Glacially related and bottom current controlled sedimentation processes on the West Antarctic continental margin –Interpretations derived from seismic reflection investigations

Carsten Scheuer

Dissertation zur Erlangung des Doktorgrades
der Naturwissenschaften

vorgelegt dem Fachbereich Geowissenschaften (FB 5)
der Universität Bremen

Bremerhaven, März 2006

Alfred-Wegener Institut für Polar- und Meeresforschung

ABSTRACT

The advances and retreats of grounded ice on the Antarctic continental shelf during glacial-interglacial cycles led to the deposition of large sediment deposits. Depositional patterns on the continental slope and rise reflect interactions between the effects of ice sheet fluctuations, mass transport processes and bottom currents. The central element of this thesis is the study of the late Cenozoic glacial history of the South Pacific continental margin of West Antarctica by interpreting the record of marine sediments there, with focus on the sedimentary successions of the outer continental shelf, slope and rise. The thesis presents the results of seismic stratigraphic analyses of multi-channel and single channel seismic reflection profiles collected on the continental margin during the course of several cruises since 1986. Seismic stratigraphic patterns are interpreted with reference to recent sedimentation models in order to differentiate between pre-glacial and glacially-influenced sediment units. In contrast to previous studies, the production and interpretation of one previously unpublished along slope seismic profile enabled the correlation of seismic units along the entire continental margin of the western Antarctic Peninsula and the Bellingshausen Sea and, thus, an evaluation of terrigenous sediment supply and distribution. Furthermore, correlation of reflectors with downhole results at the ODP Leg 178 drill sites allows the development of an age related sedimentation model and estimates of sediment deposition rates. Glacial advances and retreats appear not to have been synchronous along the continental margin. In the Bellingshausen Sea, high Pliocene and Quaternary sedimentation rates imply an increase of sediment supply to the continental rise due to frequent advances of grounded ice on the continental shelf. This is in contrast to the situation on the Antarctic Peninsula margin where increasing late Miocene and decreasing post-Pliocene sedimentation rates are observed. The modelling of isopach grids in the Southern Pacific off West Antarctica enables assessment of local variability in sediment supply from continental margins. The greatest thicknesses and deposition rates of glacial sediments are observed in front of major glacial drainage outlets, i.e. Marguerite Trough on the western Antarctic Peninsula shelf, Belgica Trough in the Bellingshausen Sea, and the trough off Pine Island Bay in the Amundsen Sea. Seismic data show differences in the width, elevation, symmetry and structure of sediment mounds and depocentres that developed on the continental rise. The characteristics of contourite drifts observed off the western Antarctic Peninsula and in the western Bellingshausen Sea can be interpreted in terms of interaction between turbidites and a westward flowing bottom current.

In addition to sediment depositions, seismic profiles provide insights into the oceanic basement structure. The topography of the ocean floor suggests that the morphology of the oceanic basement influences the shape and structure of sediment deposits. Correlations with magnetic seafloor spreading anomalies enable the verification of suspected fracture zones in the basement, which contributes to the improvement of knowledge about South Pacific plate kinematics.

TABLE OF CONTENTS

CHAPTER 1 ..... **1**

INTRODUCTION

1.1 Aims of this thesis **1**

1.2 Structure of this thesis **3**

CHAPTER 2 ..... **4**

2.1 STATE OF THE ART **4**

2.1.1 Geologic and morphologic overview 4

2.1.2 Tectonic setting of the oceanic basement 6

2.1.3 Southern ocean currents 8

2.1.4 Glacial development and transport mechanisms 9

2.2 USED METHODS **13**

2.2.1 Seismic method 13

2.2.2 Additional methods 14

REFERENCES **15**

CHAPTER 3 ..... **19**

VARIABILITY IN CENOZOIC SEDIMENTATION ALONG THE CONTINENTAL RISE OF THE BELLINGSHAUSEN SEA

3.1. Abstract **19**

3.2 Introduction **20**

3.3 Tectonic-sedimentary background **20**

3.3.1 Basement evolution 21

3.3.2 Glacial history and sediment transport 22

3.3.3 Physiographic expression 23

3.4 Magnetic database **23**

3.5. Seismic database and observations **24**

3.5.1 Basement structure 24

3.5.2 Sediment units 27

3.5.2.1 Eastern section (Profiles AWI-94003, AWI-20010001) 27

3.5.2.2 Middle section (Profiles AWI-94030, AWI 20010001) 32

3.5.2.3 Western section (Profile 92324) 32

3.6 Discussion **32**
3.6.1 Tectonic implications 32
3.6.2 Sedimentation processes 34
3.6.2.1 Geometric expression 34
3.6.2.2 Nature of sedimentary units 36
3.6.2.3 Age of sediment units 37
3.6.2.4 Sediment deposition rates 38
3.6.2.5 Faults in Unit Be1 39

3.7 Conclusions **40**

Acknowledgements **41**

REFERENCES **42**

CHAPTER 4 ..... **46**

BOTTOM-CURRENT CONTROL ON SEDIMENTATION IN THE WESTERN BELLINGSHAUSEN SEA, WEST ANTARCTICA

4.1 Abstract **46**

4.2 Introduction **46**

4.3 Study area **47**

4.4 Methods **49**

4.5 Results **50**
4.5.1 Profile BAS-92324 51
4.5.2 Profile PET-98407 51
4.5.3 Profile PET-98405 52
4.5.4 Profiles AWI-95200 and AWI-95201 54
4.5.5 Profile PET-98404 55
4.5.6 Profile PET-98403b 55
4.5.7 Profile PET-98408 56

4.6 Discussion and Conclusions **57**
4.6.1 Variations of sediment accumulation conditions 57
4.6.2 Sediment thicknesses and deposition rates 58

Acknowledgements **62**

REFERENCES **62**

CHAPTER 5 ..... **65**

GRIDDED ISOPACH MAPS FROM THE SOUTH PACIFIC AND THEIR USE IN INTERPRETING THE SEDIMENTATION HISTORY OF THE WEST ANTARCTIC CONTINENTAL MARGIN

5.1 Abstract **65**

5.2 Introduction **65**

5.3 Data and knowledge basins **67**
5.3.1 Geological setting 67
5.3.2 Previous models of total sediment thicknesses 71

5.4 Methods **71**
5.4.1 Definition of horizons 71
5.4.2 TWT [s] to depth [m]-conversion 72
5.4.3 Additional input information 74
5.4.4 Gridding of sediment thicknesses 75

5.5 Results **78**
5.5.1 Total sediment thicknesses 78
5.5.2 Pre-glacial and glacially transported sediments 80

5.6 Discussion **83**
5.6.1 Terrigenous sediment supply 83
5.6.2 Sediment accumulation rates 84
5.6.3 Influence of ocean bottom currents 86
5.6.4 Implications for geodynamics 86
5.6.5 Outlook 87

5.7 Summary and conclusions **87**

Acknowledgements **88**

REFERENCES **88**

CHAPTER 6 ..... **94**

6.1 SUMMARY **94**

6.2 OUTLOOK **96**

ACKNOWLEDGEMENTS **98**

APPENDIX A **99**

LIST OF FIGURES

Fig. 2.1: Geographic locations of Antarctica and the surrounding Southern Ocean 4
Fig. 2.2: Overview of the South Pacific continental margin of West Antarctica 6
Fig. 2.3: Gravity map of the South Pacific margin (McAdoo and Laxon, 1997) 7
Fig. 2.4: Schematic sketch of the major oceanographic features and currents of the Southern Ocean 9
Fig. 2.5: Transport and depositional processes 10
Fig. 2.6: Schematic illustration of two potential depositional processes on the continental rise 11
Fig. 2.7: Ice sheet depositional model of Cooper et al. (1991) 12
Fig. 2.8: Schematic sketch of seismic data acquisition 14

Fig. 3.1: Satellite-derived predicted bathymetric map (Smith and Sandwell, 1997) of the Bellingshausen and eastern Amundsen Sea 21
Fig. 3.2: Transport and depositional processes 23
Fig. 3.3: Seismic reflection profile AWI-20010001 25
Fig. 3.4: Profile AWI-20010001 between (a) CDP 9000 and 20000, (b) CDP 17750 and 28000 and (c) CDP 24000 and 40000 26
Fig. 3.5: Profile BAS-92324 29
Fig. 3.6: Profile AWI-94003 30
Fig. 3.7: Profile AWI-94030 31
Fig. 3.8: Illuminated satellite-derived gravity anomaly map (McAdoo and Laxon, 1997) 33
Fig. 3.9: Schematic model of sediment transport processes along the continental margin of the Bellingshausen Sea 35

Fig. 4.1: a)Track chart superimposed on a satellite-derived gravity map b)Gridded bathymetric map 48
Fig. 4.2: Schematic illustration of two potential depositional processes on the continental margin 50
Fig. 4.3: MCS profile BAS-92324 with stratigraphic units 51
Fig. 4.4: SCS profile PET-98407 with line-drawings indicating seismic reflections. 53
Fig. 4.5: SCS profile PET-98405 with line-drawings indicating major seismic reflections 53
Fig. 4.6: MCS profile ANT-95200 and ANT-95201 with line-drawings indicating major seismic reflections 54
Fig. 4.7: SCS profile PET-98404 with line-drawings indicating major seismic reflections 55
Fig. 4.8: SCS profile PET-98403b with line-drawings indicating major seismic reflections 56
Fig. 4.9: SCS profile PET-98408 with line-drawings indicating major seismic reflections. 56
Fig. 4.10: Composite seismic cross-sections of Depocentre C 59
Fig. 4.11: Estimated sediment thickness of the youngest Cenozoic sediments 61

Fig. 5.1: Overview of the South Pacific continental margin of West Antarctica 66
Fig. 5.2: Interpreted line drawings of five MCS profiles 69
Fig. 5.3: Filtered and unfiltered sediment thicknesses of the profiles Th-86-002/3/8/9 74
Fig. 5.4: Comparison between a) total sediment thicknesses, based on the latest seismic data, and b) the isopach grid from the National Geophysical Data Centre (NGDC) 76
Fig. 5.5: Isopach grid of total sediment thickness 77
Fig. 5.6: Comparison between a) the total sediment thicknesses, based on the latest seismic data, and b) predicted sediment thicknesses derived from the grid of isostatic corrected residual bathymetry from Eagles (2006) 79
Fig. 5.7: Isopach grid of pre-glacial sediments 81
Fig. 5.8: Isopach grid of glacially transported sediments 82

CHAPTER 1

INTRODUCTION

1.1 Aims of this thesis

"The White Desert", the title of a book by John Giaever (1954) is quite an appropriate description for Antarctica. Even though exploration of the southernmost continent has been the focus of a great number of surveys since the last century, wide areas of the continent and its ocean margins are still sparsely investigated, and our geological knowledge is limited. The major hindrance to investigations is ice. About 90% of the global ice mass is accumulated on Antarctica (Denton et al., 1991). About 98% of the Antarctic continent is covered by an ice sheet averaging 1 to 4 km in thickness, and parts of the continental shelves are also covered by large ice sheets (Anderson, 1999). The Antarctic ice sheet itself represents not just a limitation to research activities, but also a highly important subject for them. The Cenozoic glaciation of Antarctica is thought to have played a key role in regulating world climate, via its effects on the atmospheric and oceanic circulations. As well as this, the waxing and waning of the Antarctic ice shield influences albedo effects and sea level variations. As an example, the sea level during the last glacial maximum in the late Quaternary was about 120 m below the present sea level (Seibold & Berger, 1993). Accordingly, accurate reconstruction of Antarctic climate history is an important precondition for our understanding of the sources of global climate change and sea level variations. Hence, in order to derive the basic parameters needed to forecast climatic developments and model the future behaviour of the polar ice caps, we have to first understand the interplay of processes that operated in the past.

Reconstructions of the glacial history of the Antarctic continental margins are based on data coming predominantly from ocean drilling and seismic profiling. Investigations of sediment stratigraphic patterns on seismic profiles show evidence of ice dynamics, indicating that grounding and eroding ice streams developed on the continental shelves in glacial times. Thus, sediment accumulations on the Antarctic continental margin provide a record of the history of glaciation on the continental shelves. So far, surveys have predominantly been concentrated on the continental margins of the Antarctic Peninsula, Ross Sea, Weddell Sea, Prydz Bay and Wilkes Land (Fig. 2.1). On the other hand, knowledge of sedimentary processes in the Bellingshausen and Amundsen seas, whose remoteness and summertime ice cover make data acquisition far more difficult, is based on far sparser seismic data sets. Hence, the glacial history in this area is relatively poorly known.

The aim of this thesis is to study sediment accumulations on the South Pacific continental margin of West Antarctica, by interpreting seismic profiles and correlating them with stratigraphies known from ocean drilling sites (Fig. 2.2). Seismic data that were acquired during various expeditions between 1986 and 1995 on the outer continental shelf, slope, and rise in the Bellingshausen and Amundsen seas formed the basis for a preliminary sedimentation model, and the definition of sediment sequences related to pre-glacial and glacial times

(Nitsche et al., 1997). However, these profiles were not connected with each other, making correlation across the entire area impossible. Furthermore, these seismic data lacked adequate age control due to the lack of ocean drilling results in the region. A newer along slope seismic profile, acquired in 2001, connects these older profiles and enables correlation of seismic units along the western continental margin of the Antarctic Peninsula and Bellingshausen Sea for a distance of approximately 2000 km. The connection of this dataset to the drilling sites of ODP Leg 178, completed in 1998, allowed the development of an age related sedimentation model fur the Bellingshausen Sea, which is introduced in this thesis. To summarise, this thesis is a discussion of the sedimentation histories of the Bellingshausen and Amundsen seas, and the Antarctic Peninsula margin, which focuses on the following aspects and questions:

- The onset of sustained accumulation of glacially transported sediments is an important stage in the glacial history as it most probably marks the first phase of cooling that was strong enough to initiate the development of grounding ice on the continental shelf. Previously published investigations on the Antarctic Peninsula margin suggest that glacially transported sediment started to be deposited on the continental rise prior to 9.6 Ma. This thesis concentrates on the beginnings of glacial sediment transport in the adjacent, westward, Bellingshausen and Amundsen seas.
- Is it possible to differentiate glacial-interglacial cycles in seismic reflection profiles on the continental rise? If it were possible to identify individual glacial and interglacial periods, this would pave the way to an improved knowledge of ice sheet sensibility to climate change.
- How much sediment has been deposited, and when? The amount of sediment accumulated on the continental rise can be related to downslope sediment supply and thus, to pre-glacial and glacial conditions on- and offshore. Calculations of sedimentation rates at various sites enable comparisons of the glacial development of these sites.
- Did the dynamics of glaciation unfold synchronously over the entire South Pacific margin of West Antarctica, or is it possible to identify temporal as well as spatial differences? For example, previous studies indicated at least eight periods of grounding ice advances on the western Ross Sea continental shelf and 30 on the western Antarctic Peninsula shelf (Bart and Anderson, 2000). Different topographic settings on- and offshore in the study area suggest there should have been differences in the development of ice sheets that developed on them, or advanced and retreated over them. For instance, some authors conclude that the ice sheet onshore of the Bellingshausen and Amundsen Seas is highly sensitive to climate changes because its base lies predominantly below sea-level making it vulnerable to melting caused by warmer seawater. Pine Island Bay, in the Amundsen Sea, is fed by glaciers that drain an enormous area of the West Antarctic Ice Sheet and so may be the location of particularly strong glacial sediment transport.
- Can we identify evidence for ocean bottom currents, their velocity, or directions, or for changes in these, in the study area? The influence of bottom currents on the development of sediment deposits was verified on the continental rise of the Antarctic Peninsula. But it is not known how the current might continues to the west, and if it does so along the Bellingshausen and Amundsen Sea margins, what influence it has on sedimentation there.

1.2 Structure of this thesis

Chapter 2 gives an overview of previous knowledge of the geologic setting of Antarctica, the oceanographic pattern in the Southern Ocean, the glacial history and glacially related transport processes. Furthermore, it explains the geoscientific methods used in this thesis.

Chapter 3 focuses on the structure and the age dating of sedimentary units in the Bellingshausen Sea. Three main sediment units were identified on the basis of one seismic along-slope profile and by correlation to the continental shelf via one cross-slope profile. The lowermost unit, Be3 (older then 9.6 Ma) is interpreted as a unit representing a pre-glacial period of slow accumulation of mainly turbiditic sediments. Units Be2 and Be1 (younger then about 9.6 Ma and 5.3 Ma, respectively) may represent periods of short-lived ice advances and frequent advances of grounded ice on the continental shelf, respectively. Estimates of sedimentation rates indicate differences of the glacially and sedimentary development between the Antarctic Peninsula and the Bellingshausen Sea. Evidence for tectonic fracture zones lying perpendicular to the margin has been identified by combining several magnetic data sets and one multichannel seismic reflection profile.

Chapter 4 present a seismic study of late Cenozoic drift and levee deposits in a channel-ridge-mount system on the continental margin of the western Bellingshausen Sea in the vicinity of Peter I Island. The goal is to recognize the spatial and temporal interplay of thermohaline bottom-water flow and downslope sediment reworking by turbidity currents in response to both glacial dynamics and tectonic movements. Inspired by former studies concentrated on the western Antarctic Peninsula margin and the Bellingshausen Sea, the new data fill the gap of knowledge concerning depositional processes in the selected study area.

Chapter 5 presents models of isopach grids on the basis of a large set of seismic reflection data acquired in the South Pacific off West Antarctica. These grids provide insights into the tectonic structure and sedimentary architecture of the study area. Seismic stratigraphic models previously established on the continental margin enabled a differentiation between pre-glacial and glacially transported sediments. The adoption of the onset of glacially transported sediment supply across the shelf edge at about 10 Ma allowed approximations of sedimentation rates on the continental rise and thus, a comparison of local sedimentary developments.

Finally, chapter 6 gives a summary of this thesis, emphasizing the main conclusions with respect to the questions stated in chapter 1, and an outlook concerning further investigations.

This thesis contains the original text, tables and figures of three manuscripts that were submitted to international, peer-reviewed, journals. The first manuscript (chapter 3) is published in Marine Geology (Elsevier, Amsterdam). The second one (chapter 4) is accepted (with minor revisions) by Geo-Marine Research Letters (Springer-Verlag, Hamburg), and the third manuscript (chapter 5) is submitted to G^3 (AGU, electronic journal) in March 2006. Due to its cumulative form, repetitions within the text and the figures cannot be avoided in this thesis.

CHAPTER 2

2.1 STATE OF THE ART

2.1.1 Geologic and morphologic overview

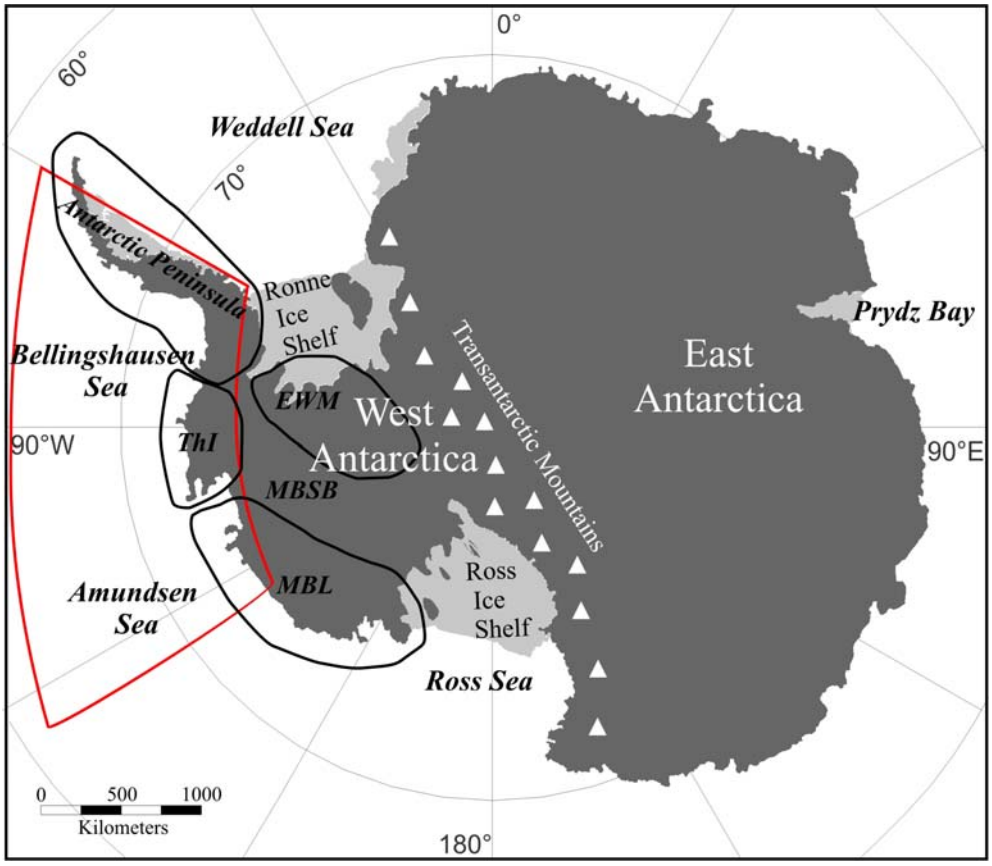

Fig. 2.1: *Geographic locations of Antarctica and the surrounding Southern Ocean. The red frame indicates the study area. The black frames encircle the four West Antarctic microplates (modified after Anderson, 1999). ThI=Thurston Island, EWM=Ellsworth-Whitmore, MBL=Marie Byrd Land Mountains, MBSB=Marie Byrd Subglacial Basin.*

The Antarctic continent consists of two major continental blocks (Fig. 2.1). The larger part is East Antarctica, a Precambrian cratone composed mainly of metamorphic basement overlain by generally flat-flying sedimentary rocks. In contrast, West Antarctica is a continental mosaic composed of at least four major microplates of predominantly Mesozoic - Cenozoic age, partially separated by deep basins (Anderson, 1999): Antarctic Peninsula, Ellsworth-Withmore Mountains, Thourston Island, and Mary Byrd Land. While the Antarctic Peninsula is a mountain chain that rises up to 1750 m altitude, the majority of the other microplates lies below sea level, even though the isostatic effect due to the overlaying ice mass is considered. East and West Antarctica are separated by the Transantarctic Mountains, on of the major mountain chains of the Earth spanning nearly 3500 km. The Antarctic continental shelves are

characterized by great depths, rough topography, and landward sloping profiles. The strong depression and the topographic shape of the shelf are also widely related to the isostatic effect during glacial periods, and to glacial erosion processes. The steepness and relief of the continental slope varies along the Antarctic margin. However, one feature that is found at many locations around Antarctica is an oceanward progradation of the shelf edge, related to the waxing and waning of grounded ice due to glacial-interglacial cycles.

Our study area is located on the West Antarctica continental margin and can be divided into three sub-regions basing on different topographic features (Fig. 2.2.): The western Antarctic Peninsula margin, and the Bellingshausen and Amundsen Sea, two epicontinental oceans as parts of the South Pacific. The continental shelf of the Antarctic Peninsula is relatively small (180 km at average), characterized by four major troughs of which Marguerite Bay Trough is largest (having maximum depressions of 1000 m). These troughs are related to glacial drainage paths for advancing ice streams during glacial maxima (e.g. Pudsey et al., 1994). The shelf is generally progradational with progradation concentrated in four lobes. The steep continental slope with gradients between 13° and 17° shows several small and great erosional channels which act as transport paths for turbidity currents. (e.g. Cunningham et al., 1994). The interaction of a westward flowing bottom current with downslope turbidity currents lead to the development of a large number of contourite drifts and sediment mounds on the sides of the channels (e.g. Larter and Cunningham, 1993; Camerlenghi et al., 1997; Rebesco et al., 1997).

While the Antarctic Peninsula margin is relatively good investigated, physiographic and geologic knowledge of the westward adjacent Bellingshausen and Amundsen Seas is limited. Previous studies predominantly base on satellite derived bathymetry data (Smith and Sandwell, 1997) and few seismic profiles. The continental shelf of the Bellingshausen Sea shows widths varying from about 390 km east of Thurston Island to about 480 km west of Alexander Island. Three lobes on the continental shelf break that may have been produced by oceanward migration can be observed. Sediment supply from the vicinity of these lobes seems to have fed large sediment depocentres on the continental rise. The continental slope in the Bellingshausen Sea is gently inclined with a gradient between 1° and 4° and thus shallower than the slope observed along the western Antarctic Peninsula (e.g. Cunningham et al., 1994; Nitsche et al., 1997).

The width of the Amundsen Sea continental shelf is similar to that of the Bellingshausen Sea but the east-west extension is less wide. The relief of the shelf is influenced by the third largest drainage outlet of the West Antarctic Ice Sheet (WAIS), the Pine Island Bay. Deepest areas of the Pine Island Bay Trough reach maximum depressions of 1100 m (Lowe and Anderson, 2002). Knowledge about the continental slope and rise is very little. One seismic profile shows a prograding shelf edge and a slope inclination of 3°- 4° (Nitsche et al., 2000). Several sediment mounds separated by channels were identified on the continental rise by seismic profiling (Yamaguchi et al., 1988).

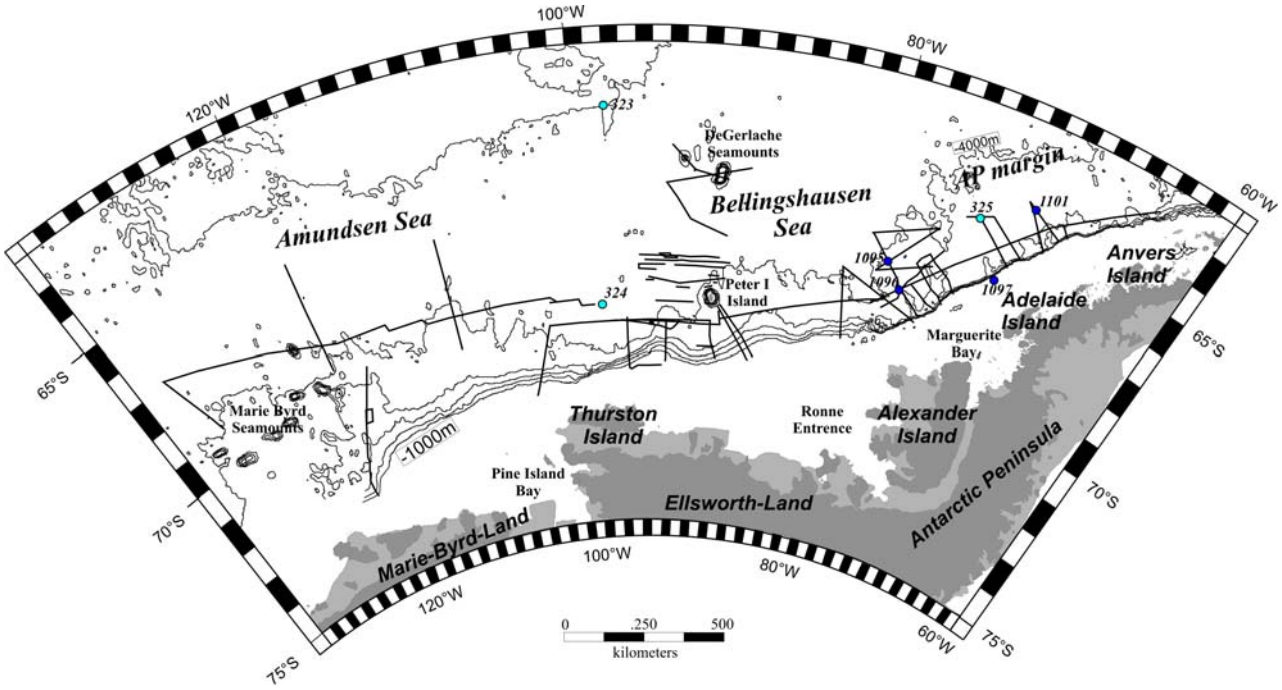

Fig. 2.2: *Overview of the South Pacific continental margin of West Antarctica, including the western Antarctic Peninsula margin, and the Bellingshausen and Amundsen Seas. The black lines indicate seismic reflection profiles analysed in this thesis. The contours base on satellite-derived predicted bathymetry from Smith and Sandwell (1997). Drill sites of DSDP Leg 35 are marked with light blue dots, those of ODP Leg 178 with dark blue dots. Dark grey areas indicate land masses, white light grey indicates recent ice shelves.*

2.1.2 Tectonic setting of the oceanic basement

Even if this thesis does not focus on plate kinematics, understanding of the evolution of the oceanic basement and its tectonic structures is important for interpretations of sediment depositions and estimation of sediment ages. This chapter gives a brief summary of present knowledge of the tectonic evolution and oceanic basement structure of the South Pacific margin of West Antarctica:

The Amundsen Sea and the Bellingshausen Sea are two different tectonic regimes, separated by a set of north-south trending tectonic lineations of which the western branch is named the Bellingshausen Gravity Anomaly (BGA), and the northern the DeGerlache Gravity Anomaly (DGGA) (Fig. 2.3). Oldest oceanic basement was identified on the passive continental margin of the Amundsen Sea where magnetic profiles indicate Cretaceous ages between 83-90 m.y. (e.g. Larter et al., 2002) This part of the oceanic crust, formally named the Bellingshausen Plate, evolved during the separation of New Zealand (i.e. Chatham Rise) from Marie Byrd Land, which began about 90 Ma. The part of the continental margin between the Amundsen and Bellingshausen Sea is most poorly studied due to its remoteness and inaccessibility. The oceanic crust in between the BGA and Peter I Island is interpreted as having formed as part of the erstwhile Charcot Plate, a remnant microplate that subducted beneath the continental margin before 83 Ma (Larter et al., 2002; Eagles et al., 2004b). Subsequent convergence at the western margin of the Charcot Plate produced the structures that are the main course of the

BGA and DGGA. This gravity anomaly corresponds to a buried basement trough where Cretaceous oceanic basement of the old Bellingshausen Plate dips beneath more elevated basement to the east. Convergent motion at this tectonic boundary occurred in the late Cretaceous from 79 Ma to 61 Ma (Gohl et al., 1997; Larter et al., 2002; Cunningham et al., 2002; Eagles et al., 2004a).

The tectonic history of the Antarctic Plate east of Peter I Island is the youngest. The former active continental margin of the Bellingshausen Sea and the western Antarctic Peninsula *was* converted to a passive margin via collisions of a spreading ridge crest that separated the Antarctic and Phoenix plates with the trench of the continental margin during the Cenozoic. The collision of the Antarctic-Phoenix ridge crest progressively migrated towards the northeast, whereas the spreading corridors that formed by the action of these ridge segments are separated from one another by fracture zones, oriented approximately perpendicular to the trench (Fig. 2.3). Such ridge crest–trench interactions began at about 50 Ma east of Peter I Island and continued until about 3 Ma at the northern end of the western Antarctic Peninsula margin at about 62.5°S (e.g. Barker, 1982; Eagles et al., 2004b). The Continental Slope Gravity Anomaly (CSGA) south of Peter I Island is interpreted as the upper part of an accretionary prism which formed during southward subduction of the Charcot and Phoenix plates (Cunningham et al., 2002).

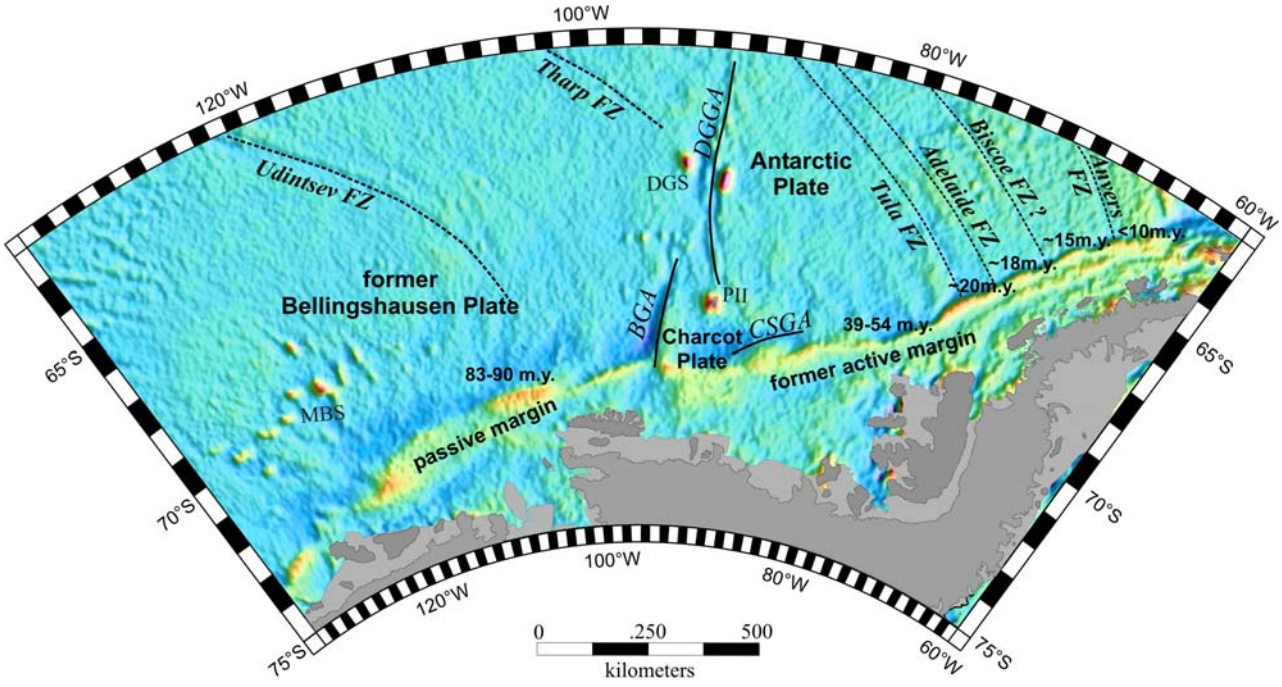

Fig. 2.3: *Gravity map, derived from altimetry data (McAdoo and Laxon, 1997) of the South Pacific margin of West Antarctica, indicating the continental shelf edge, seamounts and tectonic lineations. Bold black lines show major gravity anomalies. The dotted lines show the assumed course of tectonic fracture zones. Basement ages are denoted along the shelf edge (after Larter and Cunningham, 2002; Eagles et al., 2004b) BGA=Bellingshausen Gravity Anomaly, CSGA=Continental Slope Gravity Anomaly, DGGA=DeGerlache Gravity Anomaly, MBS=Marie Byrd Seamounts, PII=Peter I Island, DGS=DeGerlache Seamounts.*

2.1.3 Southern ocean currents

The separation of Antarctica from the African and Australian continents induced the development of the modern ocean current circulations around Antarctica. The final opening of Drake Passage in Oligocene times (about 31 +/- 2 Ma, after Lawver and Gahagen, 2003) enabled the evolution of the eastward flowing, ring-shaped, and largely wind driven Antarctic Circumpolar Current (ACC), the largest current in the Southern Ocean (Fig. 2.4). The axis of the ACC varies between 50-60° S and affects the entire water column, enabling the exchange of water masses coming from the three world oceans, the Atlantic, Pacific and Indic Oceans (e.g. Hellmer et al., 1985). Oceanographers recognize several circumpolar zones within the Southern Ocean, mainly based on their distinctive vertical stratification of temperature and salinity within the surface and intermediate levels of the water column. Narrow fronts with sharp gradients in water properties separate these zones, including the Polar Frontal Zone, the Antarctic Zone and the Continental Zone (e.g. Patterson and Whitworth, 1990; Orsi et al., 1995) (Fig. 2.4). The current system of the ACC affects both the Polar Frontal Zone and the Antarctic Zone and range to the boundary of the Continental Zone. This boundary corresponds to a region of divergent flow of surface waters, the Antarctic Divergence. This is an area of upwelling water masses caused by the southward and upward flow of Warm Deep Water (WDW) in response to the northward and downward flow of Antarctic Surface Water (AASW) (Anderson, 1999). The southernmost Continental Zone is influenced by the East Wind Drift which induces the westward flow of AASW, resulting in two large circulation gyres, the Ross Sea Gyre and the Weddell Gyre. The flow of the surface currents in the Bellingshausen and Amundsen Seas are characterized by a complex pattern of meandering, westward directed currents and small gyres (Patterson and Whitworth, 1990).

A major water mass is Antarctic Bottom Water (AABW), a loose definition including both depth and bottom waters of thermohaline origin (e.g. Hollister and Heezen, 1967). The Weddell Sea Depth Water (WSDW) defines one of these bottom waters originated by downwelling of cold Weddell Sea surface water (Patterson and Whitworth, 1990). A proportion of the WSDW escapes from the Weddell Sea gyre and flows through deep gaps in the South Scotia ridge into the southeast Pacific (Rebesco et al., 1997; Camerlenghi et al., 1997). This bottom current locally flows as contour currents along the continental slope of the western Antarctic Peninsula. Evidence comes from measurements at moored current meters. Nowlin and Zenk (1988) recorded 10-20 cm/s westward flow in the South Shetland Trench, and Camerlenghi et al. (1997) detected a weak current following the seafloor topography with velocities of 6 cm/s. The influence of bottom currents on the distribution of sediments and structures of sediment deposits along the West Antarctic continental margin is well documented by several studies analysing the development of the Antarctic Peninsula margin contourite drifts (e.g. Rebesco et al., 1997, 2002; Camerlenghi et al., 1997; Pudsey and Camerlenghi,1998).

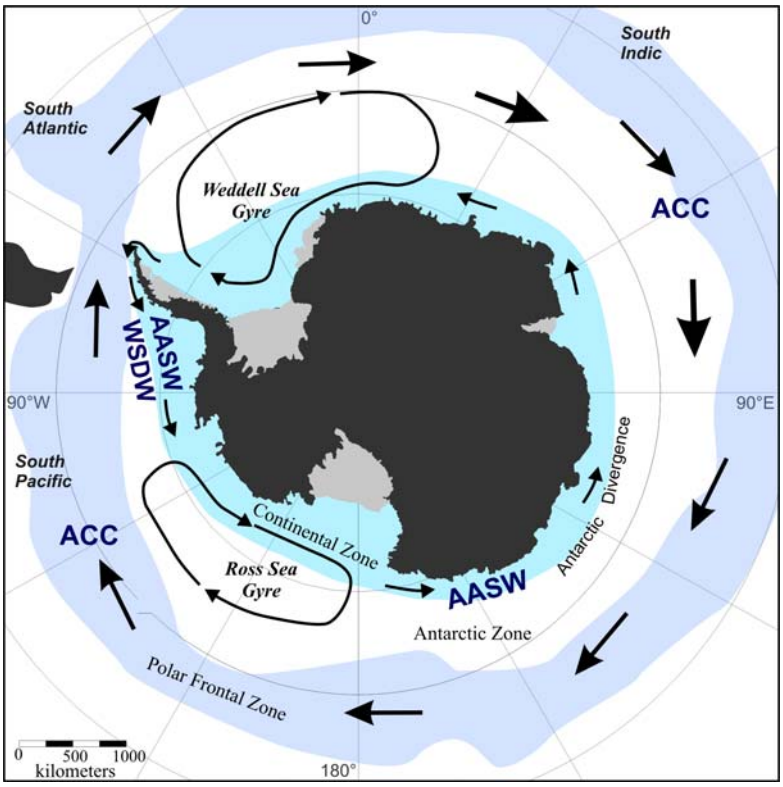

Fig. 2.4: *Schematic sketch of the major oceanographic features and currents of the Southern Ocean (modified after Anderson, 1999). ACC=Antarctic Circumpolar Current, AASW=Antarctic Surface Water, WSDW=Weddell Sea Depth Water.*

2.1.4 Glacial development and transport mechanisms

Triggered by the evolution of the ACC in Oligocene times, the West Antarctic Ice Sheet developed as a marine based ice sheet. Most of the WAIS is grounded at over 1 km below sea level and at more than 2 km in the Marie Byrd Subglacial Basin (Anderson et al., 1999). Drainage of nearly 90% from the WAIS is predominantly convergent towards the coast, creating a series of rapidly flowing ice streams (e.g. Denton et al., 1991). This most dynamic components transport large masses of terrigenous material to the continental margin. During interglacial times, ice streams lose contact with the bed at the grounding line and float as ice shelves and glacial tongues off the Antarctic mainland. The largest modern glacial outlets of the WAIS are the Weddell Sea and the Ross Sea, feeding the Ronne-Filchner Ice Shelf and the eastern section of the Ross Ice Shelf (Fig. 2.1). The third largest glacial outlet of West Antarctica is Pine Island Bay which is feed by the Pine Island Glacier and the Thwaites Glacier (e.g. Lowe and Anderson, 2002; Vaughan et al., 2001).

Glacial-marine processes are regarded as the dominant processes regulating canyon formation across the continental shelf, slope, and rise and the variation of sedimentation rates to the oceanic basin. During interglacials, pelagic, hemipelagic and glaciomarine sediments accumulate slowly on the Antarctic continental shelf and slope and little sediment is

transported off the shelf. Sea-ice cover the shelf for much of the year reducing the effect of waves, swell and currents, and the shelf mostly slopes toward the continent (e.g. Anderson, 1999). In contrast, advances of grounded ice in times of glacial maximum transported large volume of sediment across the shelf edge resulting in the deposition of unsorted sediment on the outer shelf and slope (Fig. 2.5). Deformation of subglacial till beneath ice streams is thought to be the main mechanism of sediment transport, whereas the bulldozing effect at the front of grounding ice is of minor character. The repeated advance of ice streams to the shelf edge during glacial periods resulted in a cyclicity in sediment supply to the margin. Prograding sequences and large oblique wedges developed often as tremendous sediment deposits on the outer shelf and slope. Gravity-driven mass transport processes transferred large volumes of sediment material from the continental slope to the deep basin. Numerous, large turbidity current channels which cut into the lower slope and rise are identified on many parts of the continental margin (e.g. Tomlinson et al., 1992; Rebesco et al., 2002; Dowdeswell et al., 2004). Fine to coarse grained sands have been documented at abyssal depth, hundreds of kilometres from the continental slope, and large channel-levee systems and contourite drifts are extant across the continental rise and abyssal plain as is typical for low-latitude margins (Anderson, 1999).

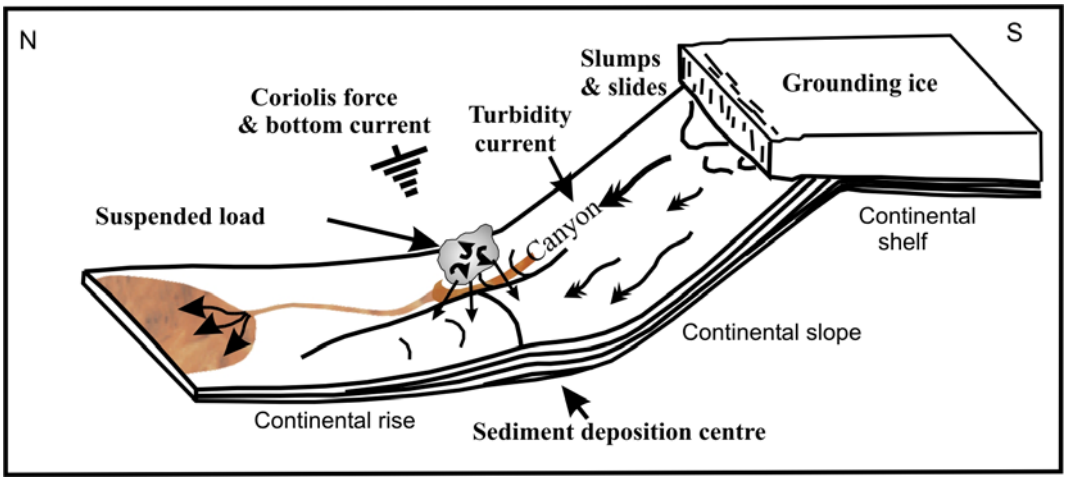

Fig. 2.5: *Transport processes of eroded sediment material across the slope and depositional processes on the continental rise along the West Antarctic margin during glacial maxima (modified after Rebesco et al., 1997).*

The records with highest resolution of Cenozoic glaciation on the Antarctic continental margins are found in the thick sediments of trough mouth fans, situated in front of bathymetric troughs that extend across continental shelves to the shelf break. This model emphasizes the delivery of large volumes of subglacial sediment to the termini of ice streams flowing along troughs, and subsequent re-deposition of this glacigenic sediment down the continental slope (e.g. Ó Cofaigh et al., 2003). The elongation of these fans can exceed 150,000 km². Examples for large Antarctic trough mouth fans are the Crary Fan in the southern Weddell Sea, or the Prydz Channel Fan off Prydz Bay in East Antarctica (e.g. Kuvaas and Kristoffersen, 1991). Channel levees and channel-related contourite drifts, interbedded with other deep-water facies,

are other widespread feature identified on the continental rise at numerous locations around Antarctica. These sediment deposits developed due to interactions of downslope-gravity-driven processes (turbidity currents), the Coriolis force and alongslope bottom currents (e.g. Rebesco et al., 1996, 1997; Faugeres et al., 1999). Channel levees represent overspill deposits composed of fine suspended sediment associated with turbidity currents. These are slightly asymmetrical, the channel walls having steep slopes, the flanks shallower slopes (Fig. 2.6, a). Along the continental margin of West Antarctica, the western levees are often higher then the eastern levees due to the Coriolis force which diverts the overspill to the left. In contrast to simple channel levees, channel-related contourite drifts are related to bottom currents that transport suspended load away from the channel. They are characterized by a strong asymmetrical shape with a steep and a gentle side (Fig. 2.6, b). The steep side often shows faults and slope failures, whereas reflections on the gentle side are rather plane and lie subparallel to parallel. Most sediment drifts rise higher above the surrounding seafloor than channel levees. As mentioned above, deep-water bottom currents flowing along Antarctic margins evolve due to thermohaline circulation in the Southern Ocean. They lead to the development of sediment drifts having dimensions directly comparable to those of deep-sea fans, ranging from small patch drifts (<100 km²) to giant elongate drifts (>100,000 km²).

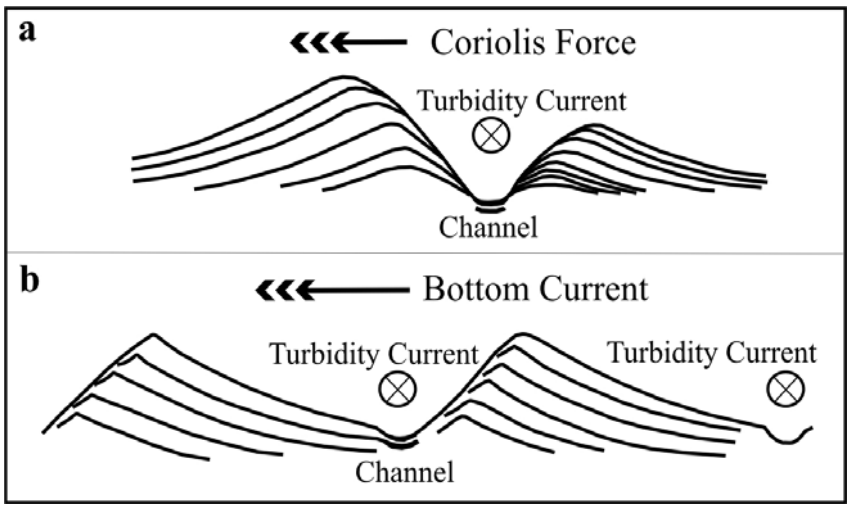

Fig. 2.6:
Schematic illustra-tion of two potential depositional pro-cesses on the continental rise fed by fine fraction of suspended material coming from turbidity currents (flow direction away from the observer). a) Channel-levee deposits are controlled by the Coriolis force, or b) deposits formed by bottom-currents resulting in the development of sediment drifts (modified after Rebesco et al., 1996).

The question when frequent deposition of glacially transported sediment on the continental slope and rise started is still subject of debate, particularly due to sparse information coming from ocean drillings. Geophysical and geological data constraining the glacial history of the South Pacific margin come from both on- and offshore, predominantly from the Antarctic Peninsula margin. A number of authors interpret compilations of benthic foraminifal oxygen isotope data (e.g. Miller et al., 1987; Zachos et al., 2001) in terms of major ice-sheet expansions at the Eocene-Oligocene boundary and in the middle Miocene. The Eocene–Oligocene shift in oxygen isotope ratios is now widely thought to be related to the development of the East Antarctic Ice Sheet and not to the development of large ice sheets on continental shelves. The earliest evidence of ice-rafted debris has been found in sediments exposed on the King George Island in the South Shetland Islands. These sediments were dated to early Eocene times by Birkenmayer et al. (1991) but have been reinterpreted as middle to

late Oligocene (26-30 Ma) sediments by Dingle and Lavelle (1998) and Troedson and Smellie (2002). The earliest offshore evidence of glaciation of any kind for the Antarctic Peninsula is ice-rafted debris at DSDP Site 325, identified in a middle Miocene core (15-17 Ma) (Hollister, Craddock et al., 1976).

Geophysical and ODP data acquired from the continental shelf and rise show evidence for ice advances and changes of conditions of sediment accumulations, suggesting a complex glaciation history of several ice advances and retreats on the continental shelves since the middle - late Miocene (e.g. Cooper et al, 1991; Bart and Anderson, 2000). Cooper et al. (1991) defined two general categories of Cenozoic acoustic sequences beneath the outer continental margin, basing on analysis of several cross-slope seismic profiles around Antarctica. Type IIA sequences principally aggrade the paleoshelf and show mostly simple geometries and gently dipping reflections. Type IA sequences are characterised by strong progradation and complex sigmoidal geometries. While Type IIA are related to little sedimentation prior to glaciation of the Antarctic continental margin, advances of grounding ice sheets are viewed as the mechanism for the development of the prograding sequences (Fig 2.7) A major change in sequence geometry (start of progradation) on the outer shelf of the western Antarctic Peninsula was dated at site 1097 of ODP Leg 178 as taking place in the late Miocene and interpreted as the start of regular advances of grounded ice to the shelf edge (Barker and Camerlenghi, 2002).

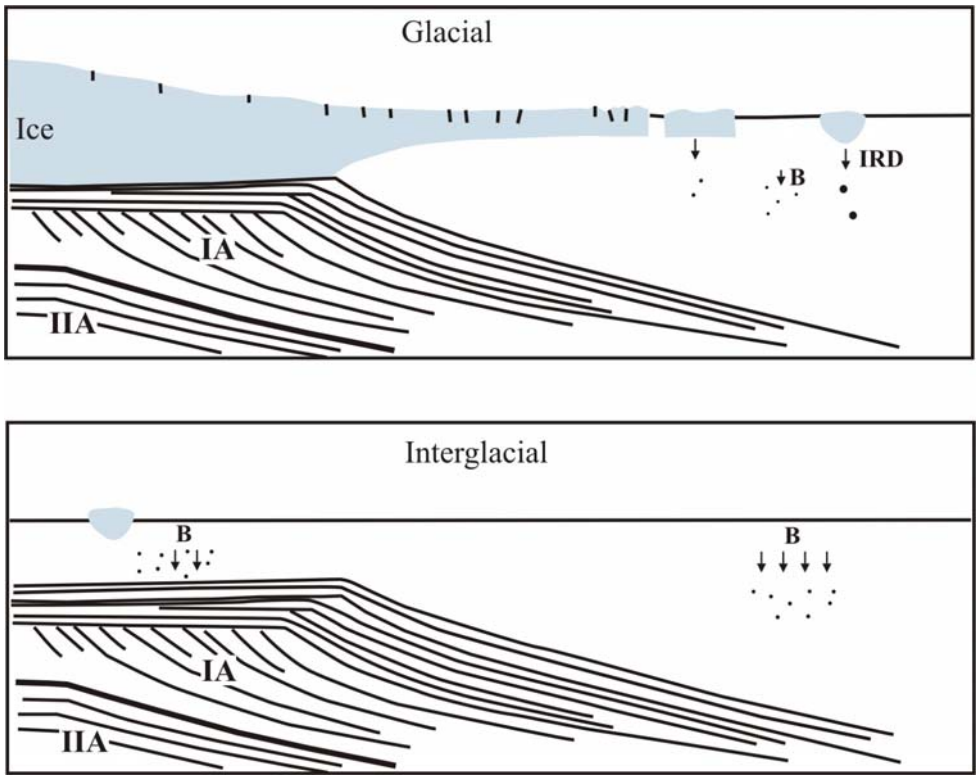

Fig. 2.7: *Ice sheet depositional model of Cooper et al, (1991), showing the major sediment sequences of Type IA and Type IIA (modified after Nitsche et al., 1998). B=Biogenic, IRD=Ice rafted debris.*

2.2 USED METHODS

2.2.1 Seismic method

Since 1973, the South Pacific continental margin of West Antarctica had been explored via seismic reflection profiling during numerous cruises, ranging from analogue recorded single channel profiles of partially low quality, to high quality, digital multi channel profiles. These profiles are the basis of investigations and interpretations in this thesis. Seismic reflection profiling is a method using acoustic waves to produce a detailed picture of the seafloor subsurface as it shows a picture of sedimentary accumulation pattern. Especially on polar continental margins, seismic profiles often show prograding and aggrading sequences that can be related to the sedimentary input during glacial and interglacial times (see 2.1.4).

The sources of the acoustic waves are airguns installed on a vessel close beneath the ocean surface (Fig. 2.8). The emitted acoustic waves cross the water column and penetrate the seafloor. At a discontinuity, i.e. where a change of seismic velocity occurs, the wave will be partially reflected back. Such velocity changes are related to density changes in sediments due to material changes, differential compactions, or changes in porosity or water content. The reflected acoustic waves are recorded with a chain of hydrophones (streamer) close beneath the ocean surface. The profiles acquired by the Alfred Wegener Institute that were analysed in this study were recorded using a 600 meter or 2400 meter hydrophone streamer and an array consisting of eight airguns with a total chamber capacity of 24 litres (except 3 x 4.3 litres for profile AWI-94030). In general, the shot interval was 12 s and the sampling interval 2 ms. The seismic data were processed with standard procedures. After demultiplexing and applying a spherical divergence correction, the data were sorted and binned into 12.5 m spaced CDP's. A bandpass filter between 10 Hz and 90 Hz was applied prior to velocity analysis, normal-moveout (NMO) correction and stacking. Finite-differences migration was required in order to correct declinations of horizons. Extensive explanations of these processing methods are given in Yilmaz (1987).

The seismic profiles named "Pet-98" were acquired during the expedition in 1998 with the *Akademik Boris Petrov*, using a single seismic hydrophone. Due to technical difficulties, the data were not digitally recorded and were only made available on paper plots. Scanning of the plots, vectorising of the seismic traces, and implementation of a new trace spacing with interpolated coordinates was required for digital interpretation.

We omit a detailed description about obtaining and processing of profiles that were previously published as these profiles were acquired during different cruises and by different companies. References to detailed descriptions are given in the respective chapters. Table A (see appendix) shows the recording methods and the year of production of all profiles used in this study.

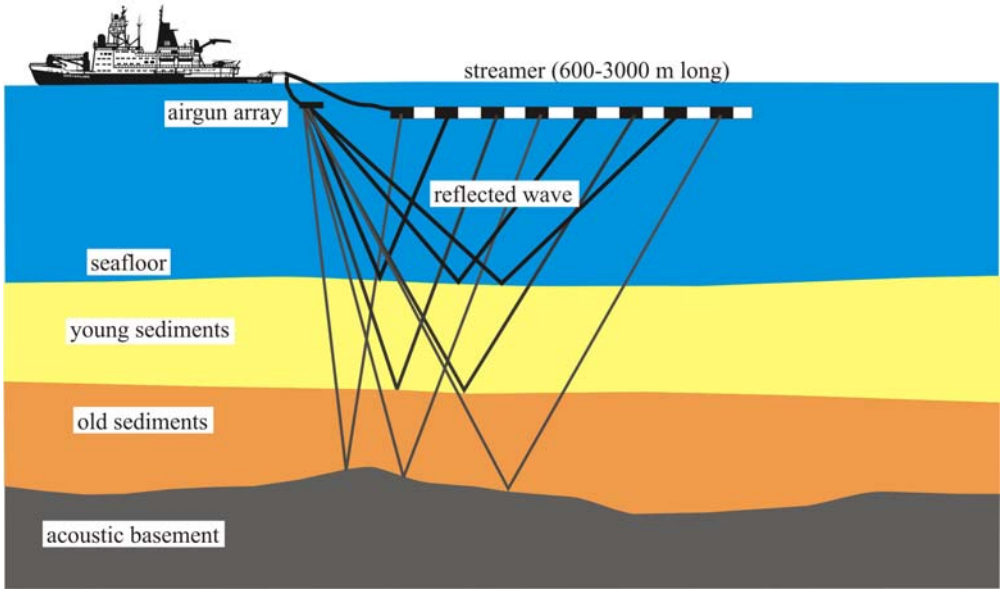

Fig. 2.8: *Schematic sketch of seismic data acquisition*

Standard processing results in a seismic profile, showing the seismic traces (i.e. shot or CDP) along the horizontal axis, and the time (two-way-traveltime in seconds) along the vertical axis. For the calculation of real sediment thicknesses the time section has to be transformed into a depth section. A common digital processing method for this time-to-depth conversion is depth-migration using acoustic velocity model of the penetrated sediments. Unfortunately, appropriate velocity models of published profiles were not available. Furthermore, low data quality due to bad ice conditions and usage of short streamers often makes generation of a reliable velocity model difficult. Other velocity information coming from refraction seismic surveys or ocean drillings are very sparse and only localized. Hence, we used the empirical relation from Carlson et al. (1986) for the time-to-depth transformation because the method successfully reproduces the decreasing seismic velocity with decreasing depth. An extensive description of this method is given in chapter 5.

2.2.2 Additional methods

Magnetic stratigraphy via detection of seafloor spreading anomalies enables dating of the oceanic basement. This method uses the potential and polarity of the magnetic field of the ocean seafloor as it is fixed during the cooling of the oceanic crust after its evolution on a mid ocean spreading ridge. The detection of a set of magnetic anomalies enables the assignment to the age of the respective section of the oceanic basement. Previously unpublished data shown in chapter 2 were acquired via a Scintrex™ caesium-vapour magnetometer towed beneath a helicopter during a RV *Polarstern* cruise in 2001. Values of total magnetic intensity (measured in nT) were sampled at 100-ms intervals. All total magnetic intensity data were subsequently processed to eliminate high-frequency noise and spikes, and the global magnetic reference field (IGRF) was then subtracted from the data.

We used bathymetry data coming from multi-beam swath bathymetry measurements along ship tracks, and data derived from satellite altimetry data (Smith and Sandwell, 1997). Furthermore, we used satellite derived gravity data (McAdoo and Laxon, 1997) in order to identify tectonic structures.

REFERENCES

Anderson, J. B., 1999. Antarctic marine geology. Cambridge University Press, pp. 289.

Barker, P.F., 1982. The Cenozoic subduction history of the Pacific margin of the Antarctic Peninsula: ridge crest interactions. J. Geol. Sci., 139, 787-801.

Barker, P.F., and Camerlenghi, A., 2002. Glacial history of the Antarctic Peninsula from Pacific margin sediments. In: Barker, P.F., Camerlenghi, A., Acton, G.D., Ramsay, A.T.S. (Eds.) Proc. ODP, Sci. Results 178 [online]. Available from World Wide Web: <http://wwwodp.tamu.edu/publications/178_SR/synth/synth.htm>.

Bart, P.J., and Anderson, J.B., 2000, Relative temporal stability of the Antarctic ice sheets during the late Neogene based on the minimum frequency of outer shelf grounding events. Earth and Planetary Science Letters, 182, 259-272.

Birkenmajer, K., 1991. Tertiary glaciation in the South Shetland Islands, West Antarctica: evaluation of data. In: Thomson, M.R.A., Crame, J.A., Thomson, J.W. (Eds.) Geological Evolution of Antarctica. Cambridge University Press, Cambridge, 629-632.

Camerlenghi, A., Crise, A., Pudsey, C.J., Accerboni, E., Laterza, R., and Rebesco, M., 1997. Ten-month observation of the bottom current regime across a sediment drift of the Pacific margin of the Antarctic Peninsula. Antarctic Science, 9, 426-433.

Carlson, R. L., Gangi, A. F., and Snow, K. R., 1986. Empirical reflection travel time versus depth and velocity versus depth functions for the deep sea sediment column. Journal of Geophysical Research, 91, 8249-8266.

Cooper, A. K., Barrett, P., Hinz, K., Traubea, V., Leitchenkov, G., and Stagg, H., 1991. Cenozoic prograding sequences of the Antarctic continental margin: a record of glacioeustatic and tectonic events. Marine Geology, 102, 175-213.

Cunningham, A. P., Larter, R. D., and Barker, P. F., 1994. Glacially prograded sequences on the Bellingshausen Sea continental margin near 90°W. Terra Antarctica, 1, 267-268.

Cunningham, A. P., Larter, R. D., Barker, P. F., Gohl, K., and Nitsche, F.-O., 2002. Tectonic evolution of the pacific margin of Antarctica: 2. Structure of Late Cretaceous-early Tertiary plate boundaries in the Bellingshausen Sea from seismic reflection and gravity data. Journal of Geophysical Research, 107 (12), 2346. doi: 10.1029/2002JB001897.

Denton, G. H., Prentice, M. L., and Burckle, L. H., 1991. Cainozoic history of the Antarctic Ice Sheet. In: Tingey, R. J. (Eds.) The Geology of Antartica, Clarendon Press, Oxford, 365-433.

Dingle, R.V., and Lavelle, M., 1998. Antarctic peninsular cryosphere: early Oligocene (c. 30 Ma) initiation and revised glacial chronology. Journal of Geological Society, 155 (3), 433-437.

Dowdeswell, J.A., Ó Cofaigh, C., and Pudsey, C.J., 2004. Continental slope morphology and sedimentary processes at the mouth of an Antarctic palaeo-ice stream. Marine Geology, 204, 203-214.

Eagles, G., Gohl, K., and Larter, R. D., 2004a. Life of the Bellingshausen plate. Geophysical Research Letters, 31, L07603.

Eagles, G., Gohl, K., and Larter, R. D., 2004b. High resolution animated tectonic reconstruction of the South Pacific and West Antarctic margin. Geochemistry, Geophysics, Geosystems, 5 (7), 1-21.

Faugères, J.C., Stow, D.A.V., Imbert, P., and Viana, A., 1999. Seismic features diagnostic of contourite drifts: Marine Geology, 162, 1–38.

Giaever, J., 1954. The White Desert, Chatto and Windus, London, pp. 304.

Gohl, K., Nitsche, F. O., and Miller, H., 1997. Seismic and gravity data reveal Tertiary intraplate subduction in the Bellingshausen Sea, southeast Pacific. Geology, 25, 371-374.

Hellmer, H. H., Bersch, M., Augstein, E., and Grabemann, I., 1985. The southern ocean: A survey of oceanographic and marine meteorological research work. Berichte zur Polarforschung, 26, Alfred Wegener Institut, Bremerhaven, pp. 115.

Hollister, C. D., and Heezen, B. C., 1967. The floor of the Bellingshausen Sea. Baltimore, 177-189, John Hopkins Press.

Hollister, C. D., Craddock, C., et al., 1976. Initial reports of deep sea drilling project. 35. U. S. Government Printing Office, Washington D. C., pp. 929.

Kuvaas, B., and Kristoffersen, Y., 1991. The Crary Fan: a trough-mouth fan on the Weddell Sea continental margin, Antarctica. Marine Geology, 97, 345-362.

Larter, R. D., and Cunningham, A. P., 1993. The depositional pattern and distribution of glacial-interglacial sequences on the Antarctic Peninsula Pacific margin. Marine Geology, 109, 203-219.

Larter, R. D., Cunningham, A. P., Barker, P. F., Gohl, K., and Nitsche, F.-O., 2002. Tectonic evolution of the pacific margin of Antarctica: 1. Late Cretaceous tectonic reconstructions. Journal of Geophysical Research. 107 (B12), 2345, doi: 10.1029/2002JB000052.

Lawver, L.A., and Gahagan, L.M., 2003. Evolution of Cenozoic seaways in the circum-Antarctic region. Palaeogeography, Palaeoclimatology, Palaeoecology, 198, 11-37.

Lowe, L. L., and Anderson, J. B., 2002. Reconstruction of the West Antarctic ice sheet in Pine Island Bay during the Last Glacial Maximum and its subsequent retreat history. Quaternary Science Reviews, 21, 1879-1897.

McAdoo, D.C., and Laxon, S., 1997. Antarctic tectonics: Constraints from an ERS-1 satellite marine gravity field. Science, 276, 556-560.

Miller, H., Henriet, J. P., Kaul, N., and Moons, A., 1990. A fine scale seismic stratigraphy of the eastern margin of the Weddell Sea. In: Bleil, U., Thiede, J. (Eds.) Geological History of the Polar Oceans: Arctic versus Antarctic. Kluwer Academ. Publ., Boston, 131-161.

Nitsche, F.-O., 1998. Bellingshausen and Amundsen Sea: Development of a sedimentation model. Berichte zur Polarforschung, 258, Alfred Wegener Institut, Bremerhaven, pp. 144.

Nitsche, F. O., Gohl, K., Vanneste, K., and Miller, H., 1997. Seismic expression of glacially deposited sequences in the Bellingshausen and Amundsen Seas, West Antarctica. In: Barker, P. F., Cooper, A. K. (Eds.), Geology and Seismic Stratigraphy of the Antarctic Margin: 2. Antarctic Research Series, 71, American Geophysical Union, Washington, DC, pp. 95-108.

Nitsche, F. O., Cunningham, A. P., Larter, R. D., and Gohl, K., 2000. Geometry and development of glacial continental margin depositional systems in the Bellingshausen Sea. Marine Geology, 162, 277-302.

Nowlin Jr., W.D., and Zenk, W., 1988. Currents along the margin of the South Shetland Island Arc. Deep-Sea Research, 35, 805-833.

Ó Cofaigh, C., Taylor, J., Dowdeswell, J.A,. and Pudsey, C.J., 2003. Palaeo-ice streams, trough-mouth fans and high-latitude continental slope sedimentation. Boreas, 32, 37-55.

Orsi, A. H., Whitworth, T., and Nowlin, W. D., 1995. On the meridional extent and fronts of the Antarctic Circumpolar Current. Deep Sea Research I, 42 (5), 641-673.

Patterson, S. L., and Whitworth, T., 1990. Physical oceanography. In: Glosky, G. P. (Eds.) Antarctic sector of the Pacific. Elsevier Oceanographic Series, 51, New York, 55-93

Pudsey, C.J., and Camerlenghi, A., 1998. Glacial-interglacial deposition on a sediment drift on the Pacific margin of the Antarctic Peninsula. Antarctic Science, 10, 286-308.

Pudsey, C.J., Barker, P.F., and Larter, R.D., 1994. Ice sheet retreat from the Antarctic Peninsula shelf. Continental Shelf Research, 14, 1647-1675.

Rebesco, M., Larter, R.D., Camerlenghi, A., and Barker, P.F., 1996. Giant sediment drifts on the continental rise west of the Antarctic Peninsula. Geo-Marine Letters, 16, 65-75.

Rebesco, M., Larter, R. D., Barker, P. F., Camerlenghi, A., and Vanneste, L. E., 1997. History of sedimentation on the continental rise west of the Antarctic Peninsula. In: Cooper, A. K., Barker, P. F. (Eds) Geology and Seismic Stratigraphy on the Antarctic Margin: 2. Antarctic Research Series, 71, American Geophysical Union, Washington, DC, pp. 29-49.

Rebesco, M., Pudsey, C.J., Canals, M., Camerlenghi, A., Barker, P.F., Estrada, F., and Giorgetti, A., 2002. Case study 27: Sediment drifts and deep-sea channel systems, Antarctic Peninsula Pacific margin, mid-Miocene to present. In: Stow, D.A.V., Pudsey, C.J., Howe, J., Faugeres, J.-C., Viana, A. (Eds.) Deep-Water Contourite Systems: Modern Drifts and Ancient Series, Seismic and Sedimentary Characteristics. Special Publication Geological Society London, Memoirs 22, pp. 353-371.

Seibold, E., and Berger, W. H., 1993. The sea floor. Springer-Verlag, Berlin, pp. 355.

Smith, W. H. F., and Sandwell, D. T., 1997. Global seafloor topography from satellite altimetry and ship depth soundings. Science, 277, 1956-1961.

Tomlinson, J. S., Pudsey, C. J., Livermore, R. A., Larter, R. D., and Barker, P. F., 1992. Long-range sidescan sonar (GLORIA) survey of the Antarctic Peninsula pacific margin. In: Yoshida, Y., Kaminuma, K., Shiraishi, K., (Eds.) Recent progress in Antarctic Earth Science. Terra Scientific Publishing Company, Tokyo, pp. 423-429.

Troedson, A.L., and Smellie, J.L., 2002. The Polonez Cove Formation of King George Island, West Antarctica: statigraphy, facies and palaeoenvironmental implications. Sedimentology, 49, 277-301.

Vaughan, D. G., Smith, A. M., Corr, H. F. J., Jenkins, A., Bentley, C. R., Stenoien, M. D., Jacobs, S. S., Kellog, T. B., Rignot, E., and Lucchitta, B. K., 2001. A review of Pine Island Glacier, West Antarctica: Hypotheses of instability vs. observations of change. In: Alley, R.B., and Bindschadler, R. A., (Eds.) The West Antarctic Ice Sheet: Behavior and Environment. AGU Antarctic Research Series. 77, 237-256.

Yamaguchi, K., Tamura, Y., Mizukoshi, I., and Tsuru, T., 1988. Preliminary report of geophysical and geological surveys in the Amundsen Sea, West Antarctica. Proceedings of NIPR Symposium of Antarctic Geoscience, 2, 55-67.

Yilmaz, O., 1987. Seismic data processing. Investigations in Geophysics. 2. Soc. Of Exploration Geophysicists, Tusla, Oklahoma, pp. 526.

Zachos, J., Pagani, M., Sloan, L., Thomas, E., and Billups, K., 2001. Trends, rythmus, and aberrations in global climate 65 Ma to present. Science, 292, 686-693.

CHAPTER 3

VARIABILITY IN CENOZOIC SEDIMENTATION ALONG THE CONTINENTAL RISE OF THE BELLINGSHAUSEN SEA, WEST ANTARCTICA

Carsten Scheuer[1], Karsten Gohl[1], Robert D. Larter[2], Michele Rebesco[3] and Gleb Udintsev[4]

[1] Alfred Wegener Institute for Polar and Marine Research (AWI), Bremerhaven, Germany

[2] British Antarctic Survey (BAS), Cambridge, UK.

[3] Istituto Nazionale di Oceanografia e di Geofisica Sperimentale (OGS), Trieste, Italy.

[4] Vernadsky Institute of Geochemistry and Analytical Chemistry, Moscow, Russia.

Published in Marine Geology (2006), 227, 279-298.

3.1. Abstract

Seismic reflection profiles, bathymetric and magnetic data collected along and across the continental margin of the Bellingshausen Sea provide new constraints and interpretations of the oceanic basement structure and Cenozoic glacial history of West Antarctica. Evidence for tectonic boundaries that lie perpendicular to the margin has been identified on the basis of one previously unpublished along-slope multichannel seismic reflection profile. By combining several magnetic data sets, we determined basement ages and verified the positions of possible fracture zones, enabling us to improve previous tectonic and stratigraphic models. We establish three main sediment units on the basis of one seismic along-slope profile and by correlation to the continental shelf via one cross-slope profile. We interpret a lowermost unit, Be3 (older then 9.6 Ma) as representing a long period of slow accumulation of mainly turbiditic sediments. Unit Be2 (from about 9.6 Ma to 5.3 Ma) may represent a period of short-lived ice advances on the continental shelf. The uppermost unit, Be1 (from about 5.3 Ma to present), apparently consists of rapidly deposited terrigenous sediment that we interpret as having been transported to the shelf edge by frequent advances of grounded ice. Listric faults are observed in Be1 and indicate sediment instability due to interactions between different depositional processes. Correlation of the sediment classification scheme with the continental rise of the western Antarctic Peninsula shows obvious differences in sediment depositional patterns. We estimate a very high sedimentation rate for Unit Be1 (up to 295 m/my) which points to an increase in glacial sediment supply due to major glacial outlets that flowed to nearby parts of the shelf edge in Pliocene and Quaternary times. This is in contrast to the situation at the adjacent Antarctic Peninsular margin and many other parts of the continental rise around Antarctica.

3.2 Introduction

Since ice sheets first advanced onto the continental shelves around West Antarctica, alternations of glacial and interglacial periods have had a major influence on the sediment supply across the shelf and into the deep sea. The patterns of deposition of late Cenozoic sediments along the slope and rise of the West Antarctic continental margin reflect interaction between the effects of ice sheet fluctuations, mass transport processes and bottom currents (Larter and Cunningham, 1993; Rebesco et al., 1996, 1997, 2002; Nitsche et al., 2000). Thus, both the sediment stratigraphy and the physiography of the sea floor reflect the history of the West Antarctic glaciation as well as the processes that eroded, transported and deposited sediments on the outer shelf, slope and rise of the continental margin.

The first multi-channel seismic profiles in the Bellingshausen Sea were collected in 1993 (Cunningham et al., 1994). In this paper we present a new profile, AWI-20010001, which connects a grid of previously recorded profiles west of the Antarctic Peninsula with a set of profiles in the western Bellingshausen Sea and eastern Amundsen Sea (Fig. 3.1). Together with slope-parallel seismic lines in the east and west, it forms a transect that is over 2000 km long and enables a correlation of deposition and transport processes along the entire West Antarctic continental rise of the south-eastern Pacific.

Previous investigations at different sites on the Antarctic continental margins show glacial related sediment supply to the continental rise since the Late Miocene and a decrease in sedimentation rates since the Pliocene (results from ODP Legs 178 and 188, see e.g. DeSantis et al., 1995; Barker and Camerlenghi et al., 2002; Iwai et al., 2002). The continuation of this survey effort into the largely unexplored Bellingshausen Sea is one of the goals of this study. In particular, this paper will discuss the influence of grounding ice development on sedimentation processes since the Late Miocene.

3.3 Tectonic-sedimentary background

This section briefly summarises previous knowledge of the tectonic and sedimentary history of the West Antarctic continental margin. An understanding of the evolution of the oceanic basement and its tectonic structures is important for the estimation of sediment ages. Furthermore, an understanding of the glacial sediment transport processes should help clarify the relationship between advances of grounded ice on the continental shelf during glacial times and the associated development and structure of sediment deposits on the continental slope and rise.

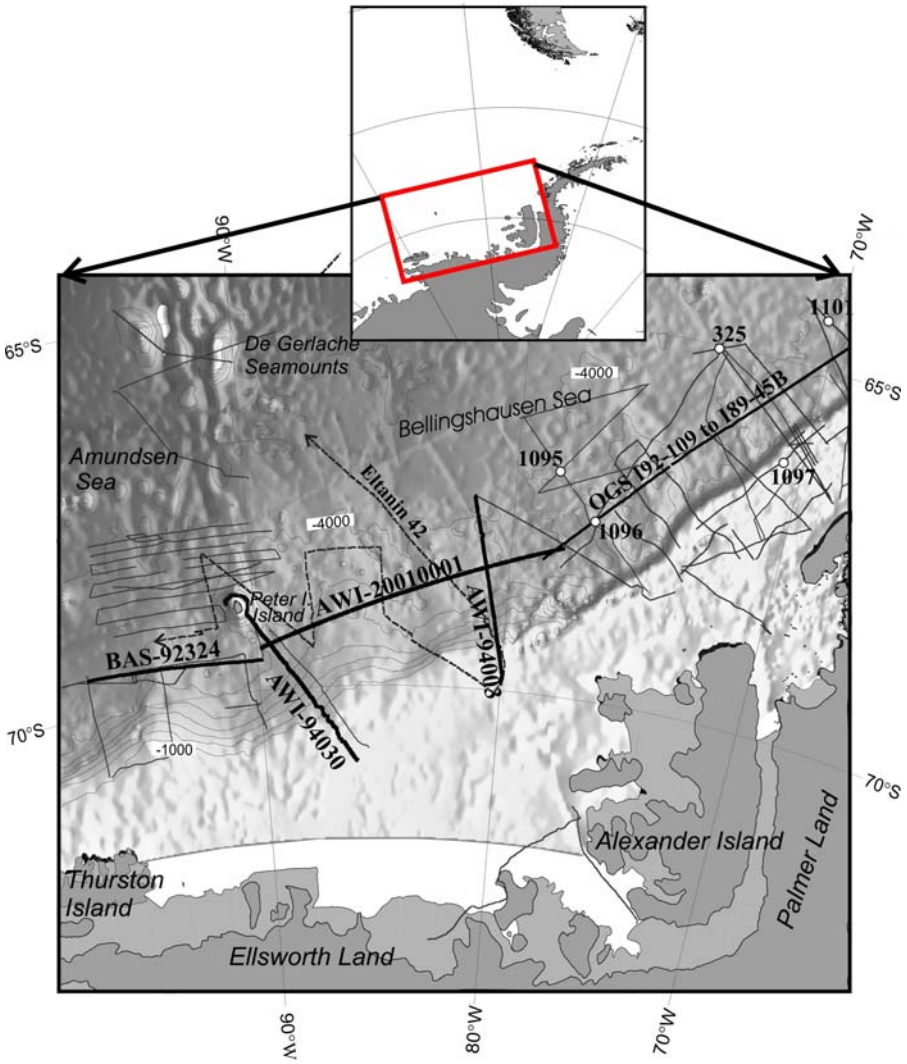

Fig. 3.1*: Satellite-derived predicted bathymetric map (Smith and Sandwell, 1997) of the Bellingshausen and eastern Amundsen Sea and the West Antarctic continental margin with tracks of seismic lines. The multichannel seismic (MCS) profiles AWI-94003, AWI-94030 and AWI-20010001 were recorded in 1994 and 2001, respectively, with RV Polarstern. The British Antarctic Survey collected MCS profile BAS-92324 during a RRS James Clark Ross cruise in 1993. The dashed line shows the track of single channel seismic data, acquired during a USNS Eltanin cruise in 1970 (e.g. Tucholke and Houtz, 1976). The thin lines show additional seismic profiles which are not used in this paper. Drill sites of DSDP Leg 35 and ODP Leg 178 are marked with white dots.*

3.3.1 Basement evolution

The active continental margin of the Bellingshausen Sea and the western Antarctic Peninsula was converted to a passive margin via a series of ridge-trench collisions of the Antarctic-Phoenix ridge that progressively migrated towards the northeast. Such ridge–trench interactions began at about 50 Ma east of Peter I Island and continued until about 3 Ma at the northern end of the Antarctic Peninsula at about 62.5°S (e.g. Barker, 1982, Larter and Barker, 1991a; Larter et al., 1997, Larter et al., 1999, Eagles et al., 2004b). The spreading corridors that formed by the action of these ridge segments are separated from one another by fracture zones that are oriented approximately perpendicular to the trench.

The boundary with the Amundsen Sea just to the west can be defined along a set of north-south trending tectonic lineations of which the western branch is named the Bellingshausen Gravity Anomaly (BGA). The BGA corresponds to a buried basement trough where Cretaceous oceanic basement dips beneath more elevated basement to the east (Gohl et al., 1997; Cunningham et al., 2002). Convergent motion at this tectonic boundary occurred in the late Cretaceous from 79 Ma to 61 Ma (Larter et al., 2002; Cunningham et al., 2002; Eagles et al., 2004a; Eagles et al., 2004b). The oceanic crust in between the BGA and Peter I Island has recently been interpreted as having formed as part of the erstwhile Charcot Plate (Larter et al, 2002, Eagles et al., 2004b).

3.3.2 Glacial history and sediment transport

Geophysical and geological data constraining the glacial history of the Antarctic Peninsula and the Bellingshausen Sea come from both on- and offshore, predominantly from the Antarctic Peninsula margin. The earliest evidence of ice-rafted debris in the region has been found in sediments exposed on the King George Island in the South Shetland Islands. These sediments were dated as early Eocene by Birkenmayer et al. (1991), but have been reinterpreted as Oligocene sediments by Dingle and Lavelle (1998) and Troedson and Smellie (2002). The earliest ice-rafted debris at DSDP Site 325 was identified in a Middle Miocene core (Hollister, Craddock et al., 1976). A number of authors interpret compilations of benthic foraminiferal oxygen isotope data (e.g. Miller et al., 1987; Zachos et al., 2001) in terms of major ice-sheet expansions at the Eocene-Oligocene boundary and in the Middle Miocene. The Eocene–Oligocene shift in oxygen isotope ratios is now widely thought to be related to development of the East Antarctic ice sheet. However, the timing of the first development of large ice sheets on West Antarctic continental shelves remains a subject of debate. Data from the Pacific margin between the Antarctic Peninsula and the Ross Sea are sparse, but geophysical and ODP data acquired from the continental shelf and rise (Location shown in Fig. 3.1) give evidence that glacially transported sediments were supplied to the continental margin in the middle to Late Miocene (e.g. Bart and Anderson, 1995; Rebesco et al., 1997; Larter et al., 1997; Nitsche, 1997; Barker and Camerlenghi, 2002). A major change in sequence geometry on the outer shelf (start of progradation) was dated as Late Miocene at ODP Site 1097 and interpreted as the start of regular advances of grounded ice to the shelf edge (Barker and Camerlenghi, 2002). A widely-held conceptual model of glacial sediment transport processes on this margin may be summarized as follows:

Deformation of subglacial till beneath ice streams is thought to be the main mechanism transporting sediment to the shelf edge, at least during the Late Miocene, Pliocene and Quaternary (Larter and Cunningham, 1993; Dowdeswell et al., 2004a). The ice grounding line advanced and retreated, controlled by climatic forcing and ice-sheet dynamics. During glacial maxima, grounded ice extended to the continental shelf edge, resulting in the transport of sediment by ice streams and deposition onto the slope (Fig. 3.2). Thus, prograding sequences and large oblique wedges developed often on the outer shelf and slope (e.g. Larter et al., 1997). Mass transport processes (slumps, slides, debris flows and turbidity currents) transported large volumes of sediment material from the continental slope to the deep basin. Numerous, large turbidity current channels, which cut on the lower slope and rise, are identified on many parts

of the continental margin (e.g. Tomlinson et al., 1992; McGinnes et al., 1997; Anderson et al., 2001, Rebesco et al., 2002; Dowdeswell et al., 2004b).

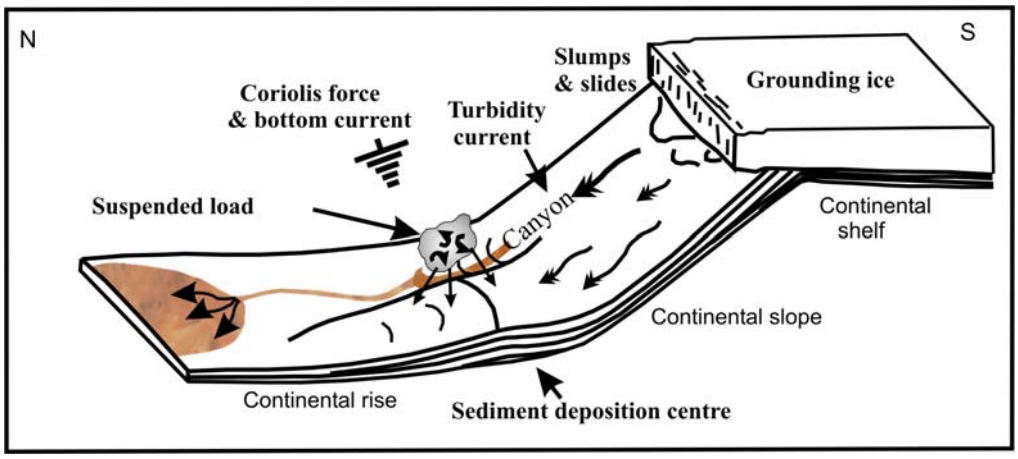

***Fig. 3.2**: Transport processes of eroded sediment material across the slope and depositional processes on the continental rise along the West Antarctic margin during glacial maxima (modified after Rebesco et al., 1997).*

3.3.3 Physiographic expression

Published data on the physiographic expression of the Bellingshausen Sea is very sparse, coming from satellite derived bathymetry data (Smith and Sandwell, 1997) and a few seismic profiles (Fig. 3.1). The satellite bathymetry suggests a relatively even continental shelf and shelf widths varying from about 390 km east of Thurston Island to about 480 km west of Alexander Island. Three lobes on the continental shelf break that may have been produced by oceanward migration can be observed. Sediment supply from the vicinity of these lobes seems to have fed large sediment depocentres on the continental rise. The continental slope in the Bellingshausen Sea is gently inclined with a gradient between 1° and 4° and thus shallower than the slope observed northeast of 77° W along the western Antarctic Peninsula (gradient between 13° and 17°) (e.g. Cunningham et al., 1994; Nitsche et al., 1997).

3.4 Magnetic database

We interpreted helicopter magnetic data that were acquired during the RV *Polarstern* cruise ANT18-5a in 2001 in the eastern Bellingshausen Sea in order to investigate basement tectonic structures. Acquisition was with a Scintrex™ caesium-vapour magnetometer. The sensor tow-length was 30 m. Altitude ranged between 150 and 300 m, and the average helicopter speed was about 80 kn. Values of total magnetic intensity (measured in nT) were sampled at 100-ms intervals. All total magnetic intensity data were subsequently processed to eliminate high-frequency noise and spikes, and the global magnetic reference field (IGRF) was then subtracted from the data.

3.5. Seismic database and observations

Two cross-slope MCS profiles, AWI-94003 and AWI-94030, permit correlations between the outer continental shelf and the along-slope MCS profiles AWI-20010001 and BAS-92324 on the continental rise and, thus, enable a determination and interpretation of the sedimentary architecture on the continental margin of the Bellingshausen Sea. The recording methods for, and processing of the two cross-slope profiles are described by Nitsche et al. (1997). The acquisition and processing of Profile BAS-92324 was described by Cunningham et al. (1994). Profile AWI-20010001 was recorded using a 96 channel, 600 meter hydrophone streamer and an array consisting of eight airguns with a total chamber capacity of 24 liters. The shot interval was 12 s and the sampling interval was 2 ms. The seismic data were processed with standard procedures. After demultiplexing and applying a spherical divergence correction, the data were sorted and binned into 12.5 m spaced CDP's. A bandpass filter between 10 Hz and 90 Hz was applied prior to normal-move out correction and stacking. We used a deconvolution filter to minimize the bubble effect and sharpen the reflection arrivals. Due to the short streamer and thus short move-out, the quality of the velocity model was not good enough for an appropriate estimate of interval velocities. Hence, all depth values in the following section are only roughly estimated by assuming an average interval velocity in sediment of 2000 m/s.

3.5.1 Basement structure

The along-slope seismic reflection profile AWI-20010001 (Figs. 3.3, 3.4a, b and c) shows a distinct sediment-basement boundary, characterised by a downwards change from weak to very strong reflectivity. The basement surface shows considerable relief, with basement highs, depressions and vertical offsets. Most conspicuous of these are a basement depression between CDPs 8000 and 11750 (up to 7.5 s TWT, about 2250 m b.s.f.), a steep basement step, of about 0.5s TWT, to the west, and a wide basement high between CDPs 22500 and 25000. This basement high rises to approximately 5.8 s TWT (about 1000 m b.s.f.) with a relief of about 0.75 s TWT on the eastern side. The basement surface west of this basement high descends slightly to 6.75 s TWT at the end of the profile.

Continuing farther west, on profile BAS 92324 (Fig. 3.5), the basement surface descends smoothly westward between CDPs 1 and 1900. The rough and elevated basement between CDPs 1900 and 4000 descends to the west at a similar angle but it is characterized by several basement steps. West of CDP 5100, the basement rises up to 6 s TWT (400 m b.s.f.) towards a wide basement high at CDP 8200 on the eastern side of the BGA. The steep westerly dipping flank of the basement high dips to more then 8.5 s TWT (>2700 m b.s.f.), indicating the tectonic boundary at the BGA.

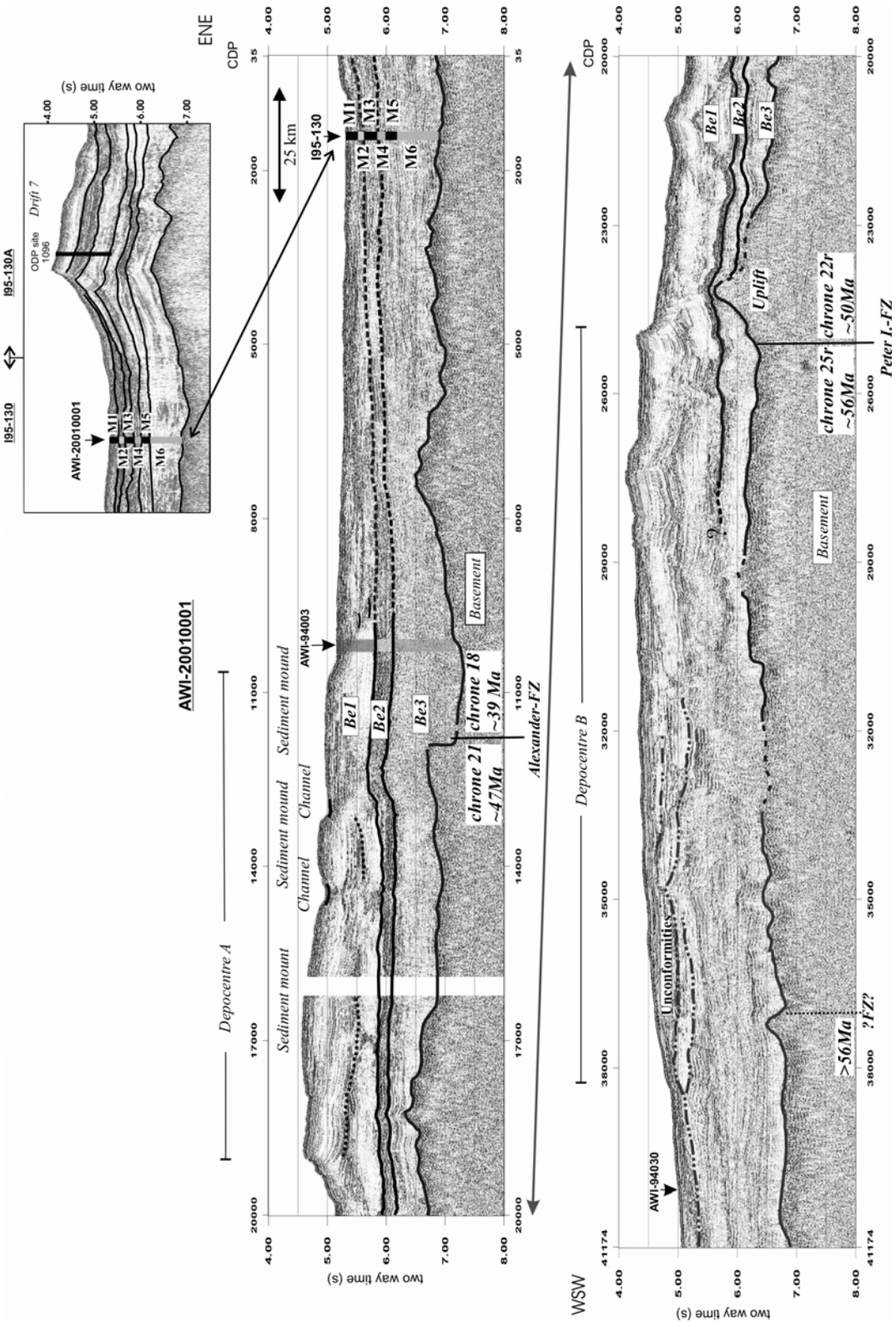

Fig. 3.3: *Seismic reflection profile AWI-20010001, showing the inferred fracture zones and sediment units Be1 – Be3. The eastward correlating profile I95-130 (shown above AWI-20010001) clarifies the age- correlation between both sediment classification schemes.*

a:

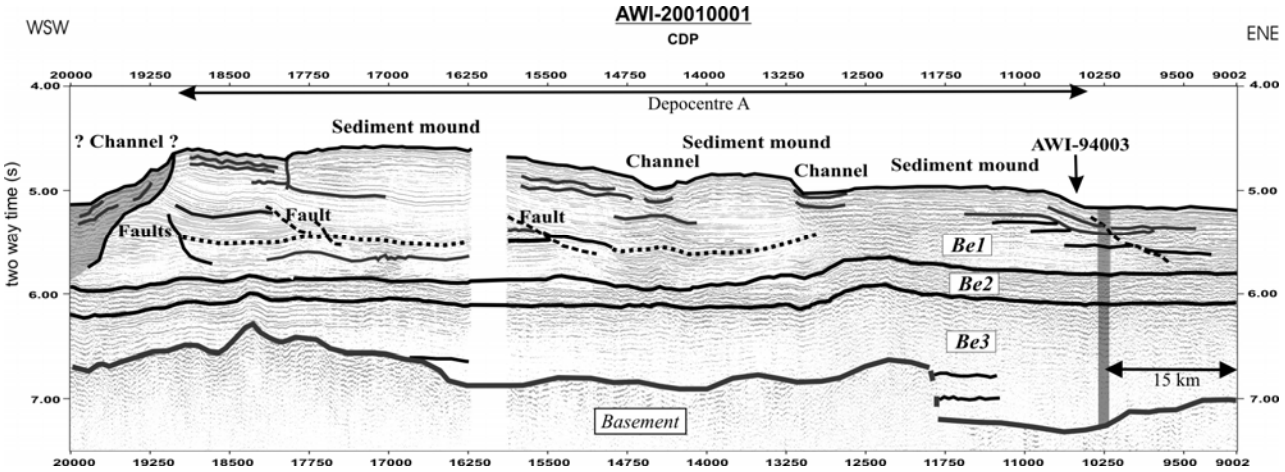

b:

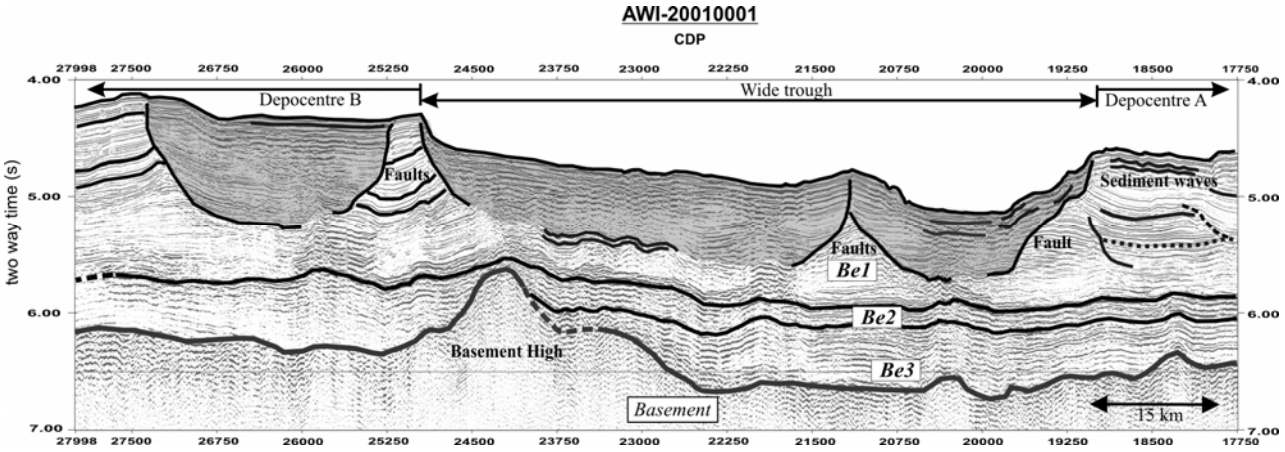

c:

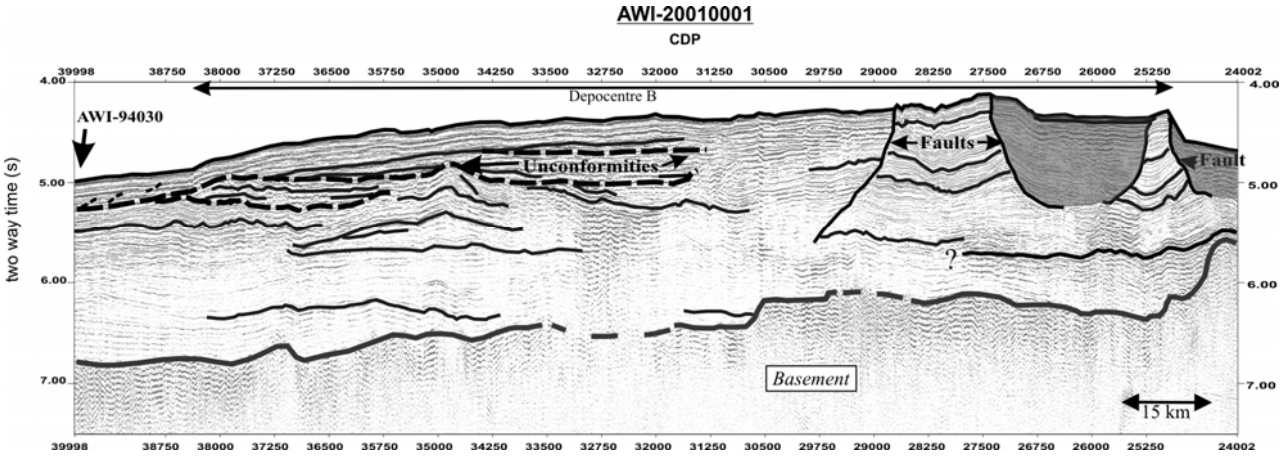

***Fig. 3.4**.: Profile AWI-20010001 between (a) CDP 9000 and 20000, (b) CDP 17750 and 28000 and (c) CDP 24000 and 40000 with detailed sediment units. Arrows mark intersections with profiles AWI-94003 and AWI-94030.*

3.5.2 Sediment units

The cross-slope profiles AWI-94003 and AWI-94030 stretch from the outer shelf to the continental rise and cross profile AWI-20010001 near its eastern and western ends (at CDPs 10500 and 40000), respectively (Figs. 3.1 and 3.3). Profile AWI-94003 (Fig. 3.6) shows three units, Unit 1 – Unit 3, previously defined beneath the outer shelf by Nitsche et al. (1997), and allows a regional continuation of their boundaries up to profile AWI-20010001 on the continental rise. This profile shows three sedimentary units, named as units Be1 - 3, whose boundaries present the distal paraconformities of the unit boundaries beneath the outer shelf. Be1 – Be3 show different seismic reflections characteristics between CDPs 10000 and 28000 (eastern section, Figs. 3.3, 3.4a, b and c). The lower unit, Be3, is characterized by low-amplitude and sub-parallel to parallel reflections, which are overlain by a set of strong reflections, unit Be2. The upper unit, Be1, is characterized by distinct parallel but weaker and faulted reflections and gentle mounds separated by channels.

In order to estimate sediment ages, we correlated the boundaries of units Be1 – Be3 with previously established seismic units on the western Antarctic Peninsula continental rise (Rebesco et al., 1997) and continued the boundaries along assumed isochron reflections of profile AWI-20010001. The classification into three units cannot be adopted on profile AWI-20010001 west of about CDP 28000, where the sedimentary reflectors are characterised by undulations and unconformities (middle section). Accordingly, we describe the western part of the profile separately. Farther west, within the domain of the BGA, the sediments are strongly affected by basement tectonics as seen on profile BAS-92324 (western section, Fig. 3.5). This profile was previously described by Nitsche et al. (1997) and Cunningham et al. (2002) and here we give only a short overview of the main seismic features that are important for the later discussion.

3.5.2.1 Eastern section (Profiles AWI-94003, AWI-20010001

Outer continental shelf units (Unit 1, Unit 2, Unit 3):

On the cross-slope profile AWI-94003, the lowermost outer shelf unit, Unit 1, consists of parallel and gently seaward dipping reflections, which are truncated seaward along the Unit1/Unit 2 boundary (Fig. 3.6). Unit 1 closely resembles the Type IIA sequence as defined by Cooper et al. (1991) at various locations along the Antarctic continental margin. Unit 2 shows upward increasing seaward inclination of the reflections and truncation of reflections on top of the shelf deposits. On the basis of identification of foreset reflections and defining Unit 2 as containing few oblique foreset truncations beneath the outer shelf, we place the Unit 1/Unit 2 boundary approximately 0.8 s deeper than Nitsche et al. (1997) did. The uppermost unit, Unit 3, shows a mainly prograding character on the outer shelf, building a sediment wedge on the slope, whereas the uppermost 0.3 s TWT near the shelf edge is characterised by a smooth decrease in progradation. In contrast to Nitsche et al. (1997), we consider the Unit 2/Unit 3

boundary to lie about 0.2 s TWT deeper, because we interpret the boundary as the deepest erosional truncation to crosses the entire outer shelf and truncate the top of Unit 2 on profile AWI-94003. Unit 3 and Unit 2 are characterized as having a Type IA geometry, after Cooper et al. (1991).

Lowermost continental rise unit (Be3):

The lowermost sedimentary unit, Be3, that we define on Profile AWI 20010001 is a succession of weak but mostly horizontal and parallel-bedded reflections with variable amplitudes (Figs. 3.3, 3.4a and b). The maximum thickness of Be3 is 0.9 s TWT in the eastern part of the profile (at about CDP 10500). Due to its low reflectivity, no distinct faults, hiatuses, or buried channels can be identified within Be3. The basal sediments fill basement troughs and onlap the basement steps and most other basement highs, indicating pre-sedimentary tectonic activity (e.g. CDP 2500, 11900). The low reflectivity of this unit changes to stronger parallel reflections between CDP 18250 and the basement high at about CDP 24000. The sediments that cover the crest of the basement high are uplifted, which indicates post sedimentary tectonic activity.

Intermediate continental rise unit (Be2):

The low-amplitude reflections of unit Be3 are covered by a set of continuous and high amplitude reflections, unit Be2 (Figs. 3.3, 3.4a and b). The transition between these two units is gradual. The thickness of Be2 varies between approximately 0.4 s TWT (e.g. CDP 14250) and 0.5 s TWT (CDP 17750). Approaching the eastern side of the basement high (at about CDP 24000), the boundary becomes less clear due to the high-amplitude character of reflectors in both Be2 and Be3.

Uppermost continental rise unit (Be1):

A change from the strong reflections of unit Be2 to the weaker reflections of unit Be1 above indicates a distinct change in depositional conditions (Figs. 3.3, 3.4a and b). Along profile AWI-20010001, Be1 can be seen to occur in two broad sediment depocentres, which we named Depocentre A (CDPs 10000-20000, east-west extent of approx. 125 km) and Depocentre B (CDPs 24500-38750, extent of approx. 180 km). Two channels divide Depocentre A into three sediment mounds (Figs. 3.3 and 3.4a). The lowermost part of Unit Be1 within Depocentre A shows low-amplitude reflections (Fig. 3.4a). This character changes upward to long, continuous, parallel, higher-amplitude, and smoothly undulating reflections. The uppermost 0.2 s TWT of Be1 show high-amplitude reflections and locally irregular sediment waves (e.g. CDPs 17000-19000). The ocean floor is rough, and two recent channels (CDPs 13000 and 14500) can be seen. Patches of chaotic and irregular reflections occur in a wide trough west of sediment Depocentre A (between CDP´s 19250 and 24750), dissected by rounded, listric faults (Fig. 3.4b). Unit Be1 shows a similar succession of reflections in Depocentre B (CDP´s 24750 to 28000), but they appear even more irregular, disturbed and wavy (e.g. CDP 28750) (Figs. 3.4b and c).

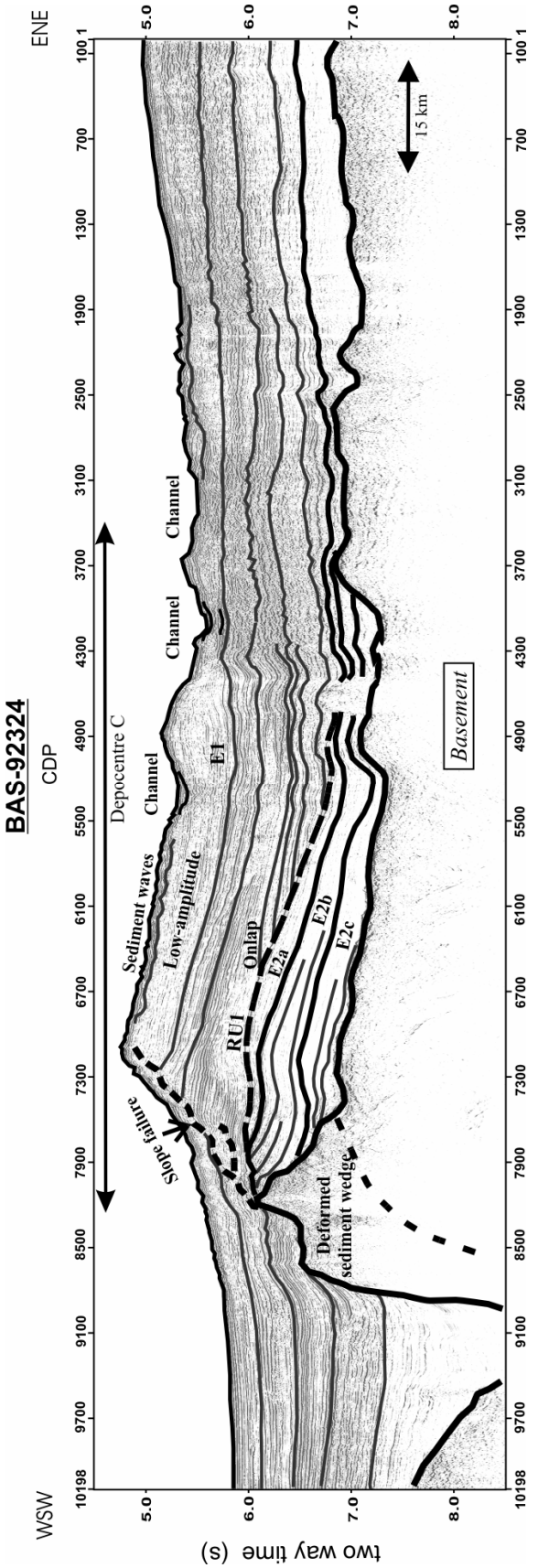

***Fig. 3.5**: Profile BAS-92324 between CDP 1 and 10200 with sediment units, modified after Cunningham et al. (2002) and Nitsche et al. (1997).*

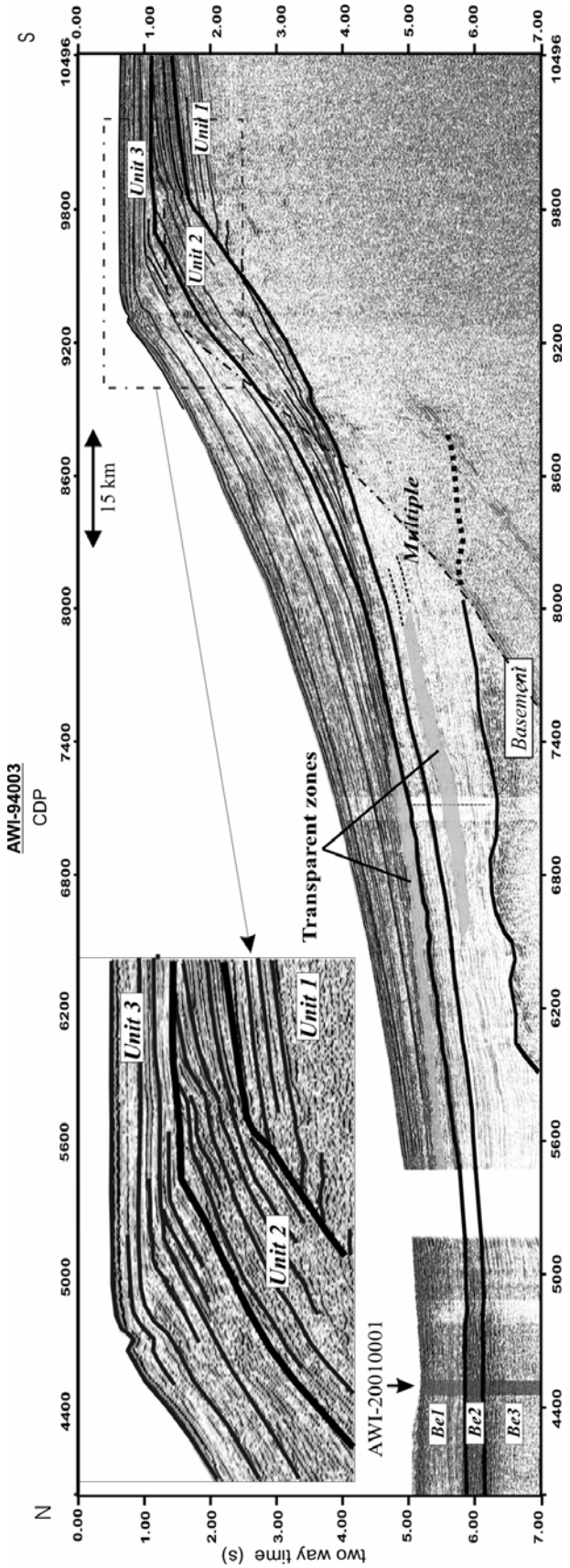

***Fig. 3.6**: Profile AWI-94003 with sediment units, Unit 1 - 3, modified after Cunningham et al. (2002) and Nitsche et al. (1997).*

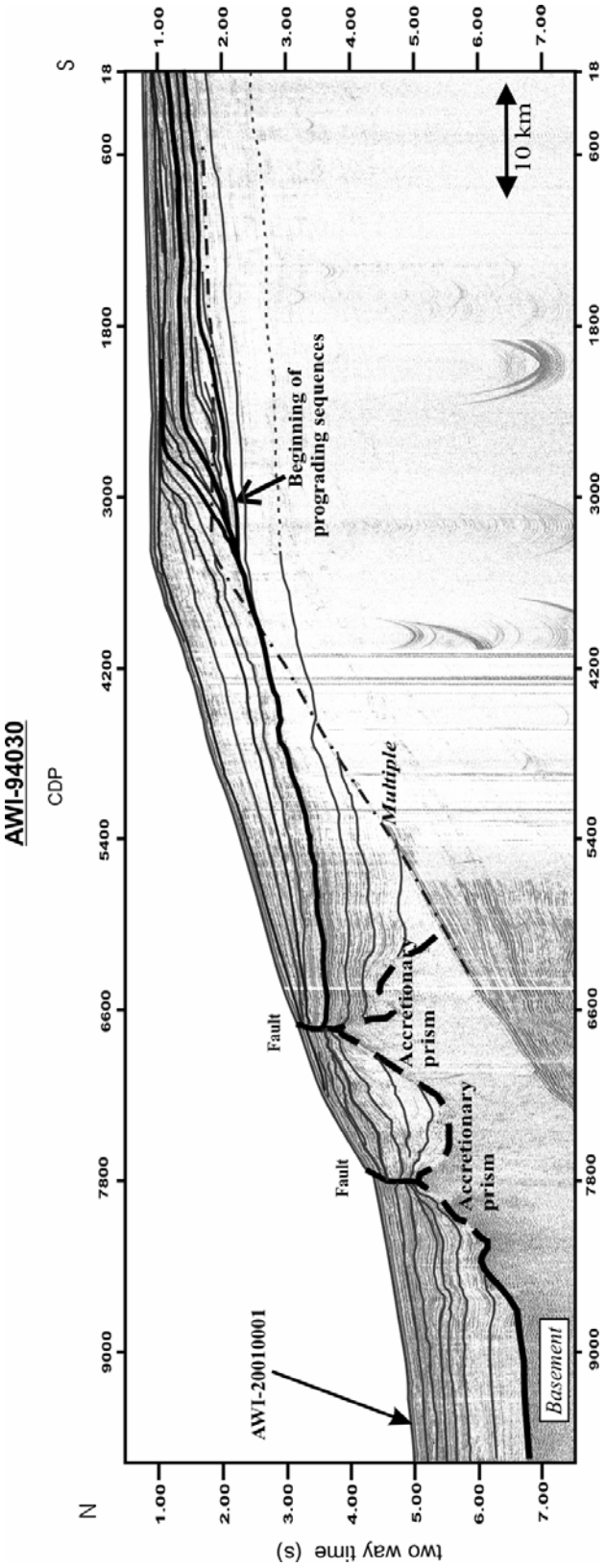

***Fig. 3.7**: Profile AWI-94030 with seismic stratigraphic sections, modified after Cunningham et al. (2002) and Nitsche et al. (1997).*

3.5.2.2 Middle section (Profiles AWI-94030, AWI 20010001)

The characteristics of the sedimentary reflections change within Depocentre B, west of approximately CDP 28000. The lowermost 0.7 – 1.0 s TWT show weak and smooth reflectivity, so that there is no clear basis for differentiation of units Be3 and Be2. The uppermost 1 – 1.5 s TWT appear more laterally variable in reflection amplitude, showing sediment bulges (CDP 34750) and buried sediment waves (between CDPs 37250 and 38750). Inside this uppermost rough section we can identify unconformities (dashed lines, Fig. 3.4c), shown by onlapping and downlapping reflectors.

The cross-slope Profile AWI-94030 serves as another seismic connection between the continental rise and shelf (Fig. 3.7). This profile reveals two acoustic basement highs on the continental slope (CDP 5700 to 8800), interpreted as the top of an accretionary wedge, and probably composed of deformed and consolidated sediments (Cunningham et al., 2002). These features are probably the source of the negative "Continental Slope Gravity Anomaly" (CSGA) between 87°W and 92°W (Fig. 3.8). We identify several sedimentary sequences on the outer shelf where the prograding character increases upwards, following Nitsche et al. (1997). The boundaries of these sequences seem to merge farther down the slope (bold line), but reflectors cannot be reliably correlated with sediment deposits on the shelf due to the acoustic basement highs and faults within the sediment sequences.

3.5.2.3 Western section (Profile 92324)

The sediments in the western section of the Bellingshausen Sea, within the domain of the BGA, are strongly affected by the underlying basement tectonics as seen on profile BAS-92324 (Fig. 3.5). An obvious sedimentary feature is a prominent unconformity, RU1, on the western side of the basement high (bold dashed line). Cunningham et al. (2002) divided the underlying sediments into three sediment units, E2a, E2b and E2c. Unit E2c consists of mostly basement-parallel reflectors and onlaps the crest of the basement high. All three units thin out to the east whereas Units E2b and E2a are truncated by RU1 to the west. This gently eastward dipping unconformity is characterised by onlap of the overlying reflectors, but it does not continue east of CDP 5000.

3.6 Discussion

3.6.1 Tectonic implications

Studies of magnetic seafloor spreading anomalies on the continental margin of the Bellingshausen Sea define basement ages ranging from 30 Ma northwest of Alexander Island (Larter and Barker, 1991a) to 45 Ma in the Bellingshausen Sea at about 87°W (McCarron and Larter, 1998) (Fig. 3.8). The basement step at CDP 11900 on Profile AWI-20010001 seems to coincide with a change in basement age from about 39 Ma (chron 18) in the east to about 47 Ma (chron 21) in the west (Figs. 3.3 and 3.8), if chron 18 is accurately extrapolated from

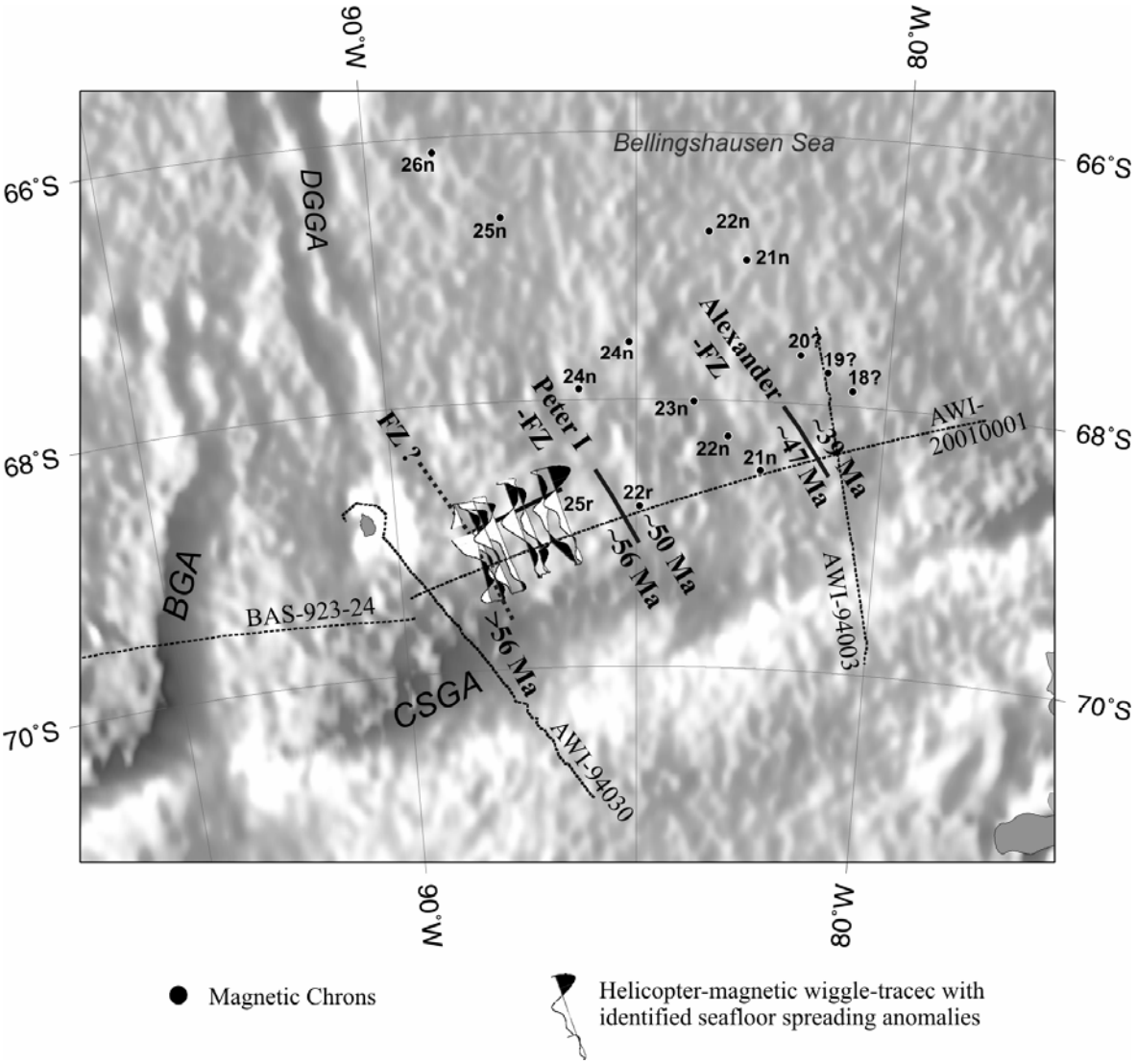

Fig. 3.8: *Illuminated satellite-derived gravity anomaly map (McAdoo and Laxon, 1997) of the Bellingshausen Sea margin with isochrons identified from several cruises´ ship-magnetic data and helicopter-magnetic data: The anomaly identifications 22n and 21n in the northwest are from a profile collected by R/V Nathaniel B Palmer 9308 (2003), which we obtained from the National Geophysical Data Center GEODAS database (available online at http://www.ngdc.noaa.gov/mgg/gdas/gd_sys.html). The anomaly identifications to the southeast marked with question marks (20n – 18n) are from a R/V Hakurei-Maru (1981) profile first published by Kimura (1982). Our interpretation of this profile is different from that published by Kimura. We interpret the anomaly he labelled as 20 as 18n. The two lines of anomaly identifications from 26n to 21n and from 24n and 22r were acquired by USNS Eltanin 42 in 1970. A synthetic magnetic anomaly profile justifying the interpretation of the anomalies on the first of these two lines is included in McCarron and Larter (1998). The helicopter-magnetic wiggle plots in the eastern Bellingshausen Sea were produced from tracks flown during a R/V Polarstern cruise in 2001.*

observed anomalies further northeast along the paleo-subduction zone. We interpret this basement step as a fracture zone (FZ), here named the Alexander FZ, although a clear identification in the satellite-derived gravity anomaly field is not possible. Another basement offset occurs at CDP 25000, with its eastern side elevated by about 0.5 s TWT. We suggest that this step may also have formed at a FZ, here named Peter I FZ (in reference to Kimura, 1982), because at the margin it separates anomaly 22r (50 Ma) in the east from anomaly 25r (56 Ma) in the west. The Alexander and Peter I FZs were previously interpreted as extensions of the Heezen and Tharp FZs, respectively (Barker et al., 1982). However, the Heezen and Tharp FZs were formed at the Pacific-Antarctic ridge and its precursor, the Pacific-Bellingshausen ridge, whereas the Alexander and Peter I FZs were formed in the Antarctic-Phoenix spreading system (e.g. Larter et al., 2002). Other basement offsets occur at CDPs 16250 and 37000, but magnetic data are to sparse to be able to say if they are related to FZs as well.

Basement ages west of the Peter I FZ, within the suggested Charcot plate fragment, remain uncertain due to a lack of reliable magnetic data. However, the lowermost sediments on the eastern part of profile BAS-92324 (CDP´s 2100 and 4000) onlap uplifted basement segments, indicating tectonic movements prior to sedimentation (Fig. 3.5). The unconformity RU1 on the eastern side of the BGA, and the lowermost, slightly elevated, sediments above the unconformity indicate post-sedimentary movements on this eastern side of the BGA, which represented a zone of convergence between 79 Ma and 61 Ma (e.g. Gohl et al., 1997; Larter et al., 2002; Eagles et al. 2004a; Eagles et al., 2004b;). If we assume that the unconformity formed at the end of uplift along the BGA at around 61 Ma (e.g. Cunningham et al., 2002), the sediments beneath this unconformity must be older than 61 Ma. It is possible that the westward thickening of the minor sedimentary units E2a, E2b and E2c (Cunningham et al., 2002) indicate a slightly westward dipping orientation of the basement before the uplift. The occurrence of three different minor units may indicate several phases of tectonic movements along the BGA (e.g. Eagles et. al., 2004b). Alternatively, it cannot be excluded that bottom currents and climate changes might have been responsible for the differing reflection characteristics and deposition rates of these minor units.

3.6.2 Sedimentation processes

3.6.2.1 Geometric expression

Based on satellite-derived predicted bathymetry (Smith and Sandwell, 1997, Fig. 3.1) and seismic profiles (Figs. 3.3 and 3.5) we identified three sediment depocentres on the continental margin of the Bellingshausen Sea, lying in front of three shelf edge lobes. We refer to these as Depocentres A, B and C, from east to west (Fig. 3.9). Channels dissect Depocentre A into three minor sediment mounds that do not show the typical characteristics of sediment drifts as those observed along the western Antarctic Peninsula. Depocentre B is the broadest and lies in front of a seafloor depression on the continental shelf indicated by bathymetric ship track data (Fig. 3.9) and verified by multibeam echo soundings surveys on the outer shelf (Larter et al., 2004; Ó Cofaigh et al., 2005). Depocentre C lies over uplifted basement along the BGA lineation and constitutes a large asymmetric sediment mound with an east-west extent of about 100 km. This mound has been interpreted as a sediment drift, characterized by a steep western and a gentle

eastern side, and two recent channels are observed on its gentle side (e.g. Nitsche et al., 1997). This entire depositional geometry on the continental rise of the Bellingshausen Sea is different to that on the adjacent Antarctic Peninsula margin where continental rise deposits developed as several discrete sediment mounds and drifts that are clearly separated by erosional channels (e.g. Rebesco et al., 1997, 2002).

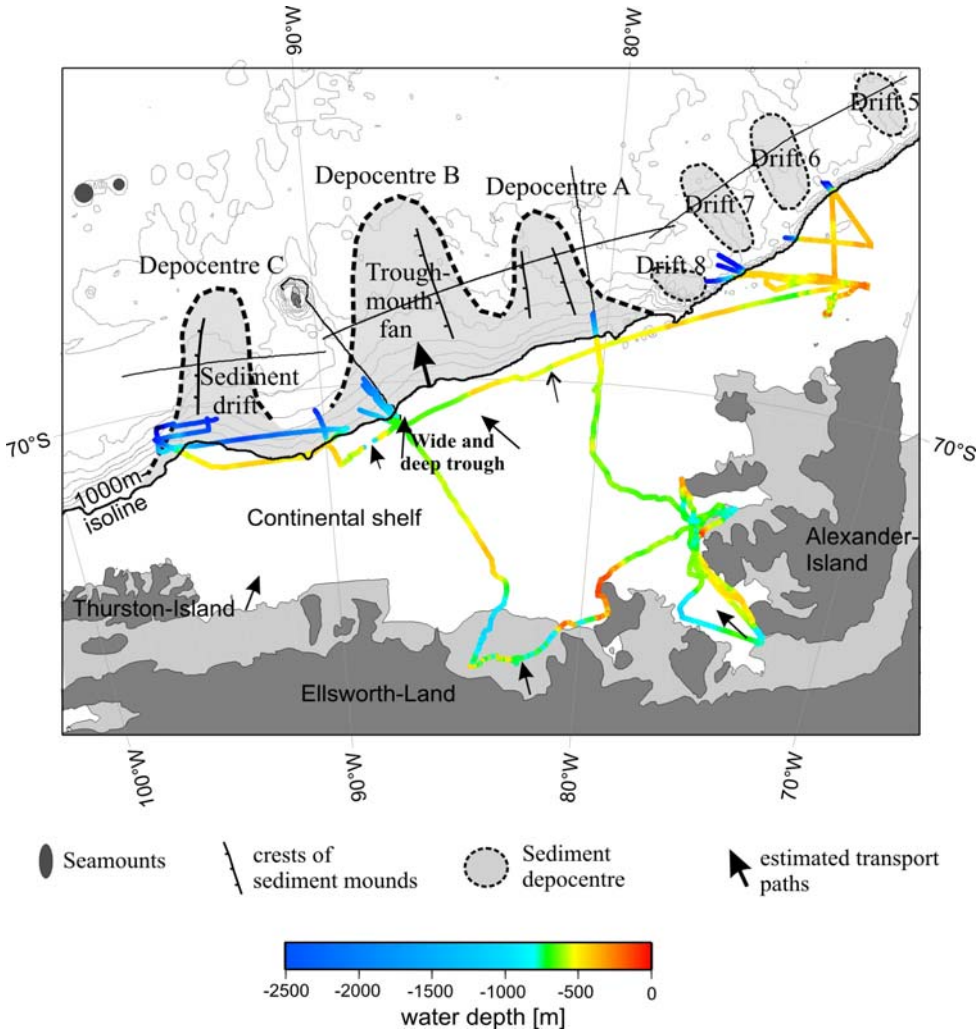

Fig. 3.9: *Schematic model of sediment transport processes along the continental margin of the Bellingshausen Sea. Sparse bathymetric ship track data over the wide continental shelf between Alexander Island and Thurston Island, acquired on RV Polarstern cruises in 1994 and 2001, reveal depressions that may be parts of major cross-shelf glacial transport pathways. They show a broad trough in front of sediment Depocentre B, with water depths of up to 680 m in the centre and about 450 m at the rim. The existence of this trough is confirmed by additional bathymetric data recently collected on RRS James Clark Ross (Ó Cofaigh et al, 2005) and is consistent with our interpretation of Depocentre B being a wide deep-sea trough-mouth fan. A further, but shallower, outer shelf depression was observed farther northeast along the shelf-edge in front of sediment Depocentre A and may indicate the presence of a further, smaller glacial trough. The locations of the sediment drifts along the Antarctic Peninsula are schematically adopted from Rebesco et al (2002).*

3.6.2.2 Nature of sedimentary units

The correlation between continental rise- and shelf deposits via profile AWI-94003 and different seismic reflection characteristics of units Be1, Be2 and Be3 shows different sediment accumulation patterns, suggesting changes of sediment supply processes. We assume a mainly turbiditic origin for the lowermost continental rise unit Be3, following the interpretation, of "Pre-drift"- and "Drift-growth" stages along the western Antarctic Peninsula by Rebesco et al. (1997). On the continental rise, the sediments infill low lying areas first and onlap onto basement topography, which is typical for turbidites. Furthermore, Early Miocene sediments, recovered in the deepest cores at DSDP Site 235, are primarily mostly terrigenous (Hollister et al., 1976).

The seismic characteristics of the outer shelf units, Unit 2 and Unit 3 (Fig. 3.6), appear similar to the sediment sequence groups S3 - S2 and S1, respectively, which were established on the continental shelf of the western Antarctic Peninsula (e.g. Larter and Cunningham, 1993; Larter et al., 1997; Barker et al., 1999). Results from site 1097 of ODP Leg 178 show glacial influences as ice rafted till in S1, S2 and the upper part of S3 (e.g. Barker and Camerlenghi, 2002). The similarities of seismic reflection characteristics between S2 and Unit 2, and S1 and Unit 3, suggest glacial sediment transport during deposition of Unit 2 and Unit 3 and their correlating units Be2 and Be1 on the continental rise. Furthermore, Unit 2 and Unit 1 resemble the Type IA sequence, as defined by Cooper et al. (1991) which was interpreted to have been influenced by glacial erosion and transport processes. However, erosional truncations of prograding foresets are rarely seen within Unit 2, which may indicate ice expansion without a strong erosional effect on the outer continental shelf. One possible origin of the strong acoustic impedance contrasts in Be2 is the presence of extensive slide/debris flow deposits interbedded with fine grained hemipelagic sediments. The question of whether or not the base of Be2 represents the time of the first advance of grounded ice to the shelf edge remains open.

We think that the truncating unconformity beneath the outer shelf, between Unit 2 and Unit 3 (Fig. 3.6) most likely represents a strong erosional advance of grounded ice to the shelf edge, but we cannot define this as the first advance or advances of grounded ice to the shelf edge, because it could have removed evidence of previous ice advances. The onset of grounded ice events on the West-Antarctic continental shelf is still the subject of controversy and cannot be clarified in this study. However, we think that the change to strongly prograding units as shown by the Unit 2/Unit 3 boundary probably represents an important change in glacial dynamics that led to more strongly erosional ice advances. The boundary between units Be2 and Be1 coincides with a distinct buried acoustic reflector identified over a wide area on the Bellingshausen Sea continental rise by Tucholke and Houtz (1976) on *Eltanin-42* single channel data (track shown in Fig. 3.1), which demonstrates the regional extend of this boundary. Tucholke and Houtz named this reflector Horizon S. Comparison with data from other parts of the Antarctic continental slope and rise shows similar variations of seismic reflection characteristics from stratified units in the deeper part of a section to faulted reflections, channel levee complexes and other products of gravity driven processes in the upper part, as seen between Be2 and Be1. This change of seismic pattern is related to glacial erosion due to glaciation on the continental shelf (e.g. Hampton et al., 1987; Miller et al., 1990b; Larter and Cunningham, 1993; Anderson, 1999).

The slightly decreasing progradation in the uppermost 0.3 s TWT of the outer shelf unit, Unit 3 (Fig. 3.6), is observed in the uppermost prograded sediments in many lines across the Antarctic Peninsula margin and elsewhere around Antarctica (e.g. Cooper et al., 1991; Bart and Anderson, 1995; Larter et al., 1997). Besides changes in climate and ice regime, a further influence on this change of progradation may be the fact that the most easily eroded sediment material is removed from the shelf by the first glaciations, leaving each subsequent glaciation with a deeper middle shelf and a more consolidated substrate. In this way, it is to be expected that erosion rates, and therefore sediment production rates, will decline with time given a sequence of glacial advances of similar magnitude. A statement on the frequency of ice advances over the continental margin of the Bellingshausen Sea is not possible with available data because the nearest age control comes from drilling at ODP Leg 178 on the western Antarctic Peninsula margin (Fig. 3.1).

3.6.2.3 Age of sediment units

Direct correlation of the continental rise units Be1 – Be3 with those of seismic profile I95-130 (of the Italian Programma Nazionale di Ricerche in Antartide, PNRA), recorded along the western Antarctic Peninsula, shows distinct differences in seismic stratigraphic pattern (Figs. 3.1 and 3.3) from which it is possible to infer differences in sediment supply and deposition on the Bellingshausen Sea and western Antarctic Peninsula margin. The units on the continental rise of the western Antarctic Peninsula were dated and classified by Rebesco et al. (1997 and 2002) by correlation with ODP-sites from Leg 178 and one DSDP-site from Leg 35. The authors defined six stratigraphic units, numbered M1 to M6 from the seafloor down (Fig. 3.3). Units M6 (36-25 Ma) and M5 (25-15 Ma) were defined as a “Pre-drift Stage” and constitute turbiditic hemipelagic/pelagic, non-glacial sediments. Units M4 (15-9.5 Ma) and M3 (9.5-5.3 Ma), whose development was influenced by bottom currents, were ascribed to a “Drift growth Stage”. The Units M2 (5.3-3.0) and M1 (3.0 Ma to the present) were interpreted as a “Drift maintenance Stage”, showing mixed influence of bottom currents and glacial sediment transport. The westward continuation of sediment units M1-M6 on profile AWI-20010001 is not advisable due to the differences of the two sediment classification schemes. However, we can estimate the ages of units Be1 – Be3 by correlating them with the units M1-M6. The correlation shows that the base of unit Be2 lies about 0.1 s TWT deeper than the base of Unit M3 (Fig. 3.3), interpreted as the base of mainly glacially derived sediment (Rebesco et al., 1997), and dated at 9.5 Ma using magnetostratigraphic data from ODP site 1095 (Iwai et al., 2002). Thus, discontinuous glacial sediment transport to the continental rise, which we infer to have produced Be2, started prior to 9.5 Ma. This conclusion is consistent with the result from ODP site 1095, where the base of glacially transported sediments was not reached and the oldest recovered material is dated at 9.6 Ma (Barker and Camerlenghi, 2002). The boundary between Be1 and Be2 coincides with the base of Unit M2, dated at 5.3 Ma (Iwai et al., 2002). With respect to our interpretation of the corresponding Unit2/Unit3 boundary on the outer continental shelf, we infer that the unit Be1/Be2 boundary indicates an increased sediment supply to the slope and rise due to grounded ice advances in the early Pliocene**.**

The change of seismic reflection characteristics west of approximately CDP 28000 of profile AWI-20010001 can be explained by changing down-slope sedimentation processes. The

acoustic basement highs along the continental slope acted as a barrier to the downslope sediment supply, as seen on Profile AWI-94030 (Fig. 3.7) and led to discontinuous sedimentation between the continental shelf and rise. This results in different sediment accumulation patterns, compared to the eastern section of the Bellingshausen Sea continental rise. The unconformities in the upper western part of profile AWI-20010001 (dashed lines, Figs. 3.3 and 3.4c) may be caused by changing patterns of downslope sediment deposition, for example in response to changes in sediment input, slope instability or bottom currents. Due to the discontinuity of reflectors across CDP 28000, it is difficult to estimate the ages of sediment units identified on profile BAS-92324 (Fig. 3.5). Only the prominent unconformity, which may record the end of an uplift phase at the BGA at about 61 Ma (e.g. Cunningham et al., 2002) constitutes a datable reflector. The sediments above the unconformity must therefore constitute the entire sediment deposition of the last 61 m.y. but a reason for the lower sedimentation rate is not obvious from available data.

3.6.2.4 Sediment deposition rates

Estimates of sediment deposition rates in the depocentres provide the opportunity to evaluate their respective glacial-derived sediment supplies and compare these to other sediment depocentres on the Antarctic continental rise. In order to roughly estimate the sediment deposition rates of units Be1, Be2 and Be3, we calculated sediment thicknesses at two locations on profile AWI-20010001 using the empirical travel-time versus depth relation of Carlson et al. (1986). We chose positions at CDPs 16500 and CDP 27400, at the crests of sediment Depocentres A and B because of their great sediment thicknesses (Fig 3.3). The results are very high sedimentation rates for Be1, with values of 247 m/m.y. (CDP 16500) and 295 m/m.y. (CDP 27500), in contrast to sedimentation rates in Be2 (112 m/m.y.) and Be3 (21 m/m.y. and 13 m/m.y.) (Tab. 1). In comparison, the highest known sedimentation rate on the western Antarctic Peninsula rise is about 180 m/m.y. in the early Pliocene (mainly Unit M2), calculated on the basis of magnetobiochronologic data from ODP site 1096 (Iwai et al., 2002). The low sedimentation rates of Be2 and Be3 are less then those of their equivalent units (M3, M4, M5, M6) farther north-east on the western Antarctic Peninsula margin (Rebesco et al., 1997). The difference could be explained by a low rate of erosion prior to Pliocene times in the source area onshore. The BEDMAP compilation of subglacial topography (Lythe et al., 2000) shows that a large part of the subglacial rock surface in Ellsworth Land is below sea level. If the situation in the early Tertiary was similar, this area is unlikely to have been a significant source of eroded sediment material supplied to the continental margin. In contrast, the axis of the Antarctic Peninsula is a plateau, with peaks higher then 2000 m, and thus a more likely site for ice sheet nucleation during the Miocene and a more plentiful source of eroded sediment material.

High sedimentation rates within unit Be1 may be associated with development of very large ice drainage basins, high erosion rates on- and offshore, and high ice flow velocities during the Pliocene and Quaternary. Furthermore, the great width of the continental shelf (up to 480 km west of Alexander Island) may have led to increased glacial basal erosion and entrainment of sedimentary material due to the long transport distance. Sparse physiographic information about the Bellingshausen Sea continental shelf make estimates about transport paths during

advances of grounded ice difficult. However, we assume that the western shelf trough indicated by swath bathymetry and sub-bottom profiler data in front of sediment Depocentre B (Fig. 3.9) acted as a major transport path for glacial sediment transport to the shelf edge. The cross-slope profile AWI-94030 shows that Depocentre B is not separated from the margin, but is in fact the lower part of a very uniform, low-angle, prograded slope (Fig. 3.7). These are typical characteristics of a trough mouth fan. Our estimation of a very high sediment deposition rate of unit Be1 and the structure and enormous width of Depocentre B support the interpretation of a trough mouth fan which seems to have been active in Pliocene and Quaternary times.

Although our calculations are crude approximations to sedimentation rates, the results nonetheless indicate a trend of increasing sediment accumulation rates since the early Pliocene. Conversely, ODP drilling on the continental margin of the western Antarctic Peninsula (Leg 178) indicate increasing deposition rates in the Late Miocene (base of unit M3) and a decrease in the Pliocene (base of unit M2, after Rebesco et al., 1997) (e.g. Iwai et al., 2002). This shows a remarkable difference in time of onset of high sediment deposition rates, which implies differences in the timing of the first erosional advance of grounded ice and, thus, variations of the glacial regime between the western Antarctic Peninsula - and the Bellingshausen Sea continental margin. Further evaluations which could explain these differences in glacial development are not possible with existing data, but a complex history of multiple glacial advances and retreats in the Bellingshausen Sea can be inferred based on the presence of several thick prograding and aggrading sequence groups beneath the outer shelf as shown on Profile AWI-94030 (Fig. 3.7).

Table 1:

CDP	Unit	TWT [s]	Compacted thickness [s]	Sub-bott. depth [m]	Compacted tickness [m]	Age [Ma]	Sediment deposition rate [m/m.y.]
16500	**Be1**	1.35	1.35	1310	1310	5.3	**247**
	Be2	1.70	0.35	1770	460	9.6	**106**
	Be3	2.20	0.50	2550	780	47	**21**
27400	**Be1**	1.55	1.55	1560	1560	5.3	**295**
	Be2 and 3	2.00	0.45	2220	660	56	**13**

Sediment depths, thicknesses and accumulation rates as estimated from the empirical travel-time versus depth relations for deep-sea sediments from Carlson et al. (1986). Depth (in km) is calculated as $Z = -(3.03 \pm 0.24) \ln [1-(0.52 \pm 0.04) T]$ *where T is two-way travel-time in s.*

3.6.2.5 Faults in Unit Be1

Various processes may account for the structures in unit Be1 that resemble faults and listric shear planes, mainly observed between sediment Depocentres A and B (between CDPs 19000 and 28000) on profile AWI-20010001 (Fig. 3.4b). We suppose that these features are the product of complex interactions between depositional processes and slope instability. The high

sedimentation rate could have led to a high pore-water content, which was expelled during diagenesis. A further important diagenetic process may have been the transformation of opal-A to opal-CT, as observed at sites 1095 and 1096 of ODP-Leg 178 (Volpi et al., 2003). Local differential compression and compaction affected the sediment pile's stability. This process may have resulted in stress-discharge of sediments to the sides of the sediment depocentres and in the development of faults. The fault between CDPs 19000 and 21000 may have developed along the migrating locus of a facies boundary between the parallel layered sediments that accumulated on Depocentre A and a more chaotic regime on its steep western flank. At about CDP 24500, we can see the influence of basement structure on the stability of the upper sediments. Here, the crest of a basement high seems to act as a vertical wedge that amplifies the instability of the overlying sediments due to differential strain. Similar patterns have been observed in inter-drift areas along other Antarctic continental margins, such as along the western Antarctic Peninsula (e.g. Rebesco et al., 1997; Volpi et al., 2003) and in the Weddell Sea (e.g. Michels et al., 2002). Additional parallel seismic and bathymetric data are required to verify our suppositions concerning the occurrence of these faults.

3.7 Conclusions

This paper provides new constraints on the tectonic and large scale sedimentary architecture of the largely unexplored continental rise of the Bellingshausen Sea, mainly based on multi-channel seismic data. This study provides the following conclusions:

1) The basement structure on the continental rise permits the identification of tectonic fracture zones. At least two fracture zones (Alexander and Peter I FZs) and the ages of four spreading corridors can be estimated from seismic and magnetic data.

2) The sediment deposits in the middle part of the continental rise in the study area show distinct vertical variations in reflectivity characteristics. We divided the deposits into three sedimentary units, Be1 – Be3, based on a correlation between the continental rise and the outer shelf via on cross-slope profile. On the continental rise, these three units can be correlated with stratigraphic Units M1-M6, identified on along-slope profiles on the western Antarctic Peninsula margin. Based on these correlations we infer:

The lowermost sedimentary unit, Be3, is older than 9.5 Ma. It probably consists of predominantly turbiditic sediments and the estimated sediment accumulation rate was low (up to 21 m/m.y.).

The intermediate sedimentary unit, Be2, was developed between about 9.5 Ma and 5.3 Ma and can be correlated with an intermediate prograding sedimentary unit on the shelf edge. We assume that unit Be2 mainly consists of sediments transported by ice advances on the continental shelf, but without strong erosion of the shelf surface. The sediment accumulation rate is estimated to be up to 112 m/m.y.

The age of the uppermost sedimentary unit, Be1, ranges from about 5.3 Ma up to present. We interpret this unit as consisting predominantly of terrigenous sediment transported across the shelf edge by strongly eroding grounded ice on the shelf, as shown by strong truncations of

underlain foresets and strong progradation. An approximate sediment accumulation rate of around 295 m/m.y. is the highest known on the west Antarctic margin.

3) The high sediment deposition rate of unit Be3 implies an increase of sediment supply to the continental rise due to frequent advances of grounded ice on the continental shelf in the Pliocene and Quaternary, which is contrary to a decrease of the sediment deposition rate since Pliocene times on other sites of the Antarctic continental margin. The reason for this discrepancy remains unclear.

4) Two wide and previously unsurveyed sediment depocentres are identified on the continental margin of the Bellingshausen Sea. We name them Depocentre A in the east and Depocentre B in the west, and we show that they have developed in Pliocene and Quaternary times. Depocentre B is interpreted as a trough mouth fan and may constitute the main discharge area for glacially-derived sediment material.

5) We interpret faults and listric shear planes inside unit Be1, mainly observed between the two sediment Depocentres A and B, as the products of complex interactions between depositional processes and slope instability, reflecting the variability of sediment stability along the continental rise.

6) In the western Bellingshausen Sea, the characteristics of seismic reflections changes entirely. Two along-slope orientated acoustic basement highs acted as barriers to sediment material supplied from the shelf, leading to a change in the conditions of sediment transport and deposition. The only clue to estimation of sediment ages west of 87° W is a prominent unconformity, identified on the elevated eastern side of a basement trough along the BGA. The unconformity is assumed to have developed at the end of tectonic uplift that occurred there around 61 Ma. The orientation of three westward thickening sedimentary minor units beneath the prominent unconformity may indicate a slightly westward dipping orientation of the basement before the uplift along the BGA.

Finally, we must emphasise that our interpretations in this paper about tectonic features and sediment deposits are mainly based on only one along-slope and one cross-slope seismic profile. To verify our conclusions and to improve knowledge about the tectonic and sedimentation history in the Bellingshausen Sea additional geophysical and geological investigations are required.

Acknowledgements

We are grateful to the masters, officers and crews of RV *Polarstern* and RRS *James Clark Ross*. This study is partly funded through grant no. GO 724/3-1 of the Deutsche Forschungsgemeinschaft (DFG). Italian contribution is supported by SEDANO and MAGICO projects of the Italian Programma Nazionale di Ricerche in Antartide (PNRA).

REFERENCES

Anderson, J.B., 1999. Antarctic Marine Geology. Cambridge Univ. Press, 289pp

Anderson, J.B., Wellner, J.S., Lowe, A.L., Mosola, A.B., Shipp, S.S., 2001. The footprint of the expanded West Antarctic Ice Sheet: ice stream history and behaviour. GSA Today, 11, 4-9.

Barker, P.F., 1982. The Cenozoic subduction history of the Pacific margin of the Antarctic Peninsula: ridge crest interactions. J. Geol. Sci., 139, 787-801.

Barker, P.F., Camerlenghi, A., 2002. Glacial history of the Antarctic Peninsula from Pacific margin sediments, in: Barker, P.F., Camerlenghi, A., Acton, G.D., Ramsay, A.T.S. (Eds.), Proc. ODP, Sci. Results 178 [online]. Available from World Wide Web: <http://wwwodp.tamu.edu/publications/178_SR/synth/synth.htm>.

Barker, P. F., Camerlenghi, A., Acton, G.D. et al., 1999. Proc. ODP, Init. Repts., 178 (CD-ROM). Available from: Ocean Drilling Program, Texas AandM University, Collage Station, TX 77845-9547, USA.

Bart, P. J., Anderson, J. B., 1995. Seismic record of glacial events affecting the Pazific margin of the northwestern Antarctic Peninsula, in: Cooper, A. K., Barker, P. F., Brancolini, G. (Eds.), Geology and seismic stratigraphy of the Antarctic margin. Antarctic Research Series, Vol. 68. American Geophysical Union, Washington, DC, 75-95.

Birkenmajer, K., 1991 Tertiary glaciation in the South Shetland Islands, West Antarctica: evaluation of data, in: Thomson, M.R.A., Crame, J.A., Thomson, J.W. (Eds.), Geological Evolution of Antarctica. Cambridge University Press, Cambridge, 629-632.

Carlson, R. L., Gangi, A. F., Snow, K. R., 1986. Empirical reflection travel time versus depth and velocity versus depth functions for the deep sea sediment column. J. Geophys. Res., 91, 8249-8266.

Cooper, A. K., Barrett, P., Hinz, K., Traubea, V., Leitchenkov, G., Stagg, H., 1991. Cenozoic prograding sequences of the Antarctic continental margin: a record of glacioeustatic and tectonic events. Marine Geology, 102, 175-213.

Cunningham, A. P., Larter, R. D., Barker, P. F., Gohl, K., Nitsche, F.-O., 2002. Tectonic evolution of the pacific margin of Antarctica: 2. Structure of Late Cretaceous-early Tertiary plate boundaries in the Bellingshausen Sea from seismic reflection and gravity data. J. Geophy. Res., 107, NO. B12., 2346. doi: 10.1029/2002JB001897

Cunningham, A. P., Larter, R. D., Barker, P. F., 1994. Glacially prograded sequences on the Bellingshausen Sea continental margin near 90°W. Terra Antarctica, 1, 267-268.

DeSantis, L., Anderson, J. B., Brancolini, G., Zayatz, I., 1995. Seismic record of late Oligocene through Miocene glaciation on the central and eastern continental shelf of the Ross Sea. Antarctic Research Series, 68, 235-260.

Dingle, R.V., Lavelle, M., 1998. Antarctic peninsular cryosphere: early Oligocene (c. 30 Ma) initiation and revised glacial chronology. J. Geol. Soc., 155, no.3, 433-437.

Dowdeswell, J.A., Ó Cofaigh, C., Pudsey, C.J., 2004a. Thickness and extent of the subglacial till layer beneath an Antarctic paleo-ice stream. Geology. 32, 13-16.

Dowdeswell, J.A., Ó Cofaigh, C., Pudsey, C.J., 2004b. Continental slope morphology and sedimentary processes at the mouth of an Antarctic palaeo-ice stream. Marine Geology. 204, 203-214.

Eagles, G., Gohl, K., Larter, R. D., 2004b. High resolution animated tectonic reconstruction of the South Pacific and West Antarctic margin. Geochemistry, Geophysics, Geosystems, Vol. 5, Nr 7, 1-21.

Eagles, G., Gohl, K., Larter, R. D., 2004a. Life of the Bellingshausen plate. Geophysical Research Letters, Vol. 31, L07603

GEODAS [online]. Available from World Wide Web: <http://www.ngdc.noaa.gov/mgg/geodas/geodas.html>

Gohl, K., Nitsche, F. O., Miller, H., 1997. Seismic and gravity data reveal Tertiary intraplate subduction in the Bellingshausen Sea, southeast Pacific. Geology, 25, 371-374.

Hampton, M. A., Eittreim, S. L., Richmond, B. M., 1987. Post-breakup sedimentation on the Wilkes Land Margin, Antarctica, in: Eittreim, S. L. and Hampton, M. A. (Eds.), The Antarctic continental margin, Geology and Geophysics of offshore Wilkes Land. Circum-Pacific Council for Energy and Mineral Recourses, Earth Science Series, 5A, 75-89.

Hollister, C. D., Craddock, C., et al. 1976. Initial reports of deep sea drilling project, 35. U. S. Government Printing Office, Washington D. C., 929 pp.

Iwai, M., Acton, G. D., Lazarus, D., Osterman, L. E., Williams, T., 2002. Magnetobiochronologic synthesis of ODP Leg 178 rise sediments from the Pacific sector of the Southern Ocean: Sites 1095, 1096 and 1101, in: Barker, P. F., Camerlenghi, A., Acton, G. D., Ramsay, A. T. S., (Eds.), Proc. ODP, Sci. Results, 178, 1-40 [CD-Rom].

Kimura, K., 1982. Geological and Geophysical Survey in the Bellingshausen Basin, off Antarctica. Antarctic Record, 75, 12-24

Larter, R. D., Cunningham, A. P., 1993. The depositional pattern and distribution of glacial-interglacial sequences on the Antarctic Peninsula Pacific margin. Marine Geology, 109, 203-219.

Larter, R. D., Barker, P. F., 1991. Effects of ridge crest-trench interaction on Antarctic-Phoenix spreading: Forces on a young subducting plate. J. Geophys. Res., 96, 19583-19608, 2345. doi: 10.1029,2000JB000052.

Larter, R.D., Dowdeswell, J.A., Pudsey, C.J., Evans, J., Hillenbrand, C.-D., Morris, P., Ó Cofaigh, C., 2004. Investigations of a major palaeo-outlet of the West Antarctic Ice Sheet in the southern Bellingshausen Sea: preliminary results from RRS James Clark Ross Cruise JR104, Terra Nostra, Schriften der Alfred-Wegener_Stiftung 2004/4, SCAR Open Science Conference Abstract Volume, 252.
http://www.scar28.org/SCAR/SCARmeeting/Wednesday/PDF/S_11_oral.pdf

Larter, R. D., Cunningham, A. P., Barker, P. F., Gohl, K., Nitsche, F.-O., 2002. Tectonic evolution of the pacific margin of Antarctica: 1. Late Cretaceous tectonic reconstructions. J. Geophys. Res., 107, NO. B12.

Larter, R. D., Cunningham, A. P., Barker, P. F., Gohl, K., Nitsche, F.-O., 1999. Structure and tectonic evolution of the West Antarctic continental margin and Bellingshausen Sea. Korean J. Polar Res., 10, 125-133.

Larter, R. D., Rebesco, M., Vanneste, L. E., Gambôa, L. A. P., Barker, P. F, 1997. Cenozoic tectonic, sedimentary and glacial history of the continental shelf west of Graham Land, Antarctic Peninsula, in: Cooper, A. K., Barker, P. F. (Eds), Geology and Seismic

Stratigraphy on the Antarctic Margin, Part 2. American Geophysical Union, Antarctic Research Series 71, American Geophysical Union, Washington, DC, pp. 1-27.

Lythe, M. B., Vaughan, D. G., BEDMAP Consortium, 2000. BEDMAP – Bedtopography of the Antarctic, scale 1:10,000,000. Brit. Antarct. Surv., Cambridge, U.K. Available from World Wide Web: <http://www.antarctica.ac.uk/aedc/bedmap/database/>

McAdoo, D.C. and Laxon, S., 1997. Antarctic tectonics: Constraints from an ERS-1 satellite marine gravity field. Science, 276, 556-560.

McCarron, J. J., Larter, R.D., 1998. Late Cretaceous to early Tertiary subduction history of the Antarctic Peninsula. J. Geol. Soc. Lond., 155, 255-268.

McGinnes, J. P., Hayes, D. E., Driscoll, N. W., 1997. Sedimentary processes across the continental rise of the southern Antarctic Peninsula. Marine Geology, 141, 91-109.

Miller, K. G., Fairbanks, R. G., Mountain, G. S., 1987. Tertiary oxygen isotope synthesis, sea-level history and continental margin erosion. Paleoceanography, 2, 1-19.

Miller, H., Henriet, J. P., Kaul, N., Moons, A., 1990b. A fine scale seismic stratigraphy of the eastern margin of the Weddell Sea, in: Bleil, U., Thiede, J. (Eds.), Geological History of the Polar Oceans: Arctic versus Antarctic. Kluwer Academ. Publ., Boston, 131-161.

Michels, K. H., Kuhn, G., Hillenbrand, C.-D., Diekmann, B., Fütterer, D. K., Grobe, H., Uenzelmann-Neben, G., 2002. The southern Weddell Sea: combined contourite-turbidite sedimentation at the southeastern margin of the Weddell Gyre, in: Stow, D.A.V., Pudsey, C.J., Howe, J., Faugeres, J.-C., Viana, A. (Eds.), Deep-Water Contourite Systems: Modern Drifts and Ancient Series, Seismic and Sedimentary Characteristics. Spec. Publ. Geol. Soc. London. Memoirs 22, pp. 305-323.

Nitsche, F. O., Cunningham, A. P., Larter, R. D., Gohl, K., 2000. Geometry and development of glacial continental margin depositional systems in the Bellingshausen Sea. Marine Geology, 162, 277-302.

Nitsche, F. O., Gohl, K., Vanneste, K., Miller, H., 1997. Seismic expression of glacially deposited sequences in the Bellingshausen and Amundsen Seas, West Antarctica, in: Barker, P. F., Cooper, A. K. (Eds.), Geology and Seismic Stratigraphy of the Antarctic Margin: 2. Antarctic Research Series 71, American Geophysical Union, Washington, DC, pp. 95-108.

Ó Cofaigh, C., Larter, R. D., Dowdeswell, J. A., Hillenbrand, C-D., Pudsey, C. J., Evans, J., Morris, P., 2005. Flow of the West Antarctic Ice Sheed on the continental margin of the Bellingshausen Sea at the Last Glacial Maximum. J. Geophys. Res., 110, doi: 10.1029. 2005JB003619

Rebesco, M., Pudsey, C.J., Canals, M., Camerlenghi, A., Barker, P.F., Estrada, F., Giorgetti, A., 2002. Case study 27: Sediment drifts and deep-sea channel systems, Antarctic Peninsula Pacific margin, mid-Miocene to present, in: Stow, D.A.V., Pudsey, C.J., Howe, J., Faugeres, J.-C., Viana, A. (Eds.), Deep-Water Contourite Systems: Modern Drifts and Ancient Series, Seismic and Sedimentary Characteristics. Spec. Publ. Geol. Soc. London. Memoirs 22, pp. 353-371.

Rebesco, M., Larter, R. D., Barker, P. F., Camerlenghi, A., Vanneste, L. E., 1997. History of sedimentation on the continental rise west of the Antarctic Peninsula, in: Cooper, A. K., Barker, P. F. (Eds), Geology and Seismic Stratigraphy on the Antarctic Margin: 2. Antarctic Research Series 71, American Geophysical Union, Washington, DC, pp. 29-49.

Rebesco, M., Larter, R.D., Camerlenghi, A., Barker, P.F., 1996. Giant sediment drifts on the continental rise west of the Antarctic Peninsula, Geo-Marine Letters, 16, 65-75.

Smith, W. H. F., Sandwell, D. T., 1997. Global seafloor topography from satellite altimetry and ship depth soundings. Science, 277, 1956-1961.

Tomlinson, J. S., Pudsey, C. J., Livermore, R. A., Larter, R. D., Barker, P. F., 1992. Long-range sidescan sonar (GLORIA) survey of the Antarctic Peninsula pacific margin, in: Yoshida, Y., Kaminuma, K., Shiraishi, K., (Eds.), Recent progress in Antarctic Earth Science, Terra Scientific Publishing Company, Tokyo, pp. 423-429.

Troedson, A.L., Smellie, J.L., 2002. The Polonez Cove Formation of King George Island, West Antarctica: statigraphy, facies and palaeoenvironmental implications. Sedimentology, 49, 277-301.

Tucholke, B. E., Houtz, R. E., 1976. Sedimentary framework of the Bellingshausen Basin from seismic profile data, in: Hollister, C. D., Craddock, C. D. et al. (Eds), Initial Reports of the Deep Sea Drilling Project, Vol. 35, U.S. Government Printing Office, Washington, DC, pp. 197-227.

Volpi, V., Camerlenghi, A., Hillenbrand, C.-D., Rebesco, M., Ivaldi, R., 2003. Effects of biogenic silica on sediment compaction and slope stability on the Pacific margin of the Antarctic Peninsula. Basin Research, 15, 339-363.

Zachos, J., Pagani, M., Sloan, L., Thomas, E. and Billups, K., 2001. Trends, rythmus, and aberrations in global climate 65 Ma to present, Science, 292, 686-693.

CHAPTER 4

BOTTOM-CURRENT CONTROL ON SEDIMENTATION IN THE WESTERN BELLINGSHAUSEN SEA, WEST ANTARCTICA

Carsten Scheuer[1], Karsten Gohl[1] , Gleb Udintsev[2]

[1] Alfred Wegener Institute for Polar and Marine Research (AWI), Bremerhaven, Germany

[2] Vernadsky Institute of Geochemistry and Analytical Chemistry, Moscow, Russia

Re-submitted after minor revision to Geo-Marine Letters, March 2006

4.1 Abstract

A set of single channel and multichannel seismic reflection profiles provide insights into the younger Cenozoic sedimentation history on the continental rise of the western Bellingshausen Sea west and north of Peter I Island. This area has mainly been influenced by glacially controlled sediment supply from the continental shelf interacting with a westward flowing bottom current. The seismic data show changes in the symmetry and structure of a prominent sediment depocentre from south to north. Its southernmost part has the characteristics of a sediment drift but this alters northwards into a large channel-levee complex with a western levee oriented in the opposite direction to the drift in the south. This change indicates a northward decreasing influence of a westward flowing bottom contour current in the study area. The topography suggests the morphologic ridges at Peter I Island to be the main features responsible for the change in bottom current influence, acting as a barrier to the bottom current and the entrained sediment material. West of Peter I Island the eastward orientated Coriolis force remains effective in deflecting the suspended load of the turbidity currents to the west and leading to a stronger growth of the western channel-levee. Calculated sediment deposition rates based on the seismic data reveal Depocentre C to consist of younger Cenozoic material supplied by glacial transport and modified by contour currents in the western Bellingshausen Sea.

4.2 Introduction

The production of sediment along the Antarctic continental margin *is primarily controlled* by glacial processes, in particular since the late Miocene when the periodic development of large and thick ice masses on the West Antarctic continent resulted in a high sediment supply to the continental margin. Grounding ice streams transported sediment material to the continental shelf and slope, and gravity-driven processes (such as slumps, slides, debris flows and turbidity currents) caused by slope failures, tectonic stress and meltwater discharge, transferred slope deposits to the continental rise (e.g. Cooper et al. 1991; Bart and Anderson 1995; McGinnes et al. 1997, Anderson 2001). In this way a variety of large sediment mounds were formed on the

continental rise. These mounds are widespread features in the Antarctic glacimarine depositional environments, as shown by numerous studies conducted along the West Antarctic Pacific margin (e.g Hampton et al. 1987, Tomlinson et al. 1992; Larter and Cunningham 1993; Rebesco et al. 1996, 1997, 2002; Nitsche et al. 1997; Lucchi et al. 2002). The development of sediment mounds is influenced by variable interactions of turbidity currents, hemipelagic sedimentation, the Coriolis force and bottom current activity (e.g. Faugeres et al. 1999; Rebesco and Stow 2001). Current measurements conducted on the continental rise of the western Antarctic Peninsula (AP) (Camerlenghi et al. 1997) and in the vicinity of the South Shetland Islands (Nowlin and Zenk 1988) show evidence of a weak south-westward flowing bottom current following the seafloor topography. These authors interpret this deep water mass as Weddell Sea Deep Water (WSDW) outflow through topographic gaps in the South Scotia Ridge. The bottom current is consistent with the development of sediment drifts on the western AP continental rise since the late Miocene. Furthermore, finely laminated silty clays deposited during the so-called 'drift-maintenance stage' were drilled during DSDP Leg 35 (sites 325 and 324, Tucholke et al. 1976), and ODP Leg 178 (sites 1095, 1096 and 1101, e.g. Barker and Camerlenghi 2002) and can be considered as contouritic sediments.

The interaction of various transport processes is controlled by factors such as the inclination of the continental slope, slope stability, grain size of the sediment material, and the strength of the bottom current. Depending on the manner of this interaction, various characteristic types of sediment mounds are produced. Channel-related contourite drifts and separated sediment mounds are observed on the Antarctic Peninsula margin (e.g. Rebesco et al. 1997), whereas a wide trough mouth fan is identified on the continental margin in the central Bellingshausen Sea (Scheuer et al. 2006). The processes that influence sediment deposition in the vicinity of Peter I Island in the western Bellingshausen Sea are still poorly understood (Fig. 4. 1). Satellite-derived gravity maps suggest that tectonic features of the oceanic crust may have an important effect on the formation of the seafloor topography in this area. Peter I Island is a relatively young volcanic island constituting an important morphologic feature which may have shifted the path of the westward flowing bottom current and, hence sedimentation in this part of the oceanic basin. In this paper, we analyze seismic reflection data to asses the influence of morphologic and tectonic structures on the sedimentation processes. It is demonstrated that the shape, structure and distribution of sediment mounds and estimates of sedimentation rates reveal the influence on bottom currents and their long term development in the past, in response to tectonic movements, ice-sheet dynamics, and deep-water formation.

4.3 Study area

The study area is located in the western Bellingshausen Sea, south-east Pacific Ocean, on the West Antarctic continental rise. The area is characterized by a rough seafloor morphology mainly caused by tectonic activity of the oceanic crust as reflected in gravity and seismic data (Fig. 4.1a). Two major gravity lineations, the Bellingshausen Gravity Anomaly (BGA) extending NNE from the margin to approx. 68°S, and the De Gerlache Gravity Anomaly

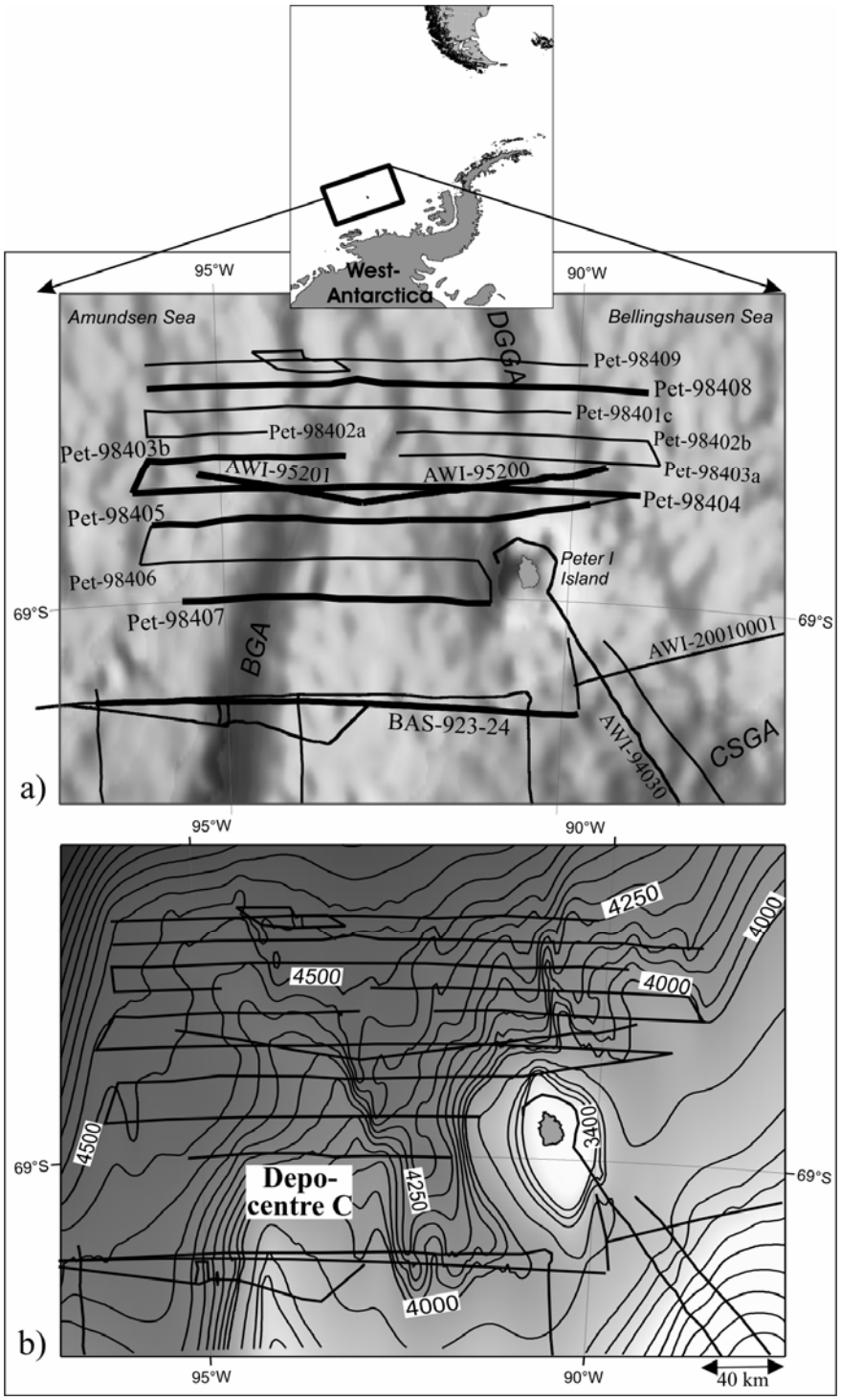

Fig. 4. 1*: a) Track chart superimposed on a satellite-derived gravity map (Smith and Sandwell 1997) of the western Bellingshausen and eastern Amundsen Sea in the vicinity of Peter I Island. Tracks of seismic profiles shown in this paper are in bold black lines. The thin black lines show other seismic profiles. Major gravity anomalies mark topographic and tectonic features (BGA = Bellingshausen Gravity Anomaly, CSGA = Continental Slope Gravity Anomaly, DGGA = DeGerlache Gravity Anomaly). b) Gridded bathymetric map of the study area derived from interpolated seismic data. The isolines show water-depths in meters.*

(DGGA), extending north from Peter I Island across the De Gerlache seamounts to approximately 62°S, mark former plate boundaries. The BGA represents the transpressional eastern boundary of the formerly independent Bellingshausen Plate (Gohl et al. 1997; Cunningham et al. 2002; Eagles et al. 2004a) which merged with the Antarctic Plate about 61 Ma. This plate boundary is characterised by a downdipping slab, a vertical basement offset of about 7 km and an accretionary sedimentary wedge (Gohl et al. 1997; Cunningham et al. 2002). The DGGA shows a tectonic scar caused by the initiation of the Phoenix-Pacific spreading ridge at about the same time (Larter et al. 2002; Eagles et al. 2004a). A set of partly exposed north-trending basement ridges underlies the DGGA (Dietmar Müller, personal communications).

The seafloor morphology is mainly characterized by two prominent topographic highs. Peter I Island, which forms the upper part of a northward-continuing seamount located approximately 400 km off the Eights Coast of the Ellsworth Land, and an elongated, northward-dipping sediment depocentre in the west (Fig. 4.1b). Water depths above the southern crest of the depocentre are around 3600 m, descending to about 4500 m in the north. Both topographic highs are separated by a south-north running valley that widens towards the north. Water depths above the valley vary from 4200 m in the south to 4600 m in the north.

4.4 Methods

The geophysical datasets used in this study were acquired during three marine expeditions (Fig. 4.1). The RV *Akademik Boris Petrov* expedition No. 29 in 1998 (Udintsev et al. 1999) resulted in the acquisition of more then 2450 km single-channel seismic (SCS) data. They represent a set of nine parallel and sub-parallel seismic lines (PET-98401c to PET-98409) north and west of Peter I Island. The data were obtained using a single seismic hydrophone. Due to technical difficulties, the data were not digitally recorded for their major part and were only made available on paper plots. We scanned the plots and vectorised the seismic traces for digital processing. As part of the process, a new trace spacing had to be implemented with interpolated coordinates. The multi-channel seismic (MCS) profiles AWI-95200 and AWI-95201 were acquired during the RV *Polarstern* cruise ANT-XII/4 in 1995 using an array of eight 3-litre airguns and a seismic streamer with an active length of 2400 m**.** Acquisition and processing of profile BAS-92324, which was acquired during a RRS *James Clark Ross* cruise in 1993, is described in Cunningham et al. (1994). For interpretation we selected five SCS profiles from the data set recorded during the RV *Boris Petrov* cruise and three MCS profiles from the RV *Polarstern* and RRS *James Clark Ross* cruises (Fig 1a, bold lines). Due to the low quality and low resolution of the SCS profiles, the basement surface and the reflections of deep sediments can be identified only in a few locations. Reflections from younger sedimentary sequences are of better quality. The distinct and continuous reflections of the MCS profiles AWI-95200 and AWI-95201 were used to constrain the analyses of the adjacent SCS lines PET-98404, PET-98403a and PET-98403b.

In order to convert the two-way-traveltime [s] of the seismic profiles into depths [m] for subsequent estimates of sediment thicknesses and deposition rates, we used the interval-velocities in the sediment analysed via processing of the MCS data. The average interval

velocity of profile ANT-95201 inside the western levee (above the unconformity LB) determinated in this way is about 1700 m/s. We adopted this velocity for estimates of the sediment thicknesses of unit E1a of the sediment drift and of the channel-levees along the other profiles.

4.5 Results

Sediment drifts and channel-levees, interbedded with other deep-water facies, are widespread features on the Antarctic continental margins due to interactions of episodic turbiditic events, along slope bottom currents and the Coriolis force. Two characteristic types of sediment mounds were identified in the study area: (1) *Channel levees* representing overspill deposits composed of fine suspended sediment associated with turbidity currents (Fig. 4.2a). These are slightly asymmetrical, the channel walls having steep slopes, the flanks shallower slopes. Along the continental margin of West Antarctica, the western levees are often higher then the eastern levees due to the Coriolis force which diverts the overspill to the left. (2) Channel-related sediment drifts characterized by a strong asymmetrical shape with a steep and a gentle side (Fig. 4.2b). The steep side often shows faults and slope failures, whereas reflections on the gentle side are rather plane and lie subparallel to parallel. In contrast to channel levees, most sediment drifts rise higher above the surrounding seafloor and are related to bottom currents that transport suspended load away from the channel. In the following, the analyzed profiles are described from south to north.

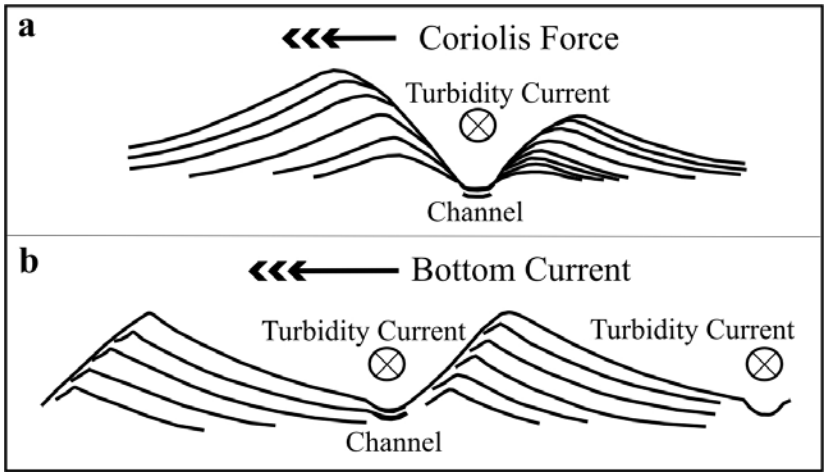

***Fig. 4.2**: Schematic illustration of two potential depositional processes on the continental rise fed by the fine fraction of suspended material coming from turbidity currents (flow direction away from the observer). a) Channel-levee deposits are controlled by the Coriolis force, or b) deposits formed by bottom-currents resulting in the development of sediment drifts (modified after Rebesco et al. 1996).*

4.5.1 Profile BAS-92324

Profile BAS-92324 (Fig. 4.3) is located closest to the continental margin. It crosses one of the largest sediment mounds (about 130 km wide and 700 m high) of the West Antarctic continental margin, referred to as Depocentre C by Scheuer et al. (2006). This mound developed on the elevated basement at the eastern side of the tectonic boundary defined by the BGA. It is characterized by a steep western and a gentle eastern side and so resembles a sediment drift. Cunningham et al. (2002) defined two major sedimentary units, unit E1 and E2, separated by unconformity RU1 (Fig. 4.3). Unit E2 is divided in subunits E2a, E2b and E2c, presenting different stages of sedimentation prior to and during uplift (Cunningham et al. 2002; Scheuer et al. 2006). Precise observations of unit E1 indicate various stages of drift development on the gentle drift side, which also makes a division into subunits E1a and E1b reasonable. Whereas unit E1b shows mainly parallel and continuous high-amplitude reflections, the reflections in unit E1a are disturbed and of weak and laterally variable amplitudes. Three recent channels have been developed on the lower end of the western, gentle side separated by sediment mounds. The middle and oldest channel, channel 2, which has a more elevated levee to the west, shows the deepest depression. The seismic reflections suggest the development of channel 2 from the base of unit E1a.

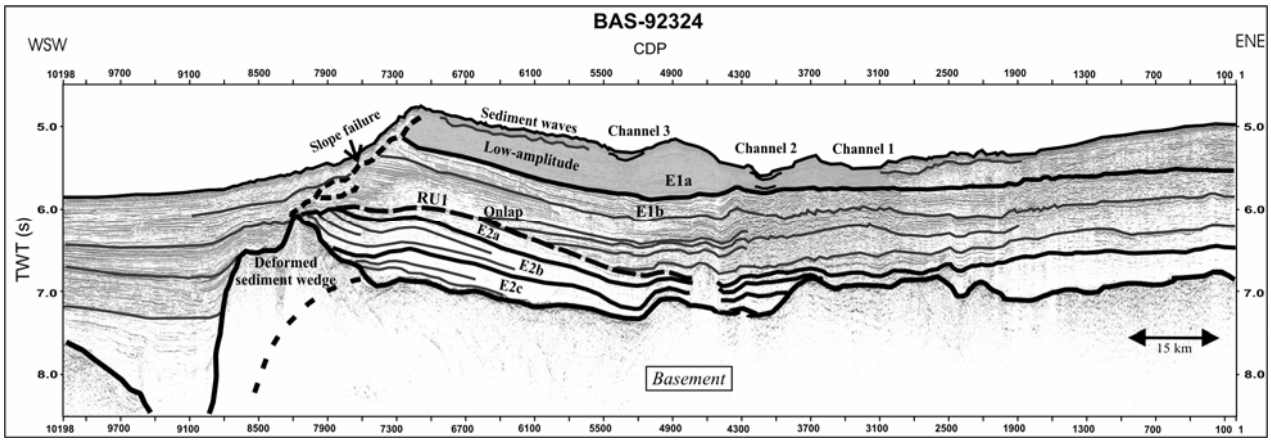

***Fig. 4.3**: MCS profile BAS-92324 with stratigraphic units modified after Nitsche et al. (1997), Cunningham et al. (2002), and Scheuer et al. (in press). The unconformity RU1 is supposed to be caused by tectonic uplift of the seafloor east of the BGA until about 61 Ma (Cunningham et al. 2002; Larter et al. 2002). The subunits E2a, E2b and E2c may present different stages of sedimentation prior to and during uplift (Cunningham et al. 2002; Scheuer et al. in press). Changing reflection characteristics of Unit E1 indicate various stages of drift development on the gentle drift side, which makes a division into subunits E1a and E1b reasonable.*

4.5.2 Profile PET-98407

Profile PET-98407 (Fig. 4.4), west of Peter I Island, is the southernmost of the SCS profiles, approximately 55 km north of BAS-92324. The seafloor topography is characterized by an asymmetrical channel-levee system. The deep channel at trace 700 is flanked by a small (about

0.08 s two-way-traveltime [TWT]) and gently westward-dipping eastern levee, and a wide and strongly elevated (about 0.3 s TWT) western levee. The western levee extends up to trace 1750, representing an asymmetrical sediment mound with a steep eastern and a gentle western side. Its east-west extension is about 140 km. The uppermost part of the western levee (0.2 s TWT) is characterized by reflections parallel to the surface. The base of this levee cannot be clearly identified due to the low data quality, but the reflections below 6.0 - 6.1 s TWT have a different orientation leading us to estimate the base of the levee at about 6.1 s. Reflections between 6.1 and 6.6 s TWT reveal a depression at trace 1000 of which the western flank ascends until trace 1500. The inclination corresponds to that of the unconformity RU1 on profile BAS-92324 (Fig. 4.3). Reflections of basement structures and deep sediment deposits are sparse. However, changing amplitudes on the corresponding analogue plot indicate faint basement structures below 6.8 s TWT.

4.5.3 Profile PET-98405

The eastern part of profile PET-98405 (Fig. 4.5) crosses the rising northern flank of Peter I Island (Fig. 4.1). To the west, the profile shows the distal continuation of the asymmetrical channel-levee system seen on profile PET-98407. The elevation difference between both levees is 0.2 s TWT. The uppermost 0.25 s TWT of the eastern levee is characterized by smooth undulating and sub-parallel reflections. The western levee gently slopes downward towards the west up to trace 2650. Although the base of this levee cannot be defined accurately, horizontal reflections possibly constituting the basis reflectors are identified at 6.3 s TWT between traces 2300 and 2500. At the western end of the profile (trace 3300), a depression of the seafloor may indicate another channel.

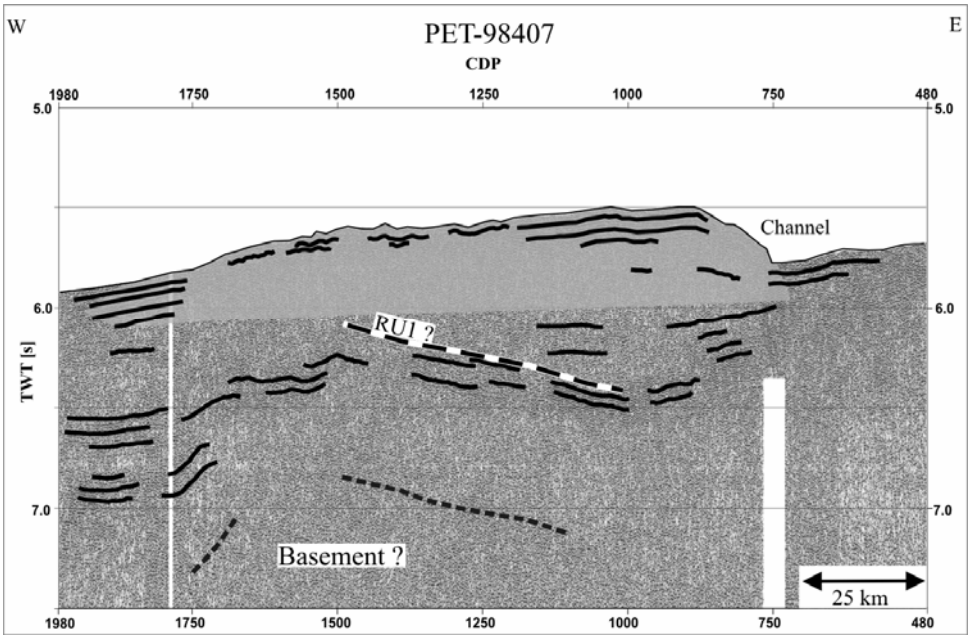

***Fig. 4.4**: SCS profile PET-98407 with line-drawings indicating seismic reflections. The western channel levee is marked in transparent grey. The black/white dashed line displays the unconformity RU1 which was defined on profile BAS-92324 (Fig. 4.3). The black dashed line shows faint basement structures as identified on the original analogue plot.*

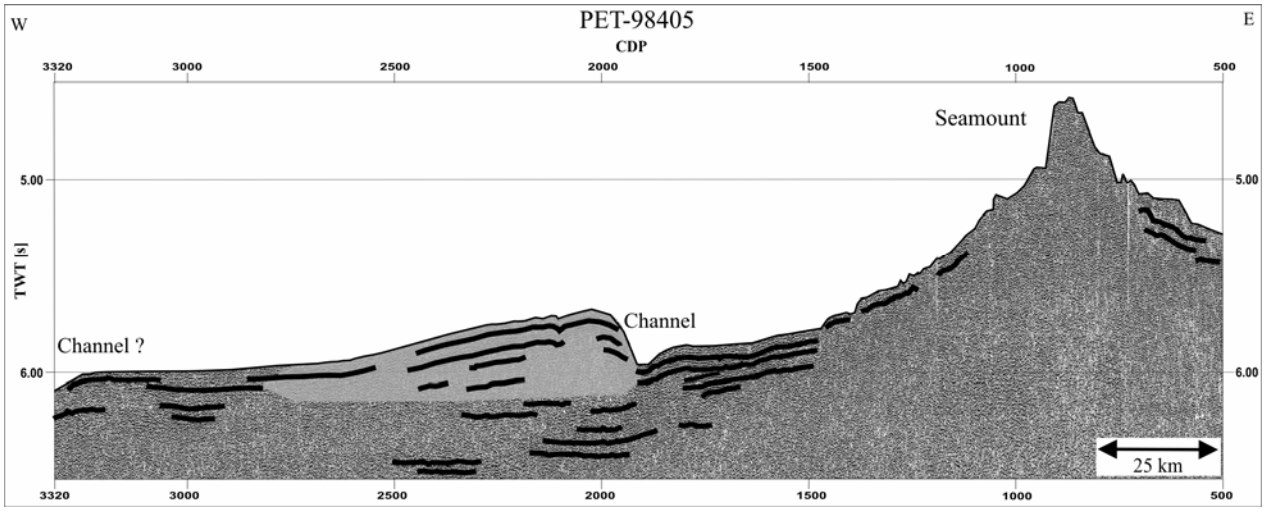

***Fig. 4.5**: SCS profile PET-98405 with line-drawings indicating major seismic reflections. The western channel levee is marked in transparent grey.*

4.5.4 Profiles AWI-95200 and AWI-95201

The MCS profiles AWI-95200 and AWI-95201 are oriented obliquely to the SCS profiles and cross profile PET-98404 at Common Depth Points (CDPs) 3200 and 2000, respectively (Fig. 4.6). The profiles cover the elevated seafloor in the east and the channel-levee system in the west. An unconformity, named LB, marking the base of the levee extends across the entire profile at a depth of about 6.2 s TWT. On profile AWI-95200, the parallel reflections above LB dip towards the west whereas parallel and sub-parallel orientated reflections below LB are horizontal. On profile AWI-95201, LB can be clearly identified as the base reflector of the western channel levee, highlighted by the downlapping reflections. The unconformity constitutes the paleo-seafloor prior to the development of the channel levee system. Reflections below LB are horizontal and sub- parallel to parallel, showing variable amplitudes. The deepest sedimentary reflections of this seismic transect are observed at 7.4 s TWT below the western channel-levee in a basement trough beneath the BGA (between CDP 1500 and 2700). The seismic data show a rough basement-sediment boundary and subsidence of the basement west of the BGA (CDP 2700 - 3200). Two narrow and seismically opaque domes suggest magmatic intrusions north of Peter I Island (at CDP 1500 of AWI-95200) and west of the BGA (at CDP 3500 of AWI-95201).

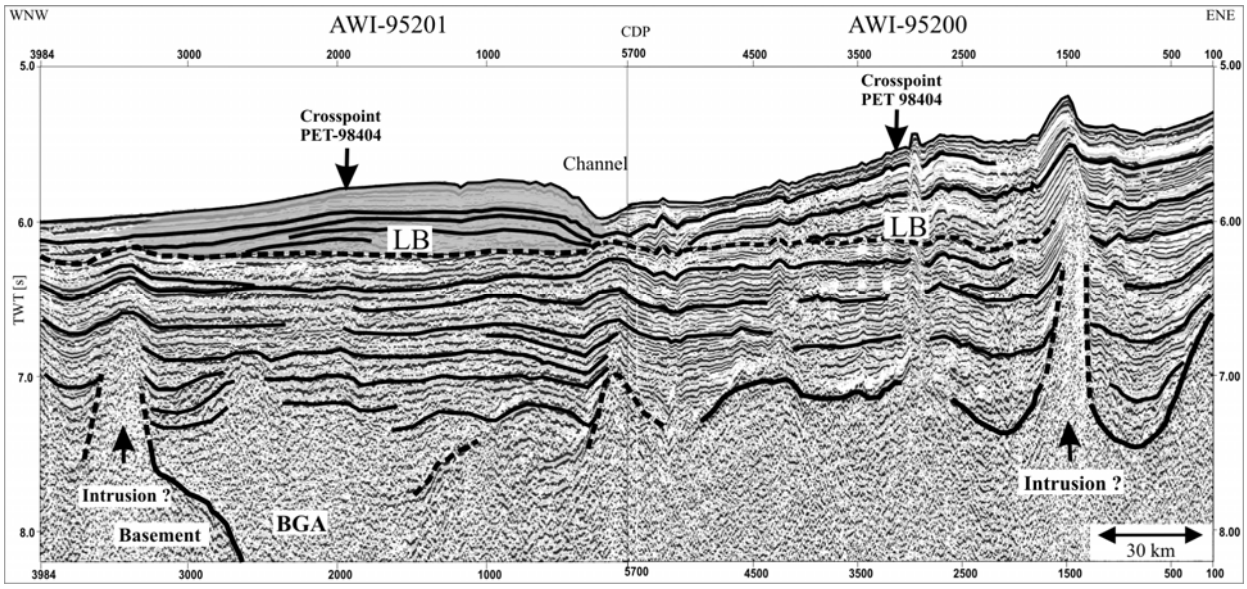

***Fig. 4.6**: MCS profile ANT-95200 and ANT-95201 with line-drawings indicating major seismic reflections. The western channel levee is marked in transparent grey. The dashed line displays the base of the channel-levee (LB).*

4.5.5 Profile PET-98404

The eastern part of profile PET-98404 (Fig. 4.7) shows rough seafloor north of Peter I Island which is cut by several gullies and channels (between trace 2300 and 3000). The uppermost sediments (0.3 s TWT) show smoothly undulating reflections oriented in parallel to the westward declining seafloor to a channel at trace 1600. The difference in elevation between the eastern and the western channel levee is 0.1 s TWT. The bulge of the western levee extends to trace 900, showing a width of about 65 km. It is characterized by parallel surface reflectors in the uppermost 0.2 s TWT. In contrast to the levee reflections, the reflections between 6.3 and 6.6 s TWT show a smooth depression at trace 1250. Between traces 500 and 600, the deformed reflections below 6.3 s TWT may indicate the southern continuation of the magmatic intrusions seen on profiles AWI-95200 and AWI-95201.

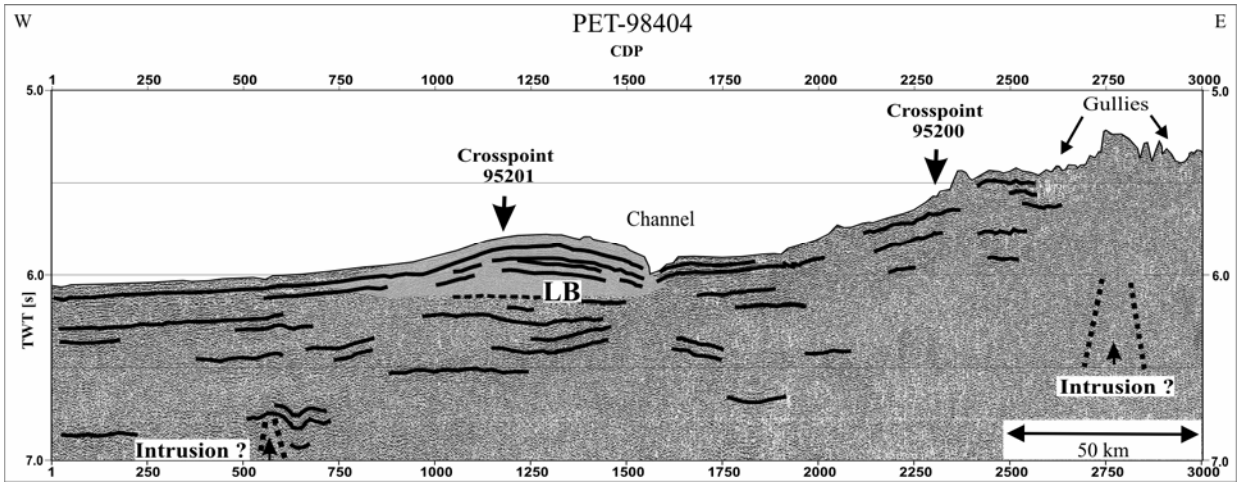

***Fig. 4.7**: SCS profile PET-98404 with line-drawings indicating major seismic reflections. The western channel levee is marked in transparent grey.*

4.5.6 Profile PET-98403b

The section of the channel-levee system shown on profile PET-98403b (Fig. 4.8) shows a lower relief than the profiles to the south. A prominent feature of the western levee is its division into three small sediment mounds (m1, m2 and m3) which widen from east to west. The uppermost 0.1 – 0.2 s TWT of the western levee are characterized by smooth undulating reflectors parallel to the seafloor. The base of the western levee can be approximated by near-horizontal reflectors at about 6.2 s TWT below m1 and m2, as well as by downlapping westward dipping reflections west of trace 1100.

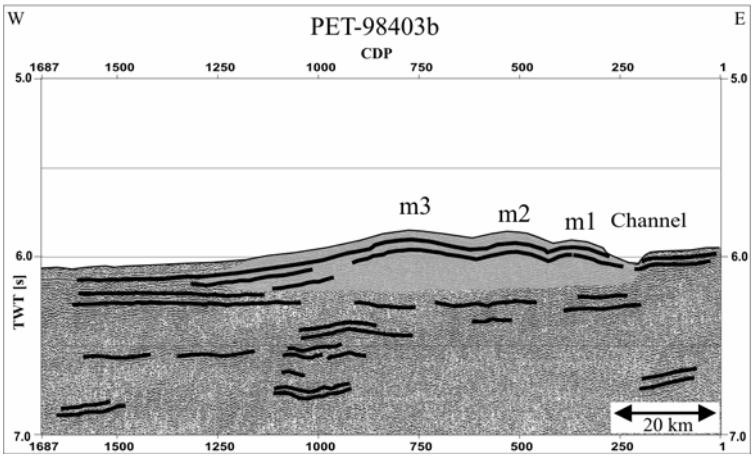

Fig. 4.8: *SCS profile PET-98403b with line-drawings indicating major seismic reflections. The western channel levee is marked in transparent grey.*

4.5.7 Profile PET-98408

Profile PET-98408 (Fig. 4.9), which represents the northernmost profile of this study, has the smoothest relief. The eastern part of the profile is characterized by high amplitude and smoothly undulating reflections in the uppermost 0.3 s TWT. Single wave-shaped reflections are recognised down to 6.8 s TWT. Reflections that can be interpreted as the base of the western levee appear at 6.3 s TWT. To the west (at about CDP 3500), we see a smooth depression of the seafloor. Reflections at trace 3400 indicate a bulge between 6.6 and 7.0 s TWT.

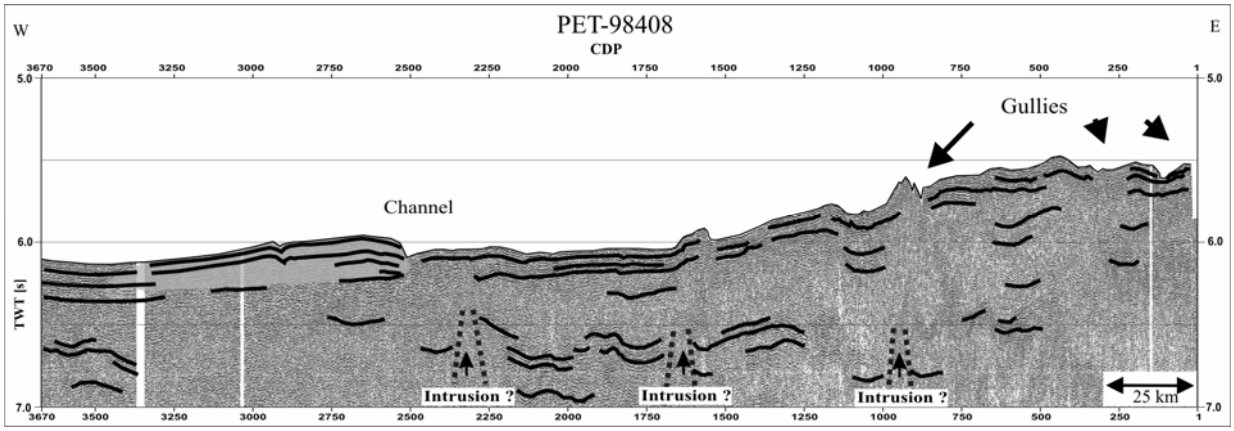

Fig. 4.9*: SCS profile PET-98408 with line-drawings indicating major seismic reflections. The western channel levee is marked in transparent grey.*

4.6 Discussion and Conclusions

4.6.1 Variations of sediment accumulation conditions

The compilation of the SCS and MCS profiles from the continental rise around Peter I Island (Fig. 4.10) reveals changes in the conditions of sediment deposition and a topographically rough seafloor from the upper rise northwards into the deep-sea basin. The structure of the southern part of Depocentre C shows the characteristics of a sediment drift (profile BAS-92324) previously described in detail by Nitsche et al. (2000), Cunningham et al. (2002) and Scheuer et al. (2006). These characteristics are very similar to those of contourite drifts identified further east on the continental rise of the western Antarctic Peninsula, which are suggested to have been developed under the influence of a bottom contour current flowing eastward along the continental slope (e.g. Rebesco et al. 1996, 1997, 2002). The drift structure on the southern part of Depocentre C can thus be seen as an indicator that a bottom current also affected sedimentation in the western Bellingshausen Sea. Instead of recording a continuation of this sediment drift structure to the north, we observe a classical channel-levee structure approximately 55 km farther north on profile PET-98407. The symmetry of the wide western levee shows a short eastern flank dipping steeply into the channel and a long and gentle western flank which is contrary to the symmetry of the sediment drift in the south. In addition, slope failures observed on the steep drift side on profile BAS-92324 are not seen on profile PET-98407. This change clearly indicates a marked change in the conditions of sedimentation from a sediment drift to a channel-levee system, implying a decreasing influence of the bottom current to the north. Furthermore, we do not see a continuation of all three channels to the north, as observed on profile BAS-92324. Either the three channels merge into one channel somewhere between both profiles, or only one channel continues toward the deeper continental rise (Fig. 4.10). The higher elevation of the western levee is caused by the influence of the Coriolis force. It caused a deflection of the suspended turbiditic sediment load to the west and thereby enhanced sediment accumulation on the western channel side. Exact reconstruction of the change of sedimentation conditions between profiles BAS-92324 and PET-98407 was not possible due to a lack of direct correlation between individual reflections. The existence of channel levees beneath channel related sediment drifts is a relatively common feature of the Antarctic continental rise, having been reported from the western Antarctic Peninsular (Rebesco et al. 2002) and the Riiser Larsen Sea (Kuvaas et al. 2004). Contourites often appear close to the slope, associated with proximal turbidites, while the deeper parts of the continental rise and abyssal plains are dominated by distal turbidites. However, the observed transformation of a contourite drift into a ‘simple’ channel-levee system over a distance of approximately 55 km, as revealed on Depocentre C, is so far unique on the Antarctic continental margin.

Further north, the western levee becomes narrower and steeper on the eastern side (Fig. 4.10). Highly energetic turbidity currents flowing through the channel may be responsible for the large steepness of its eastern flank. The narrowing of the levee may be further evidence for the decreasing influence of bottom current flow on the sedimentation. The three mounds (m1-m3) on profile PET-98403b may constitute three minor depocentres of mainly turbiditic material. Whether this suggests a stronger influence of bottom currents on sediment deposition than on profile PET-98405, which is mainly affected by the Coriolis force, remains unclear (Fig. 4.9).

Separation into three mounds by low-energy erosional channels may be another explanation, although the seismic data do not indicate any high-amplitude reflections consistent with consolidated sediments at the base of erosional channels. In any case, this division of the channel levee into a number of minor mounds is only localized. The northernmost profile PET-98408 shows a weakly developed and undivided western channel levee, indicating decreasing energy of distal turbidity currents.

The unconformity RU1 defined on profile BAS-92324 (Fig. 4.3) is supposed to be caused by tectonic uplift of the seafloor east of the BGA until about 61 Ma (Cunningham et al. 2002; Larter et al. 2002). RU1 seems to continue to the north, as indicated by the inclination of the deeper reflections on profile PET-98407 (dashed line in Fig. 4.4). However, reflections showing a similar inclination cannot be identified on profiles further north. We therefore infer the disappearance of the unconformity to be due to a decrease in uplift to the north. The seismic data north of Peter I Island show a decreasing roughness of the seafloor to the north. Small and narrow depressions in the western part of profile PET-98404 suggest that channels and gullies produced by erosional downslope processes become less steep to the north, as indeed seen on profile PET-98403a and PET-98408. Furthermore, magmatic intrusions have affected the sedimentation almost up to the present-day seafloor, as seen on profile ANT-95200. Unfortunately, the low quality of the SCS data does not allow the influence of intrusions and other basement structures on the sediments to be better constrained.

4.6.2 Sediment thicknesses and deposition rates

As outlined in the methods, estimates of sediment deposition rates are based on sediment thicknesses and estimated sediment ages. As illustrated in Fig. 4.11, thicknesses vary between 600 m (BAS-92324) and less then 100 m (PET-98409),. The thickest segment of the levee on profile ANT-95201 at CDP 800 (about 0.22 s TWT, Fig. 4.6) is approximately 360 m thick. The generation of a time scale for the individual sediment layers, which is required for the estimation of deposition rates is difficult due to the lack of drill data in this area. Correlations of sedimentary units of the study area with the nearest ODP sites (1095 and 1096 of Leg 178) have large uncertainties, as shown in the western part of seismic profile AWI-20010001 in Scheuer et al. (2006). Accretionary wedges, formed during Late Cretaceous to early Tertiary subduction along the continental margin are interpreted from the Continental Slope Gravity Anomaly (CSGA) (Cunningham et al. 2002). These wedges may have acted as a barrier for down-slope transported sediments, leading to different forms of sediment accumulations and deposition rates on the continental rise of the Bellingshausen Sea (Scheuer et al. 2006). Site 324 of DSDP Leg 35, located west of the BGA, only penetrated down to a depth of 218 m in Pleistocene and Pliocene sediments of mainly unconsolidated clay (Hollister and Craddock 1976) and, therefore, did not reach the sediments deposited at the base of the levee.

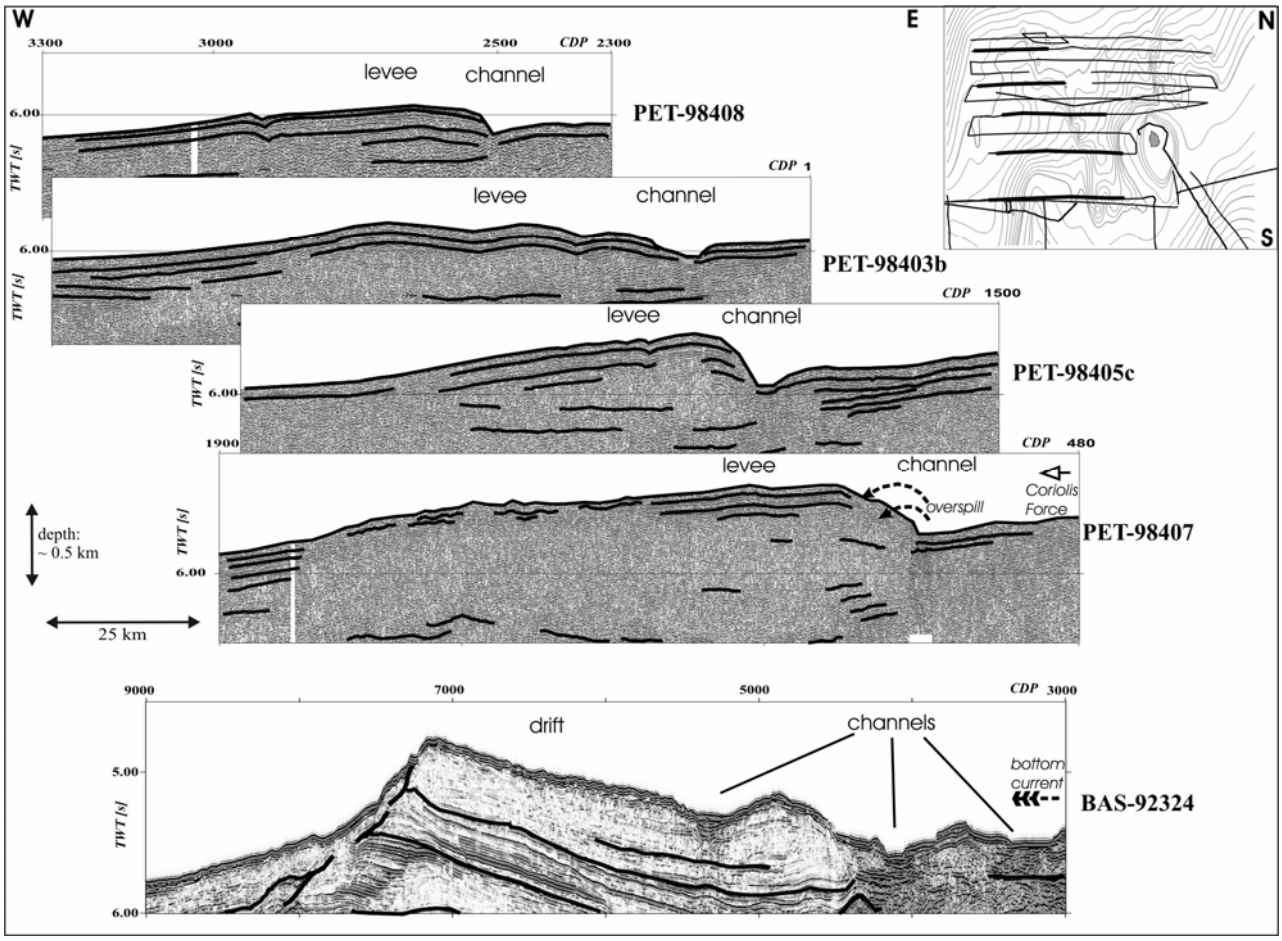

***Fig. 4.10**: Composite seismic cross-sections of Depocentre C showing the structural changes from south to north. Profile BAS-92324 is closest to the continental slope and shows a sediment drift structure with a steep side to the west and a gentle side to the east. In contrast, the four PET-profiles show a channel-levee system with an opposite orientation of the steep and the gentle side of the western levee.*

However, for the calculation of sediment deposition rates we can make assumptions about the onset of channel-levee development. It is likely that the channel-levee system developed with the onset of strong glacial sediment supply to the continental rise caused by regularly advancing grounding ice on the continental shelf (e.g. Rebesco et al. 1997). High sediment accumulation rates on the continental slope may have resulted in a more frequent occurrence of turbidites and, thus, the deposition of turbiditic sediments along the margins of the erosional channels. The oldest drilled glacial sediment sequences on the western Antarctic Peninsula shelf were dated at about 9.6 Ma (e.g. Iwai et al. 2002; Barker and Camerlenghi 2002). We use this age for the calculation of the deposition rates along the SCS and MCS profiles, shown in Table 2.

Table 2:

profile	CDP/ trace	compacted thickness TWT [s]	compacted thickness [m]	deposition rate (age of levee basis ~9.6 Ma) [m/m.y.]
BAS-92324	**4900**	0.80	680	**72**
PET-98407	**1050**	0.55	468	**49**
ANT-95201	**1000**	0.50	425	**45**
PET-98403b	**750**	0.38	323	**34**
PET-98408	**2650**	0.24	204	**21**

Maximum sediment thicknesses and deposition rates of unit E1a on profile BAS-92324, and of the western levee on the other determinated profiles, measured and calculated at one CDP of each profile. The used seismic interval velocity for the calculation of the sediment accumulation rate used here is 1700 m/s, having been derived from the analysis of MCS profile AWI-95201.

Although the calculation of sediment deposition rates is a spot check without considering the true width and the volume of the levees, it indicates a decline in sedimentation rate towards the north (Fig. 4.11). The deposition rate is highest along profile BAS-92324 (72 m/m.y.) and strongly decreases northwards to 21 m/m.y. on profile PET-98407. The validity of these values can be assessed by a comparison with sedimentation rates calculated for other sediment depocentres of the West Antarctic continental margin. The highest sedimentation rates on the continental rise of the Antarctic Peninsula during the early Pliocene are about 180 m/m.y., calculated on the basis of magnetobiochronologic data from ODP site 1096 on Drift 7 (Iwai et al. 2002). The highest known sedimentation rates along the West Antarctic continental margin since the Pliocene is about 295 m/m.y. in a trough-mouth fan east of Peter I Island, referred to as Depocentre B and located approximately 150 km east of Depocentre C (Scheuer et al. 2006). This trough-mouth fan developed at the foot of a shelf trough and appears to be the main sediment depocentre of terrigenous sediment material eroded and transported by grounded ice on the shelf between Alexander – and Thurston island. This trough-mouth fan may be the origin for a large part of the early Cenozoic sediments deposited on the southern part of Depocentre C, delivered by the westward flowing bottom current (Scheuer et al. 2006, Ó Cofaigh et al. 2005). The maximum sedimentation rate of 72 m/m.y. on the southern part of Depocentre C suggests a lower downslope input of sediments during the late Cenozoic compared to these main sediment deposition areas (Depocentre B and Drift 7). Due to the partial low quality of the seismic data and the lack of age control by ocean drilling we are neither able to differentiate single turbiditic or contouritic sediment sequences, nor make inferences about glacial cycles that influenced the sediment supply in the western Bellingshausen Sea. Furthermore, indicators of palaeoceanographic conditions are, at present, too scarce to reconstruct the development of the bottom current during glacial and interglacial periods and, thus, the variability of the influence of the current on the sediment accumulation. However, the large size of Depocentre C and its unique sitting on an uplifted area of oceanic

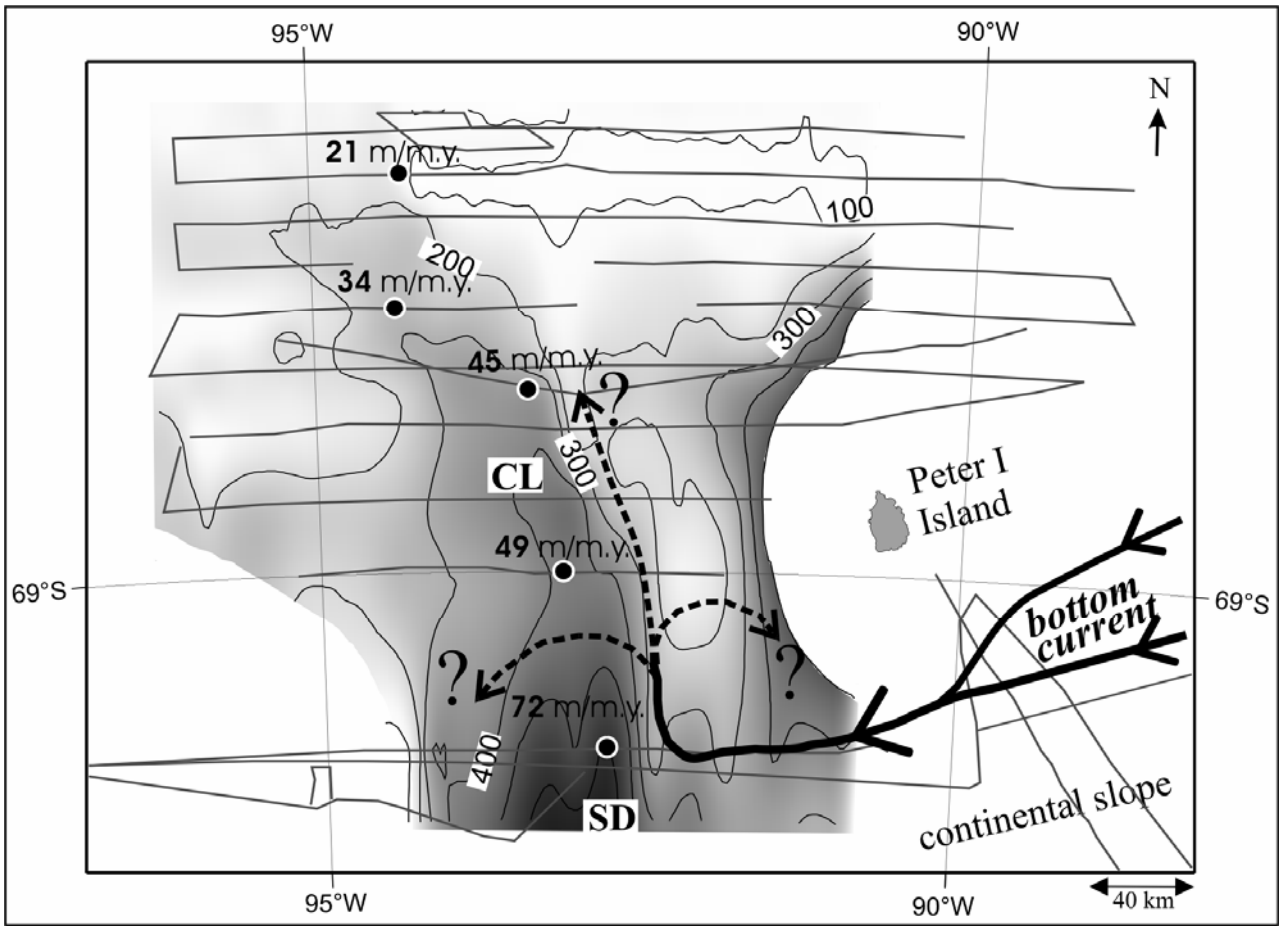

***Fig. 4.11**: Estimated sediment thickness of the youngest Cenozoic sediments (unit E1a of the sediment drift [SD] and the western channel-levee [CL]). The isolines show the thickness in meters [m]. The base of this sediment body was estimated from the seismic profiles (LB on Fig. 4.3-10). Five calculated maximum sediment deposition rates are marked with black/white points in the respective locations. The arrows display the estimated direction of the westward flowing bottom current along the continental margin between Peter I Island up to the sediment drift [SD]. The further continuation of the current remains uncertain (dashed arrows).*

basement indicate it as an important example of how changes in bottom current parameters influence the sediment accumulation on the Antarctic continental margin. We assume that the structure of Depocentre C and the sediment accumulations north of Peter I Island picture the course of the westward flowing bottom current (Fig. 4.11). The submarine foot of Peter I Island acts as a topographic barrier. North of Peter I Island, sediment accumulations such as sediment drifts along the sides of the seafloor depressions are not observed and do not indicate bottom current activity. The main part of the current probably flows between the continental slope and Peter I Island, causing the development of the sediment drift on profile BAS-92324. Similar to the measurements of recent bottom current activity on Drift 7 (Rebesco et al. 2002), the current may be diverted to the north, following the topography as a contour current without provoking the continuation of the sediment drift to the north. Instead, the Coriolis force becomes the decisive factor for the sedimentation. Nevertheless, the course of the current north of profile BAS-92324 remains unclear.

Acknowledgements

We are grateful to the captain and crew of the RV *Akademik Boris Petrov* for their support during Cruise No. 29. The cruise was funded by the Alfred Wegener Institute for Polar and Marine Research, the Vernadsky Institute of Geochemistry and Analytical Chemistry and the Russian Foundation for Fundamental Investigation (RFFI). We thank Dr. A.F. Beresnev, Dr. P.N. Efimov and Ing. V.N. Poberzhin of the Vernadsky Institute for the acquisition of the seismic data. We also thank the British Antarctic Survey, especially Dr. Rob Larter, who provided the seismic data of profile BAS-92324.

REFERENCES

Anderson JB, Wellner JS, Lowe AL, Mosola AB, Shipp SS (2001). The footprint of the expanded West Antarctic Ice Sheet: ice stream history and behaviour. GSA Today, 11, 4-9

Barker PF, Camerlenghi A (2002) Glacial history of the Antarctic Peninsula from Pacific margin sediments. In: Barker PF, Camerlenghi A, Acton GD, Ramsay ATS. (eds.), Proc. ODP, Sci. Results 178 [online]. Available from World Wide Web: <http://wwwodp.tamu.edu/publications/178_SR/synth/synth.htm>

Bart PJ, Anderson JB (1995) Seismic record of glacial events affecting the Pacific margin of the northwestern Antarctic Peninsula. In: Cooper AK, Barker PF, Brancolini G (eds.), Geology and seismic stratigraphy of the Antarctic margin. Antarctic Research Series 68 American Geophysical Union, Washington, DC: 75-95

Camerlenghi A, Crise A, Accerboni E, Laterza R, Pudsey CJ, Rebesco M (1997) Ten-month observation of the bottom current regime across a sediment drift on the Pacific of the Antarctic Peninsula. Antarctic Science, 9, 424-431

Cooper AK, Barrett P, Hinz K, Traubea V, Leitchenkov G, Stagg H (1991) Cenozoic prograding sequences of the Antarctic continental margin: a record of glacioeustatic and tectonic events. Marine Geology, 102, 175-213

Cunningham AP, Larter RD, Barker PF, Gohl K, Nitsche FO (2002) Tectonic evolution of the pacific margin of Antarctica: 2. Structure of Late Cretaceous-early Tertiary plate boundaries in the Bellingshausen Sea from seismic reflection and gravity data. J Geophy Res 107 (B12), 2346 DOI 10.1029/2002JB001897

Cunningham AP, Larter RD, Barker PF (1994) Glacially prograded sequences on the Bellingshausen Sea continental margin near 90°W. Terra Antarctica 1: 267-268

Faugeres J-C, Stow DAV, Imbert P, Viana A (1999) Seismic features diagnostic of contourite drifts. Marine Geology 162: 1–38

Eagles G, Gohl K, Larter RD (2004) Life of the Bellingshausen plate. Geophys Res Letters Vol. 31, L07603 DOI 10.1029/2003GL019127

Gohl K, Nitsche, FO, Miller H (1997) Seismic and gravity data reveal Tertiary intraplate subduction in the Bellingshausen Sea, southeast Pacific. Geology 25: 371-374

Hampton MA, Eittreim SL, Richmond BM (1987) Post-breakup sedimentation on the Wilkes Land Margin, Antarctica. In: Eittreim SL and Hampton MA (eds.) The Antarctic

continental margin, Geology and Geophysics of offshore Wilkes Land. Circum-Pacific Council for Energy and Mineral Recourses, Earth Science Series, 5A, 75-89

Hollister CD, Craddock C, (1976). Intruduction, principal results . Leg 35 deep sea drilling project. Initial reports of deep sea drilling project, 35. U. S. Government Printing Office, Washington D. C., 929 pp

Iwai M, Acton GD, Lazarus D, Ostermann LE, Williams T (2002) Magnetobiochronologic synthesis of ODP Leg 178 rise sediments from the Pacific sector of the Southern Ocean: Sites 1095, 1096 and 1101. In: Barker PF, Camerlenghi A, Acton GD, Ramsay ATS (eds.) Proc ODP Sci Results, 178: 1-40 [CD-Rom]

Kuvaas B, Kristoffersen Y, Guseva J, Leitchenkov G, Gandjukhin V, Kudryavtsev G (2004) Input of Glaciomarine Sediments along the East Antarctic Continental Margin; Depositional Processes on the Cosmonaut Sea Continental Slope and Rise and a Regional Acoustic Stratigraphic Correlation from 40° W to 80° E. Mar Geophys Res, 25, 3-4: 247-263

Larter RD, Cunningham AP (1993) The depositional pattern and distribution of glacial-interglacial sequences on the Antarctic Peninsula Pacific margin. Marine Geology 109: 203-219

Larter RD, Cunningham AP, Barker PF, Gohl K and Nitsche FO (2002). Tectonic evolution of the pacific margin of Antarctica: 1. Late Cretaceous tectonic reconstructions. J Geophys Res, 107, NO. B12 2345 DOI 10.1029/2000JB000052

Lucchi RG, Rebesco M, Camerlenghi A, Busetti M, Tomadin L, Villa G, Perisco D, Morigi C, Bonci MC, Giorgetti G (2002) Mid-late Pleistocene glacimarine sedimentary processes of a high-latitude, deep-sea sediment drift (Antarctic Peninsula Pacific margin). Marine Geology 189: 343-370

McGinnes JP, Hayes DE, Driscoll NW (1997) Sedimentary processes across the continental rise of the southern Antarctic Peninsula. Marine Geology 141: 91-109

Nitsche FO, Cunningham AP, Larter RD, Gohl K (2000) Geometry and development of glacial continental margin depositional systems in the Bellingshausen Sea. Marine Geology 162: 277-302

Nitsche FO, Gohl K, Vanneste K, Miller H (1997) Seismic expression of glacially deposited sequences in the Bellingshausen and Amundsen Seas, West Antarctica. In: Barker PF, Cooper AK (eds.), Geology and Seismic Stratigraphy of the Antarctic Margin: 2. Ant Res Ser 71, American Geophysical Union, Washington, DC, 95-108

Nowlin WD, Zenk W (1988) Westward bottom currents along the margin of he South Shetland Island Arc. Deep Sea Research, 35, No.2, 269-301

Ó Cofaigh C, Larter RD, Dowdeswell JA, Hillenbrand C-D, Pudsey CJ, Evans J, Morris P (2005) Flow of the West Antarctic Ice Sheed on the continental margin of the Bellingshausen Sea at the Last Glacial Maximum. J Geophys Res, 110, doi: 10.1029. 2005JB003619

Rebesco M, Stow D (2001) Seismic expression of contourites and related deposits. Special Issue. Mar Geophys Res 22 (5-6): 303-308

Rebesco M, Pudsey CJ, Canals M, Camerlenghi A, Barker PF, Estrada F, Giorgetti A (2002) Sediment drifts and deep-sea channel systems, Antarctic Peninsula Pacific margin, mid-Miocene to present. In: Stow DAV, Pudsey CJ, Howe J, Faugeres J-C and Viana A. (eds.)

Deep-Water Contourite Systems: Modern Drifts and Ancient Series, Seismic and Sedimentary Characteristics. Spec Publ Geol Soc London. Memoirs 22: 353-371

Rebesco M, Larter RD, Barker PF, Camerlenghi A, Vanneste LE (1997) History of sedimentation on the continental rise west of the Antarctic Peninsula. In: Cooper AK, Barker PF (eds.), Geology and Seismic Stratigraphy on the Antarctic Margin: 2. Antarctic Research Series 71, Am Geophys Union, Washington, DC: 29-49

Rebesco M, Larter RD, Camerlenghi A, Barker PF (1996) Giant sediment drifts on the continental rise west of the Antarctic Peninsula. Geo-Marine Letters 16: 65-75

Scheuer C, Gohl K, Larter RD, Rebesco M, Udintsev G (2006). Variability in Cenozoic sedimentation along the continental rise of the Bellingshausen Sea, West Antarctica. Marine Geology, 227, 279-298

Smith WHF, Sandwell DT (1997) Global seafloor topography from satellite altimetry and ship depth soundings. Science, 277: 1956-1961

Tomlinson JS, Pudsey CJ, Livermore RA, Larter RD, Barker PF (1992). Long-range sidescan sonar (GLORIA) survey of the Antarctic Peninsula pacific margin. In: Yoshida Y, Kaminuma K, Shiraishi K, (eds.) Recent progress in Antarctic Earth Science, Terra Scientific Publishing Company, Tokyo, 423-429

Tucholke BE, Houtz RE (1976) Sedimentary framework of the Bellingshausen Basin from seismic profile data. In: Hollister CD, Craddock CD, et al. (eds.) Initial Reports of the Deep Sea Drilling Project, Vol 35, U.S. Government Printing Office, Washington, DC, 197-227

Udintsev GB, Schenke GW, Schöne T, Beresnev AF, Efimov PN, Kol'tsova AV, Knyazev AB, Tererin DE, Kurentsova NA, Bulychev AA, Gilod DA (1999) New data on the floor structure of the Bellingshausen Sea, Western Antarctica. Doklady Earth Sciences 367A, No. 6: 876-880

CHAPTER 5

GRIDDED ISOPACH MAPS FROM THE SOUTH PACIFIC AND THEIR USE IN INTERPRETING THE SEDIMENTATION HISTORY OF THE WEST ANTARCTIC CONTINENTAL MARGIN

Carsten Scheuer, Karsten Gohl, Graeme Eagles

Alfred Wegener Institute for Polar and Marine Research (AWI), Bremerhaven, Germany

Submitted to Geochemistry, Geophysics, Geosystems (G^3), AGU online journal, in March 2006

5.1 Abstract

Large scale maps of sediment thicknesses are essential prerequisites for the next generation of high resolution paleobathymetric reconstructions. In addition, maps of sediment thicknesses on continental margins are useful for studies of terrigenous sediment supply and sediment distribution on the ocean floor. Based on a compilation of more than 10,000 km of single and multichannel seismic reflection data and correlations with ocean drilling sites, we model isopach grids of the Southern Pacific margin of West Antarctica. Following recent seismic stratigraphic models, we differentiate between “pre-glacial” and “glacially transported” sediments. The subsequent modelling of sediment thickness grids allows us to compare the pre-glacial and glacial sedimentary development in the study area. Based on available drillhole dates, we estimate the onset of accumulation of glacially transported sediments to have occurred at about 10 Ma, based on approximate sediment deposition rates. The thickest glacial sediment accumulations occur in front of major glacial drainage outlets, i.e. Marguerite Trough on the western Antarctic Peninsula margin, Belgica Trough in the Bellingshausen Sea, and the trough off Pine Island Bay in the Amundsen Sea. Sedimentation rates between 140 and 170 m/m.y. are calculated for these sites.

5.2 Introduction

The separation of Antarctica from the Australian and South American continents in Cenozoic times initiated the development of southern ocean currents, which were important for climate change (e.g. Kennett, 1977). The opening of the Tasmanian and Drake Passage gateways enabled the final development of the ring-shaped Antarctic Circumpolar Current (ACC), an important component of the modern oceans. This process may also have led to the gradual climatic isolation of Antarctica (Kennett, 1977) and thus has been the main focus of various climate model experiments investigating the glacial development of Antarctica (e.g. Sijp and England, 2004). However, the opening of gateways is only one of the factors that influenced

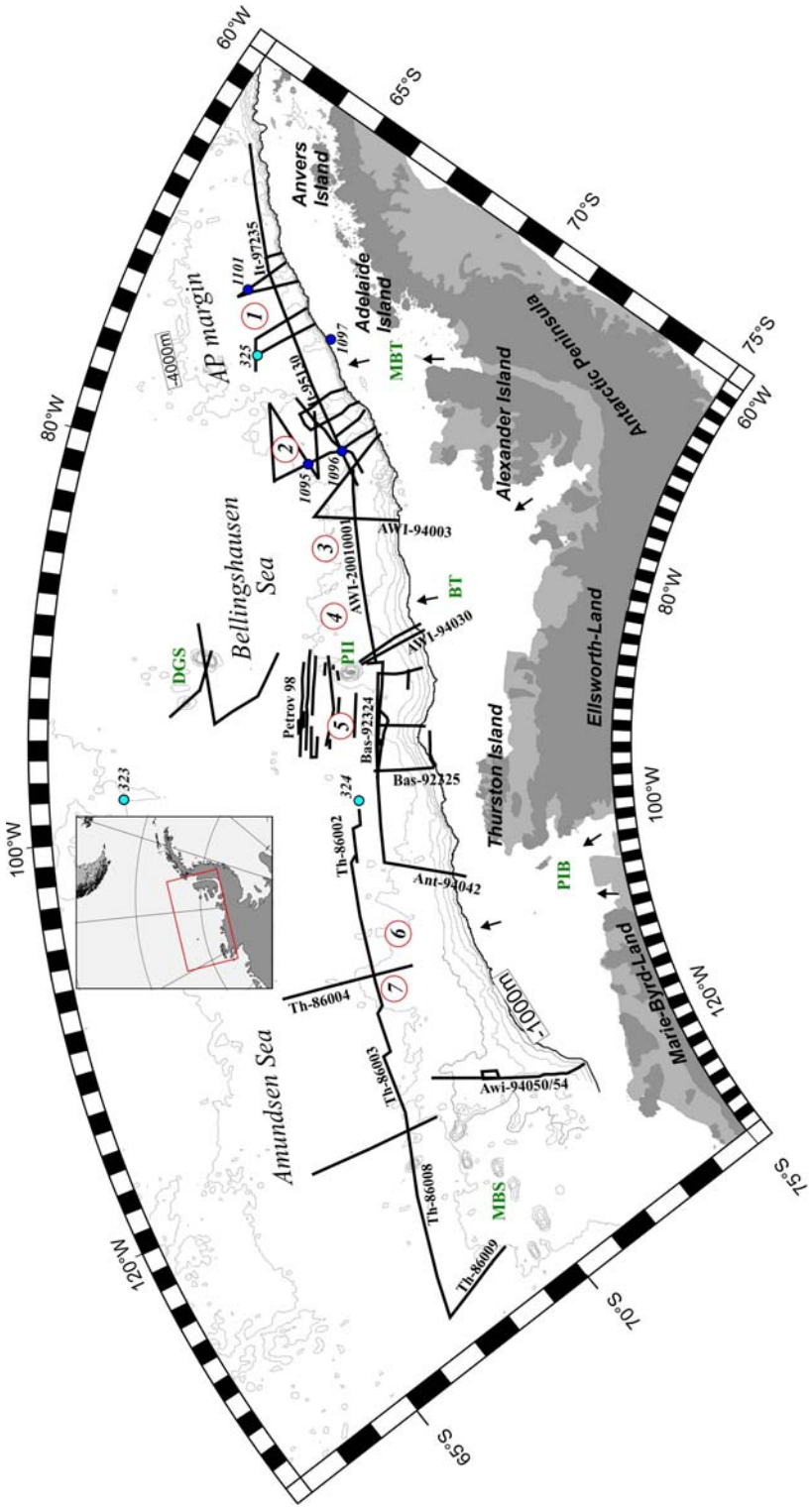

Fig. 5.1*: Overview of the South Pacific continental margin of West Antarctica, showing a network of digital available multi-channel (MC) and single-channel (SC) seismic profiles (black lines) and contours of the satellite-derived predicted bathymetry from Smith and Sandwell (1997) (faint lines). Drill sites of DSDP Leg 35 and ODP Leg 178 are marked with black circles. Dark grey areas indicate land masses, white light grey indicates ice shelves. Important topographic locations are notated. MBS = Marie Byrd Seamounts, PII = Peter I Island, DGS = DeGerlache Seamounts, PIB = Pine Island Bay, BT = Belgica Trough, MB = Marguerite Bay. The numbers in red circles indices the positions of some of the main sediment accumulation areas. 1: drifts 3 and 4, 2: drifts 6 and 7, 3: Depocentre A, 4: Depocentre B, 5. Depocentre C, 6: mounds Am3 and 3, 7: mound Am4.*

the development of circum-Antarctic currents. Several studies have shown that the ACC and Antarctic Bottom Water (AABW) are strongly guided by seafloor topography (e.g. Lazarus and Caulet, 1993; Rack, 1993). Recent palaeobathymetric models were based on the kinematics and thermal subsidence rates of oceanic crust (e.g. Sykes et al., 1998; Brown et al., 2005), but lack any consideration of the effects of sediment distribution. Hence, sediment accumulations should also be taken into account in the next generation of paleobathymetric reconstructions. To do so will require gridded maps of sediment thickness.

In this study, we present gridded sediment isopachs for the Pacific margin of West Antarctica. As well as their importance for climate modelling, these maps enable analyses of the distribution of sediment accumulations. High latitude continental margins are characterized by thick sediments deposited during glacial periods when grounding and eroding ice streams developed on the continental shelf. These thick sediment deposits provide an indirect record of glacial climate (e.g. Cooper et al., 1991; Tomlinson et al., 1992; Larter et al., 1997; McGinnes et al., 1997; Anderson et al., 2001, Rebesco et al., 1996). It is possible to identify features in seismic data that are consistent with the change from pre-glacial to glacial sedimentation, and thus to produce isopach maps for each. The adoption of a date for the first development of grounding ice allows approximations of sedimentation rates and thus comparisons of local glacial sedimentation histories on the West Antarctic continental margin. Furthermore, comparisons of sedimentary structures on the Antarctic Peninsula and Amundsen Sea continental rises enable some speculations on the role of bottom currents in the Amundsen Sea.

5.3 Data and knowledge basins

Our calculation of sediment thicknesses is based on single- and multi-channel reflection seismic profiles acquired between 1989 and 2001. Most of the seismic data are publicly available in the digital database of the SCAR Seismic Data Library System (SDLS). Seismic data that are not yet available in digital form are not included in this study. In addition, we have taken account of drilling data from Deep Sea Drilling Project (DSDP) Leg 35 and Ocean Drilling Program (ODP) Leg 178. All the seismic profiles and the ocean drilling sites are shown in Figure 5.1.

5.3.1 Geological setting

The highest-resolution records of Cenozoic glaciation of West Antarctica are found in the thick sediments of trough mouth fans, such as the Crary Fan in the southern Weddell Sea (e.g. Kuvaas and Kristoffersen, 1991) or the recently mapped Belgica fan in the Bellingshausen Sea (Ó Cofaigh et al. 2005; Scheuer et al., 2006). Thick sediments have also accumulated on sediment mounds, channel levees, and contourite drifts that developed due to interactions between turbidity currents and alongslope bottom currents (e.g. Rebesco et al., 1996, 1997; Faugeres et al., 1999).

The date of the onset of grounding ice advances and glacial sedimentation at the West Antarctic margin is still the subject of debate, as data remain sparse. Many authors use features observed in seismic profiles in order to evaluate the glacial influence of the terrigenous

sediment input. Studies have shown that these features include strong prograding sequences on the outer continental shelf, thick sediment wedges on the slope, unconformities overlain by sediment mounds or drifts on the rise, and erosional channels caused by turbidity currents (e.g. Hampton et al., 1987; Cooper et al., 1991; Rebesco et al., 1997; DeSantis et al., 2003; Cunningham et al., 2002; Nitsche et al., 2000; Rebesco et al., 2000, 1997; Cooper et al., 1995). The correlation of seismic patterns with ODP results suggests that a dominantly glacial environment has existed along the SE Pacific margin forat least 10 m.y. (e.g. Rebesco et al., 1997; Barker and Camerlenghi, 2002, Scheuer et al., 2006). By considering such seismic patterns, we establish a differentiation between predominantly pre-glacial and predominantly glacially transported sediments on the continental margin of West Antarctica. In the following, we give a brief overview of the topographic setting and recent knowledge of the sedimentation processes of the area offshore of the Antarctic Peninsula, the Bellingshausen Sea, and the Amundsen Sea.

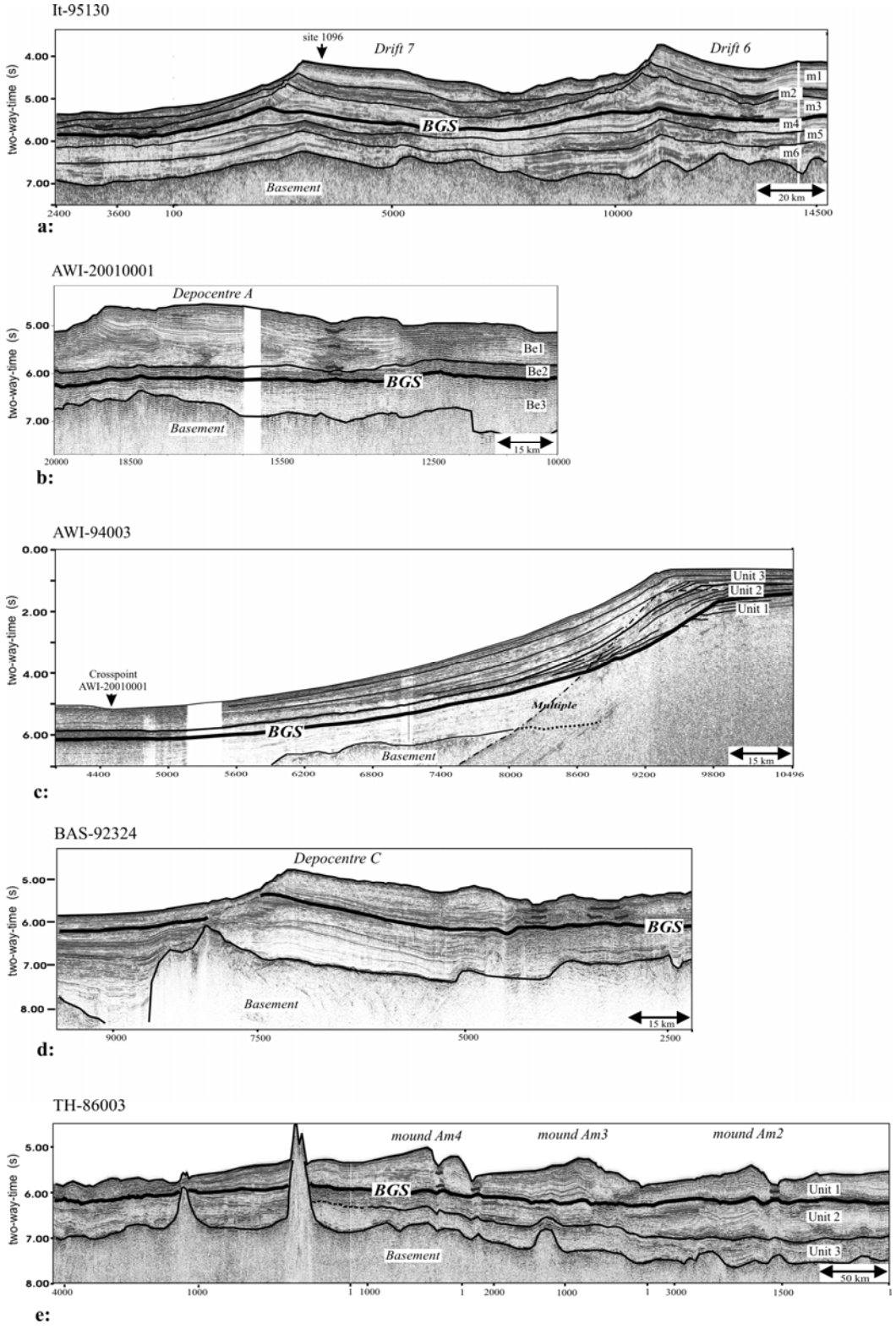

Fig. 5.2a, b, c, d, and e: *Interpreted line drawings of five MCS profiles on the South Pacific continental margin of West Antarctica. Interpretation of profile IT-95130 (2a) refers to Rebesco et al. (1997), AWI-20010001 and AWI-94003 (2b, c) to Scheuer et al. (2006), BAS-92324 (2d) to Cunningham et al. (2002) and Scheuer et al. (2006), and TH-86003 (2e) to Yamaguchi et al. (1988). In consideration of these interpretations we defined the basis of glacially transported sediments (BGS).*

Western Antarctic Peninsula continental margin

A large number of seismic and bathymetric data (e.g. Rebesco et al., 1996, 1997, 2002, Larter and Cunningham, 1993, Dowdeswell et al., 2004b, McGinnis et al., 1997, Bart and Anderson, 1995) and the results of DSDP Leg 35, site 325 (e.g. Hollister and Craddock et al., 1976) and ODP Leg 178 (e.g. Barker and Camerlenghi, 2002) gave insights to the sedimentation history of the western Antarctic Peninsula margin (Figure 5.1). The interaction of a westward flowing bottom current with downslope turbidity currents led to the development of eight contourite drifts and three sediment mounds on the sides of downslope turbidity channels (e.g. Larter and Cunningham, 1993; Camerlenghi et al., 1997; Rebesco et al., 1997). Rebesco et al. (1996, 1997) identified six sedimentary units, numbered M1 to M6, and related the M3/M4 boundary, where they observed amplified development of sediment drifts and the onset of erosional channels on the continental rise, to the onset of grounding ice advances on the shelf. (see Drift 6 and Drift 7 as examples on Figure 5.2a). Ocean drilling at ODP site 1095 of Leg 178 recovered sediment dated at 9.6 Ma that was related to glacial sediment transport just above the M3/M4 boundary, but did not reach the lower boundary of glacial sediments.

Bellingshausen Sea

Seismic data from the Bellingshausen Sea are sparse, but enable the identification of three wide sediment depocentres on the continental shelf (Figure 5.1). The largest, Depocentre B, is interpreted as a trough mouth fan (Ó Cofaigh et al., 2005; Scheuer et al., 2006). The correlation of the aggrading and prograding sequences, named units 1 – 3, and identified on the continental shelf/upper slope by Nitsche et al. (1997), with sediments on the continental rise near the easternmost depocentre, A, allowed the definition of three continental rise units, named Be1 to Be3 (see examples at Figures 5.2b and c). Correlation with the Antarctic Peninsula margin stratigraphy (Rebesco et al., 1997) and ODP Leg 178 drilling results indicated that Be1 and Be2 consist of glacially derived sediments above a pre-glacial Be3. No such correlation was possible for the western Bellingshausen Sea and Amundsen Sea, due to changing characteristics of seismic pattern (Scheuer et al., 2006). Depocentre C is situated on a basement uplift along a north-south trending Late Cretaceous tectonic lineation, giving rise to the prominent Bellingshausen Gravity Anomaly (e.g. Gohl et al., 1997; Larter et al., 2002) (Figure 5.1). On the upper continental rise, Depocentre C resembles a sediment drift, but distally it has the features of a simple channel levee (Cunningham et at., 1994; Nitsche et al., 2000; Scheuer et al., 2006). According to Scheuer et al. (accepted), the base of the drift and channel-levee may indicate enhanced sediment supply to the continental rise due to advances of grounding ice on the continental shelf (Figure 5.2d).

Amundsen Sea

The relief of the continental shelf is influenced by a large drainage outlet of the West Antarctic Ice Sheet in Pine Island Bay, which is fed by the Pine Island and Thwaites glaciers (e.g. Lowe and Anderson, 2001; Vaughan et al., 2001). Knowledge about the continental slope and rise is very limited. One seismic profile shows a prograding shelf edge (Nitsche et al., 2000). The Japan National Oil Company published seismic profiles which show several sediment mounds

separated by channels in the east, and shallow basement and decreasing sediment thickness to the west near the Marie Byrd Seamounts (Yamaguchi et al., 1988) (Figures 5.1 and 5.2e). Kimura (1982) classified three sediment units, A, B and C. The uppermost, units A and B, are interpreted as consisting of post-middle Miocene terrigenous turbidites, ice-rafted detritus and pelagic sediments. Site 323 of DSDP-Leg 35, drilled in the abyssal plain, revealed ice rafted debris in sediment of middle Miocene age at a depth of approximately 300 m b.s.f. (Hollister and Craddock et al., 1967).

5.3.2 Previous models of total sediment thicknesses

The first sediment isopach maps of the South Pacific region were compiled by Houtz et al. (1973) and Rodrigues et al. (1986), based on sparse and mainly analogue seismic data acquired during early *RV Eltanin* cruises (e.g. Tucholke and Houtz, 1976), and on surveys related to DSDP Leg 35 (e.g. Hollister and Craddock et al., 1976). Hayes and LaBreque (1991) published a revised version of this sediment isopach map by adding data from more recent seismic reflection profiles and DSDP/ODP. The Hayes and LaBrecque dataset was incorporated into the world isopach maps of Laske and Masters (1997) and the National Geophysical Data Center (NGDC, available online). Since publication of this second compilation, ODP Leg 178 was completed on the western Antarctic Peninsula margin (e.g. Barker and Camerlenghi, 2002) and new digital seismic data were acquired along the West Antarctic continental margin.

Eagles (2006) modelled a thermally subsided South Pacific oceanic lithosphere using Stein and Stein's (1992) subsidence relationship, and removed it from predicted bathymetry (Smith and Sandwell, 1997) to produce residual bathymetric anomalies. Under the assumption that most of this anomaly can be attributed to the presence of sediments on the seafloor, he used a polynomial for isostatic correction (Sykes et al., 1996) to predict total sediment thickness in the South Pacific.

5.4 Methods

5.4.1 Definition of horizons

In order to calculate sediment thicknesses and to differentiate between "pre-glacial" and "glacially transported" sediments, we defined the seafloor, the lower boundary of mainly glacially transported sediments, and the acoustic basement, by picking points along correlatable seismic reflections. Reflections from the acoustic basement surface were in most cases clearly identifiable, with the exception of some of the single-channel R/V *Boris Petrov* 1998 profiles where reflection amplitudes were too low, or beneath the continental slope where seafloor multiples obscure them (Figure 5.1). In order to define the base of glacially transported sediments (BGS), we used the seismic stratigraphy described in section 2.2. In the Amundsen Sea, where the published stratigraphy does not explicitly define a BGS horizon, we defined BGS at the bases of sediment mounds where we observe the initial occurrence of channels, following the interpretation of similar features on the Antarctic Peninsula margin. The horizon we defined closely resembles the base of Yamaguchi's (1988) Unit A. We

interpolated the horizons in regions where low data quality, inconclusive seismic stratigraphy, or tectonic boundaries prevented correlations. After picking the horizons, we extracted the horizons (in two way travel time (TWT) [s]) in steps of 50 CDPs or traces.

5.4.2 TWT [s] to depth [m]-conversion

Sound velocities in the sediments of the Antarctic margin are sparsely known. Downhole measurements of velocity at ocean drilling sites are very sparse and the use of short streamers during acquisition (due to ice conditions) often excludes the generation of a reliable velocity model. The study of Volpi et al. (2001), for example, shows enormously different seismic stacking velocities to downhole velocities measured during ODP Leg 178. We used an empirical relation (Carlson et al., 1986) for the transformation of TWT [s] into depth [m], which is based on 233 correlated depths from Deep Sea Drilling Project (DSDP) data, ranging up to a depth of 1.4 s (TWT). Sub-bottom depth (in km) is calculated as $Z = -(3.03 \pm 0.24) \ln [1-(0.52 \pm 0.04) T]$ where T is two-way travel-time in [s]; the rms-error is 26 m in depth. The method successfully reproduces the generally decreasing seismic velocity with decreasing depth and has previously been applied to seismic data acquired on the western Antarctic Peninsula and Bellingshausen Sea continental rises (Rebesco et al., 1997; Scheuer et al., 2006). A comparison of the downhole velocities in glacially transported sediments at sites 1095 and 1096 of ODP Leg 178 (Volpi et al., 2001) to calculated velocities shows a good agreement, and thus allows confidence in the calculated depth of the BGS horizon. The comparison also shows increasing differences with increasing depth, as shown by differing depth of the acoustic basement (Tab. 3).

A small number of sound velocities were determined with sonobuoys deployed along the seismic profiles TH-86002-009 in the Amundsen Sea (Yamaguchi et al., 1988). Tab. 4 shows comparisons of the sonobuoy data with the values calculated after Carlson et al. (1986). The comparison indicates that our calculated thicknesses and sound velocities are slight underestimates. Unfortunately, details of the sonobuoy deployments, processing method and exact values are not published, making it impossible to evaluate the reliability of the sonobuoy sound velocities. Hence, we decided to retain the sediment thicknesses calculated after Carlson et al. (1986) in the Amundsen Sea.

The formula from Carlson et al. (1986) has some limitations. TWT-to-depth conversions for values higher then 1.4 s TWT are extrapolated and thus not associated with an rms-error. Furthermore, the formula becomes insolvable for values higher than 3.8 s TWT. Therefore, we converted all TWT-values greater than 3.0 s to depth by assuming an average-velocity of 3200 m/s. This assumption affects only ~9% of the data points of the acoustic basement horizon, mainly observed on the continental slope/rise transition, and none of the BGS picks.

Table 3:

	ODP site 1095			Seismic data at CDP 1276 on Profile It-95135a		
	subbottom depth TWT [s]	**subbottom depth [m]**	**sound velocity [m/s]**	**subbottom depth TWT [s]**	**subbottom depth [m]**	**sound velocity [m/s]**
BSG (M3/M4-boundary)	580	505	~1740	550	480	~1735
Basement	1380 *	1430 *	~2070 *	1305	1286	~1970
	ODP site 1096			**Seismic data at CDP 4276 on Profile It-95130a**		
BSG (M3/M4-boundary)	1100 *	950 *	~1730 *	1116	1060	1900
Basement	2180 *	2155 *	~1980 *	2148	2477	2306

* =extrapolated

Comparison of sub bottom depths in [m], TWT in [ms] and sound velocities in [m/s]. The values in the right columns were calculated with the empirical formula of Carlson et al. (1986) using seismic data from profiles IT-95135a (CDP 1276) and IT-95130a (CDP 4276). The comparative values come from core measurements on site 1095 and 1096 of ODP Leg 178 (Fig.5. 1).

Table 4:

		Data from sonobuoy				Data from seismic profiles			
Location	Profile / Trace	seafloor [m]	depth to basement [s TWT]	sedthick [m]	**velocity [m/s]**	seafloor [m]	depth to basement [s TWT]	sedthick [m]	**velocity [m/s]**
SB 1	86002a / 300	4280	1.57	1800	**2300**	4455	1.70	1792	**2108**
SB 2	86003a / 2300	4180	2.28	3420	**3000**	4215	2.04	2290	**2245**
SB 4	86004c / 2650	4560	2.01	2410	**2400**	4451	1.94	2124	**2194**
SB 7	86006 / 1550	4160	0.99	940	**1900**	4109	0.81	714	**1770**

Comparison of depth, sediment thicknesses and sound velocities coming from sonobuoy data and seismic profiles which were acquired on the continental rise of the Amundsen Sea during the TH-86 cruise of the RV-Hakurei-Maru. Sonobuoy data were read off a figure published by Yamaguchi et al. (1988). The comparative data were calculated on the basis of the digital seismic profiles TH-86002-009 at the approximate sonobuoy locations, using the formula of Carlson et al. (1991).

5.4.3 Additional input information

Due to strong seafloor multiples, we were not able to define acoustic basement on most profiles crossing the continental shelf. Here, we used estimates of total sediment thickness from gravimetric models made along seismic profiles BAS-92325 and AWI-94003 instead (Cunningham et al., 2000; Alfred Wegener Institute, unpublished gravimetric data). We exclude estimates of sediment thicknesses on the innermost shelf due to the total lack of reliable data.

In addition to this, in order to maintain a realistically smooth appearance of the grids in areas remote from seismic data control it was necessary to include about 50 further estimates of total sediment thickness. On the continental slope and rise, our estimates were either reasonable guesses based on the physiographic context, or by comparison to the nearest seismic profile. We also referred to regional trends in the predicted sediment thickness grid of Eagles (2006). As the abyssal plain is largely uncovered by newer seismic profiles, we included estimates of total sediment thicknesses coming from the NGDC dataset, originally produced by Hayes and LaBrecque (1991), in the area north of 63°S and west of 80°W, sampled at 1° spacing. To us, this section of the dataset appears reliable as it is based on analogue seismic profiles and results from site 323 of DSDP Leg 35 (Figures 5.4a and b).

Continuous identifications of the BGS horizon on the cross-slope profiles are difficult due to discontinuous seismic reflections beneath the continental slope, which requires interpolation of the BGS horizon along the profiles. We added control points where necessary along the 1000 m bathymetric contour based on the average thickness (1800 m) of glacially transported sediments seen in profile crossings of this contour. To approximate thicknesses of glacial related sediments on the central abyssal plain, we assumed that the ice rafted material drilled in a depth of approximately 300 m at ocean drilling site 323 represents the distal complimentary boundary to the BGS horizon. Due to lack of data we excluded estimates of pre-glacial and glacially transported sediments on the Bellingshausen Sea and western Amundsen Sea abyssal plain.

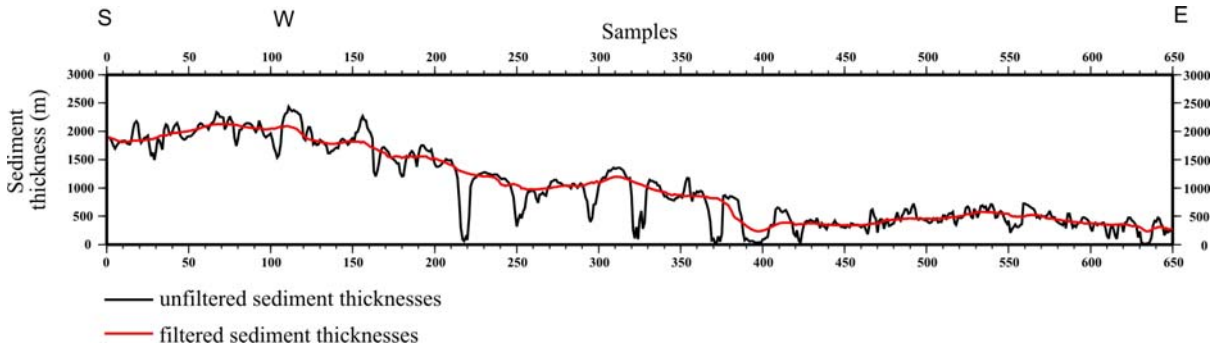

Fig. 5.3: Filtered and unfiltered sediment thicknesses of the profiles Th-86-002/3/8/9, along-slope orientated in the Amundsen Sea. The filtertype was a Gaussian filter with a filter width of 50 traces.

5.4.4 Gridding of sediment thicknesses

We produced isopach grids of total sediment thicknesses and of pre-glacial and glacially transported sediments of the South Pacific region between 60°W and 133°W and 62°S and 72°S, with a grid spacing of 2x2 minutes, using a continuous curvature gridding algorithm (*surface* algorithm, see GMT manual from Wessel and Smith, 2004). We used a low tension factor in view of the large areas to be interpolated between data profiles. Before gridding, a high cut cosine filter was applied to the input profile data along slope in the Amundsen Sea in order to prevent short wavelength anomalies related to seamounts having an effect on the finished grid (example of filtering in Figure 5.3). Elsewhere, and for the BGS horizon, low relief means that no filtering was required.

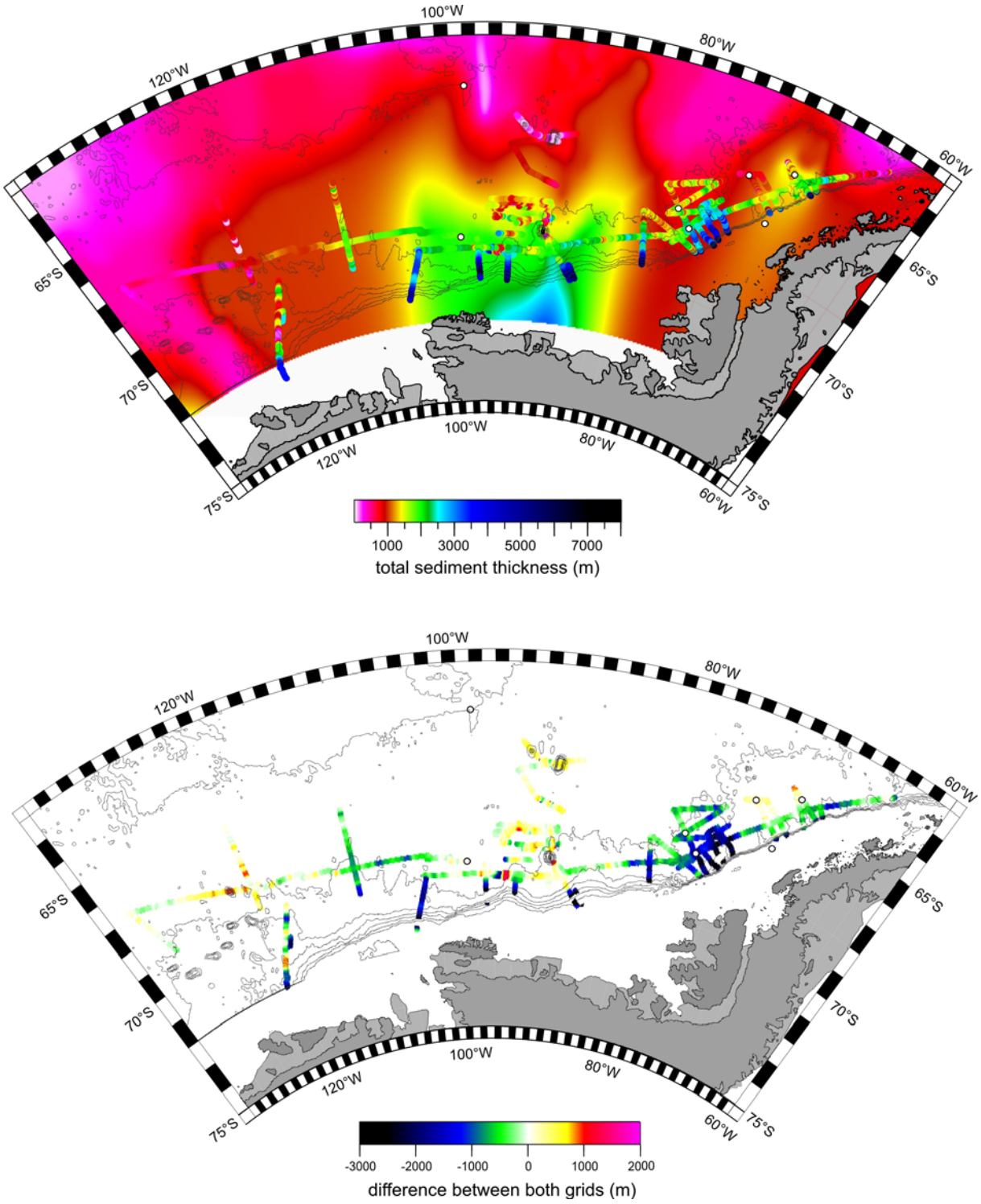

Fig. 5.4a, and b: a) *Comparison between total sediment thicknesses, based on the latest seismic data (displayed along the seismic tracks), and the isopach grid from the National Geophysical Data Centre (NGDC) (online available), previously published by Hayes and LaBrecque (1991) (color image in the background). b) The differences between both grids imaged along the seismic tracks.*

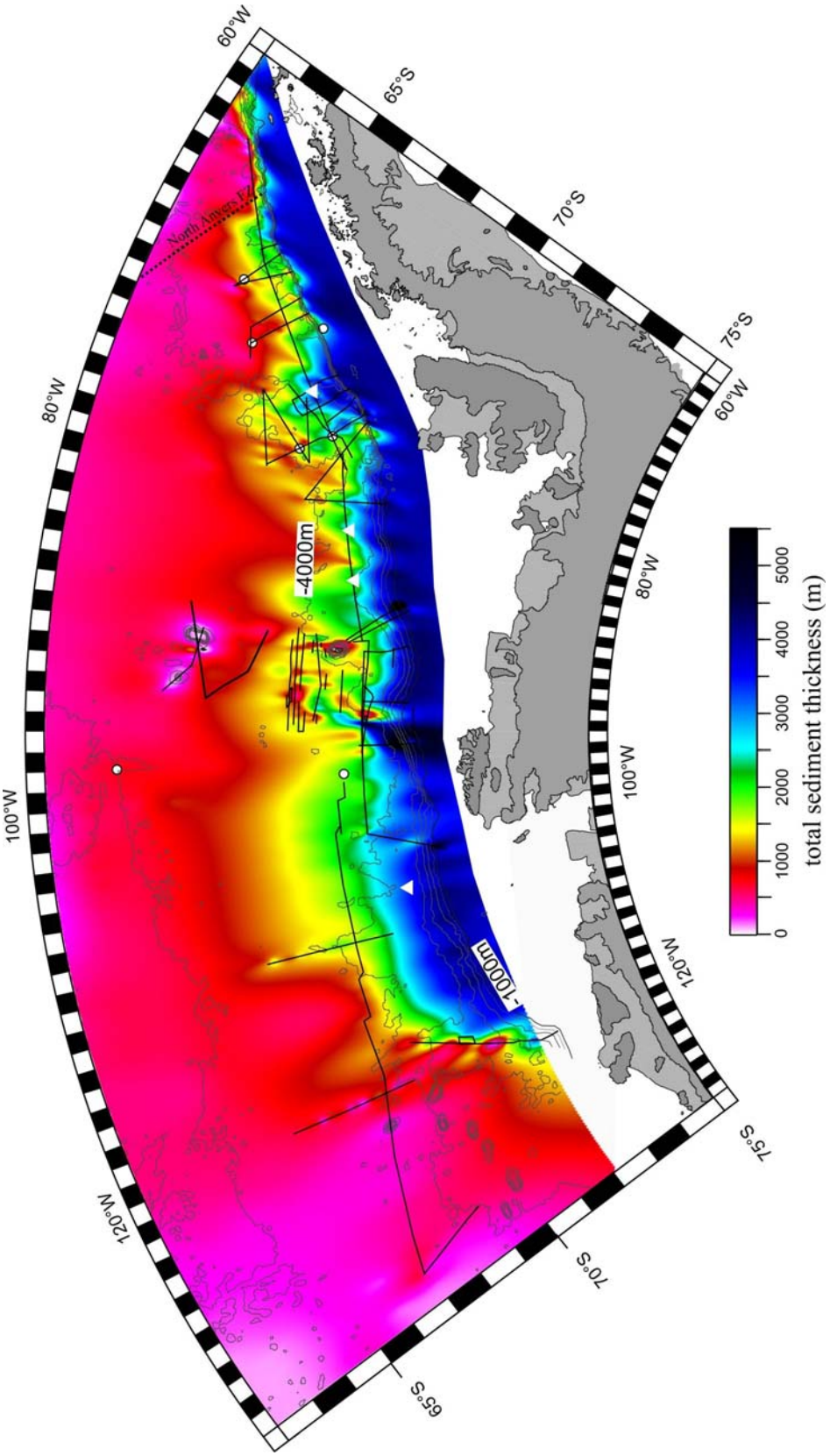

Fig. 5.5*: Isopach grid of total sediment thickness, calculated on the basis of MCS and SCS data*

5.5 Results

5.5.1 Total sediment thicknesses

Figures 5.4a and 5.4b allow a comparison between the isopach grid of Hayes and LaBrecque (1991) and our total sediment thicknesses calculated along the seismic tracks. The Hayes and LaBrecque isopachs do not show the general trends of thick sediment accumulations on the shelf and slope, and decreasing thicknesses to the deep sea that recent cross-slope seismic profiles produce in our grid. Numerous sediment mounds, drifts and channels on the continental rise only appear in our grid. In contrast, thicknesses on the abyssal plain correspond well, as the two compilations are largely based on the same data there. Our TWT-to-depth-conversion is more complete than that applied by Hayes and LaBrecque who assumed an average sound velocity of 2 km/s in sediment, unless other sound velocities had been noticed in the original works.

Some of the features shown for the first time by the new grid of total sediment thickness are described here (Figure 5.5). Peak thicknesses, exceeding 4000 m, occur along the continental shelf and slope of the entire SE-Pacific continental margin with a general decrease towards the deep sea (e.g. to 700 m at site 323, DSDP Leg 35). An east to west trend of increasing sediment thicknesses on the continental rise and abyssal plain can be observed across the entire grid. Discrete sediment mounds, drifts and wide depocentres are shown on the continental rise. Drift 3, north of Adelaide Island (thickness up to 2700 m on profile It-97235) and Drift 6 and Drift 7 (Figures 5.5 and 5.2a), north of Alexander Island (maxima of 3200 m at Drift 6 on profile It-95130) are observed on the western Antarctic Peninsula margin. Depocentres A, B and C in the Bellingshausen Sea can also be clearly identified, with thicknesses of up to 2500 m (Depocentre A, Figures 5.5 and 5.2b) and 2600 m (Depocentre B) on profile AWI-20010001. Depocentre C shows a north–striking step in sediment thickness, downwards to the west from 4500 to 450 m, which is related to the underlying basement step (profile BAS-92324, Figures 5.5 and 5.2d). North of Peter I Island, low sediment thicknesses coincide with the northwards extension of the Peter I Seamount. Profiles TH-86002 and 003 show widespread thick sediment cover in the eastern Amundsen Sea (Figures 5.5 and 2d). Maximum thicknesses of 2200 m are observed on profile TH-86003, and thick sediments are recorded along the northern part of profile TH-86004. To the west of this profile sediment thicknesses show a marked decrease to less then 250 m.

A comparison between our grid of total sediment thickness and that of predicted sediment thicknesses from Eagles (2006) is shown on Figure 6a and b. The sediment thicknesses calculated from residual gravity anomalies are generally much higher than those measured in our seismic profiles. Peak differences of about 7 km occur on the upper continental slope and on the continental rise of the western Amundsen Sea. In general, the greatest differences on the continental rise, of around 2000 m, are shown in areas of high sediment thicknesses such as at Drift 6/Drift 7. In the western Bellingshausen Sea and near Peter I Island, predicted sediment thicknesses are up to 4 km greater than seen in seismic profiles. Elsewhere, the predicted thicknesses are consistently 1–3 km thicker than seismic data show.

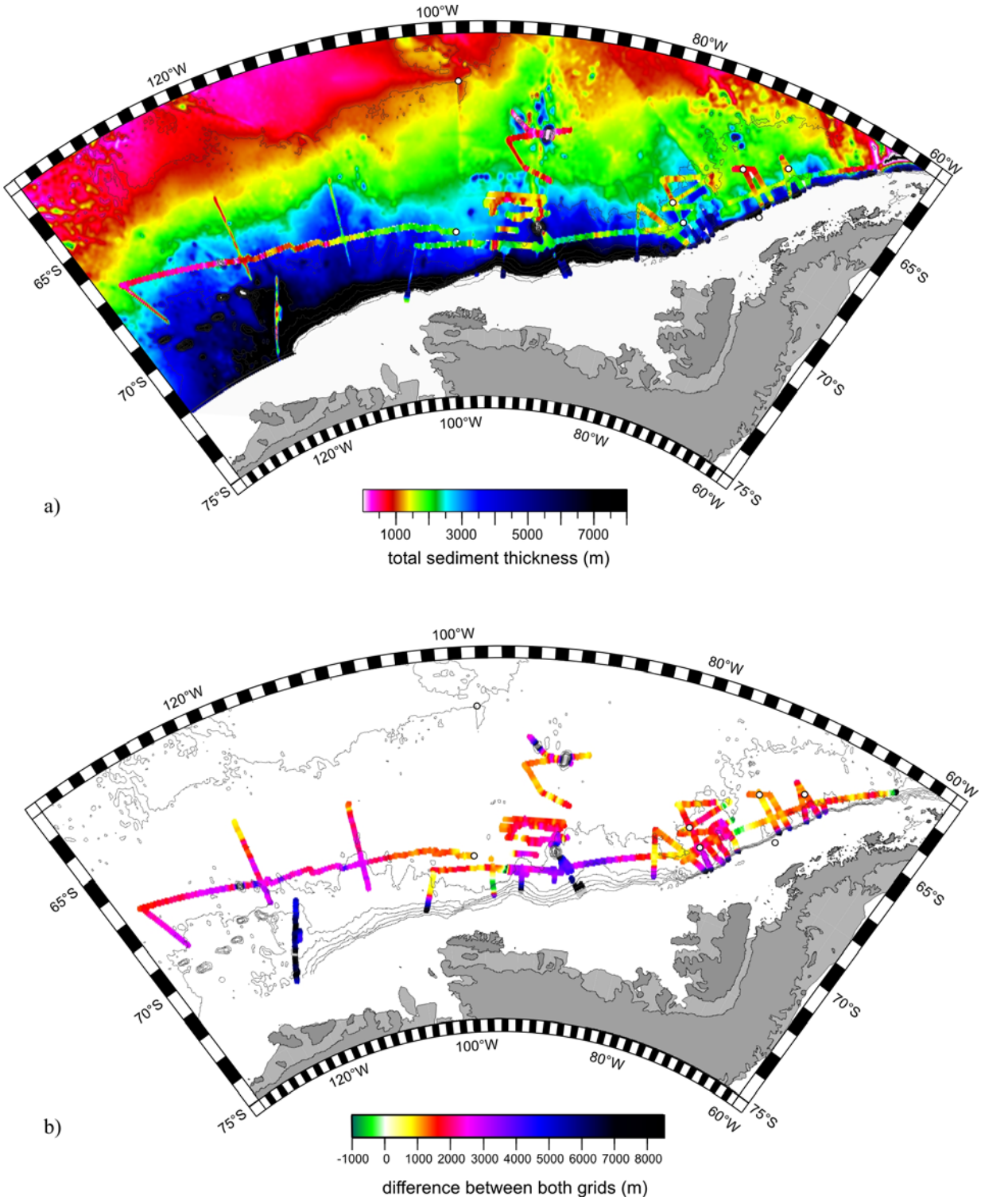

***Fig. 5.6a, and b**: a) Comparison between the total sediment thicknesses, based on the latest seismic data (displayed along the seismic tracks), and predicted sediment thicknesses derived from the grid of isostatic corrected residual bathymetry from Eagles (2006) (colour image in the background). b) The differences between both grids, imaged along the seismic tracks.*

5.5.2 Pre-glacial and glacially transported sediments

We observe an overall trend of westward increasing thicknesses of pre-glacial sediments on the continental rise (Figure 5.7), similar to the grid of total sediment thicknesses. Thick sediments of more than 1500 m were accumulated at drifts 6 and 7, depocentres B and C and in the eastern Amundsen Sea. Prominent basement highs, probably related to magmatic intrusions around Peter I Island, or depressions such as that along the Bellingshausen Gravity Anomaly (thicknesses exceeding 3500 m) can be clearly seen. The low pre-glacial sediment thicknesses in the central Bellingshausen Sea (100 – 500 m), and in the western Amundsen Sea near the Marie Byrd Seamounts are conspicuous. No pre-glacial sediments exist on the northernmost margin of the Antarctic Peninsula, northwest of the North Anvers fracture zone, where the oceanic basement is younger than 10 Ma.

The distribution of highs and lows in the thickness of mainly glacially transported sediments resembles that for total sediment thickness. The greatest thickness, of about 2000 m, is observed on the outer continental shelf (e.g. profile AWI-94003), and overall thicknesses decrease towards the deep sea. The thickest sediments on the continental rise are observed at the sediment depocentres, mounds and drifts on the continental slope and rise (Figure 5.7; e.g. 1200 m at Drift 3 and 1400 m at drifts 6 and 7 on profiles IT-97235 and IT-95130). Sediment thicknesses west of Drift 7 decrease to 250 m in a wide seafloor trough. Very high thicknesses of glacial sediments are seen on depocentres A and B (up to 1500 m and 1700 m on profile AWI-20010001). Values north of profile AWI-20010001 can only be guessed at, as there are no other data. We suppose these depocentres extend further out to sea than drifts 6 and 7, because of the thicker glacially transported sediments and the gentler continental slope inclination. Glacial sediment thicknesses decrease west of Peter I Island, as shown on profile BAS-92324 crossing sediment Depocentre C near the continental slope (maximum thickness of 750 m). The Petrov 98 profiles indicate a strong northward decrease of sediment thicknesses to less then 200 m. The northernmost of these profiles, in the vicinity of the DeGerlache Seamounts, show no features that enable us to define the BGS horizon.

The seismic profiles in the Amundsen Sea show sediment mounds and drifts separated by channels, similar to those on the Antarctic Peninsula margin (Figures 5.2a and e). Sediment thicknesses along profile TH-86002 and the eastern section of TH-86003 indicate four sediment mounds, which we refer to as Am1 – Am4 from east to west. Profile TH-86003 shows sediment thicknesses that increase to the west on the sediment mounds. The north-south trending profile TH-86004 indicates maximum thicknesses of about 700 m and a wide northward extent of mound Am4. From here, sediment thicknesses decrease to the west.

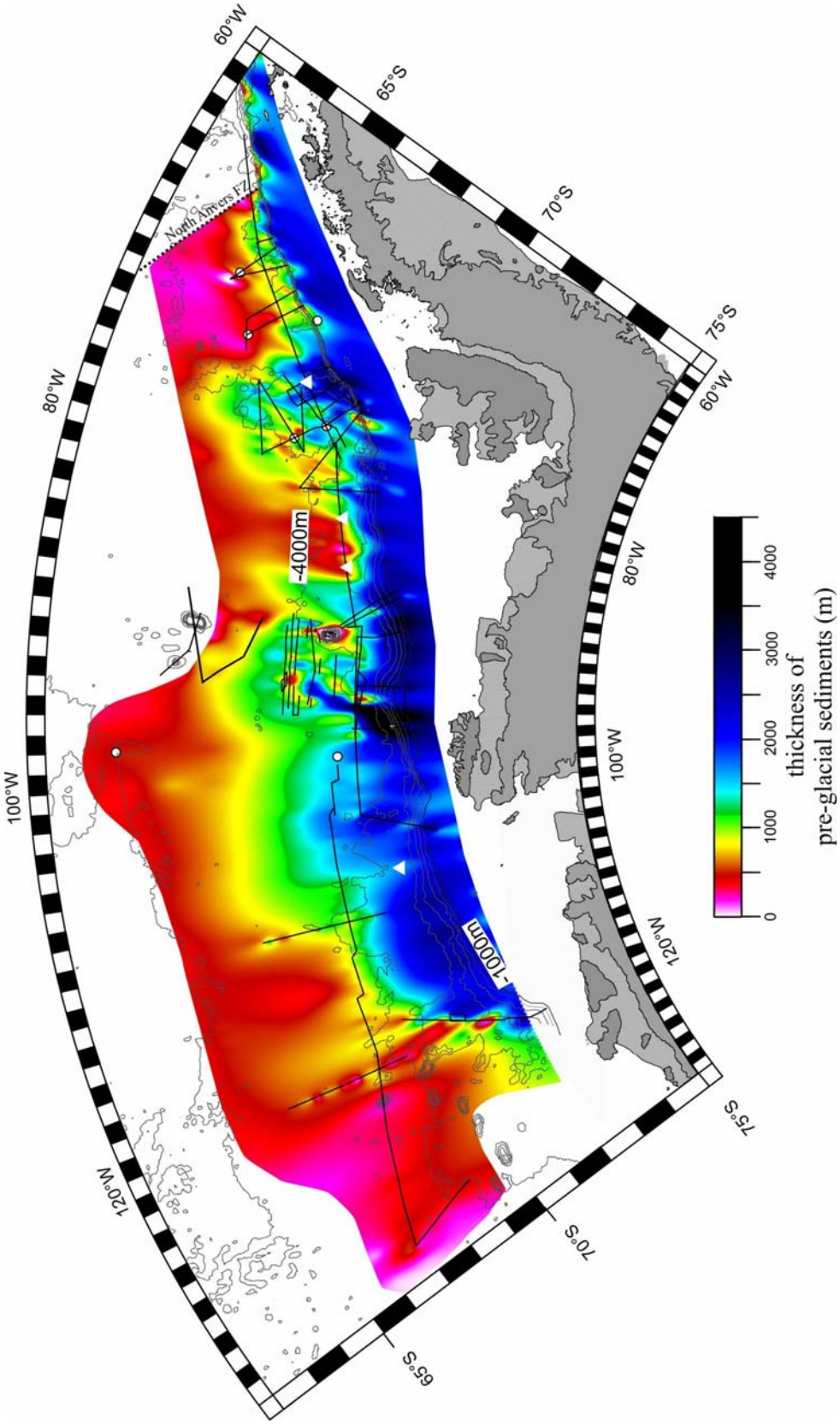

Fig. 5.7: *Isopach grid of pre-glacial sediments, calculated on the basis of MCS and SCS data.*

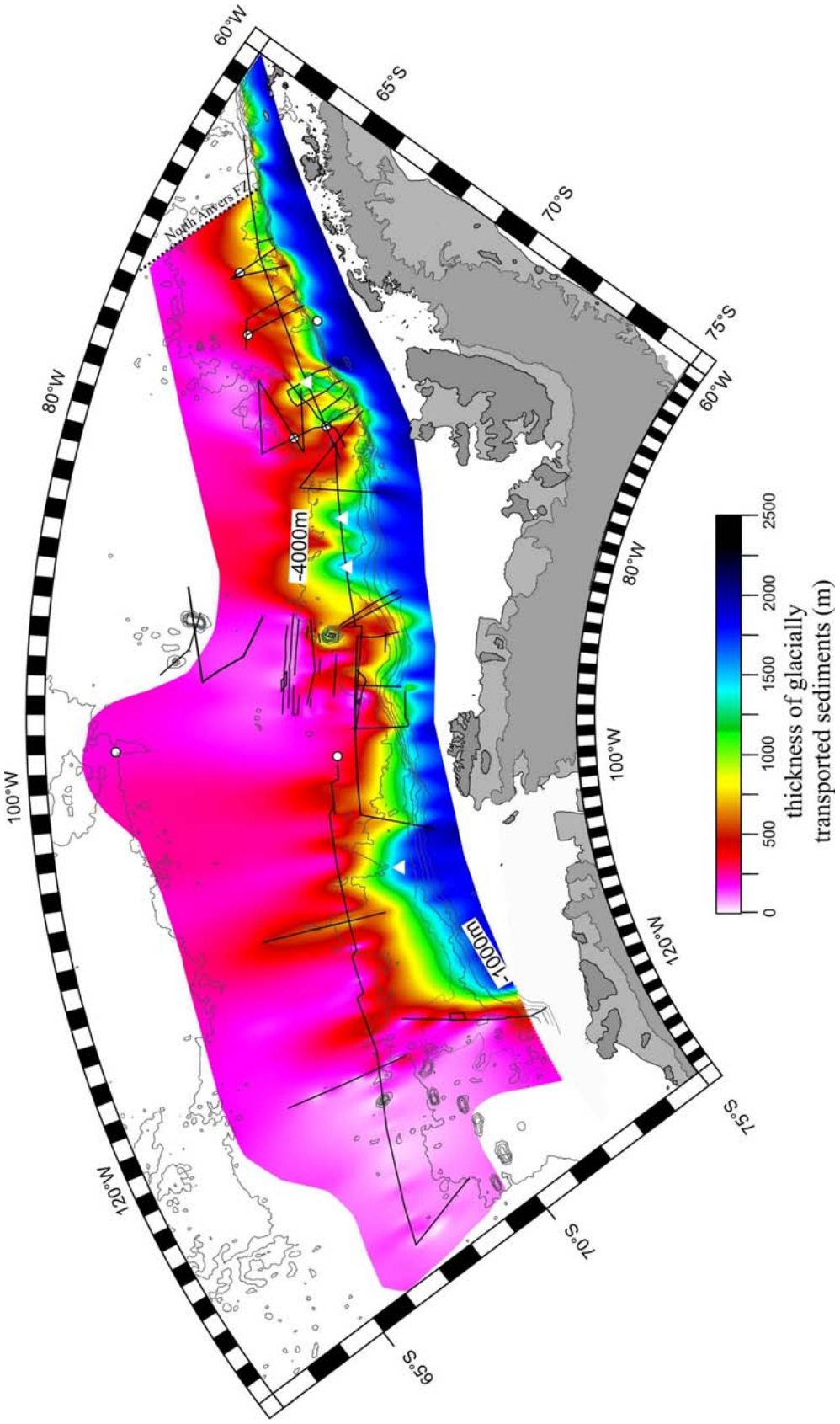

Fig. 5.8: *Isopach grid of glacially transported sediments, calculated on the basis of MCS and SCS data.*

5.6 Discussion

5.6.1 Terrigenous sediment supply

The main reason for the overall east to west trend of increasing total and pre-glacial sediment thicknesses on the continental rise and abyssal plain is the variation in the age of underlying oceanic crust, which is mostly due to oblique subduction at the continental margin. Oceanic basement ages vary from about 3 Ma on the northern Antarctic Peninsula margin to about 90-83 Ma in the Amundsen Sea. (e.g. Barker et al., 1982; Larter and Barker, 1991; McCarron and Larter, 1998; Cunningham et al., 2002; Eagles et al., 2004).

The western half of the Antarctic Peninsula is divided into four major ice drainage basins, which during glacial times fed sediment to turbidity channels offshore and, finally, sediment mounds and drifts on the continental rise (e.g. Rebesco et al., 2002). The greatest sediment thicknesses are found off these main glacial drainage areas (Figures 5.5 and 5.7), indicating that the supply of sediment by grounding ice streams during glacial periods is the decisive factor for the sediment distribution on the West Antarctic continental margin. The greatest sediment thickness is observed at drifts 6 and 7 off Marguerite Trough, the deepest depression on the western Antarctic Peninsula continental shelf, excavated by fluctuation of palaeo-ice streams between Alexander and Adelaide islands (e.g. Ó Cofaigh et al., 2002).

The topography and the development of sediment accumulations on the Bellingshausen Sea continental margin east of Peter I Island shows some distinct variation compared to the western Antarctic Peninsula continental margin. Instead of several smaller turbidity channel-related sediment mounds and drifts, large depocentres have developed. Bathymetric investigations conducted on the Bellingshausen Sea outer continental shelf revealed a wide trough named Belgica Trough, which is interpreted as the path of palaeo-ice streams and which may represent a major glacial drainage trough between Alexander and Thurston islands (Ó Cofaigh et al., 2005; Scheuer et al., 2006). Depocentre B developed below this trough and thus was interpreted as a trough mouth fan by Scheuer et al., which we will refer to as the Belgica Fan. The thickness of glacially transported sediments on Depocentre C is low compared to depocentres A and B, which may indicate a lesser supply of downslope sediments on the continental margin west of Thurston Island. After Scheuer et al. (accepted) we suggest that the majority of glacial sediments in Depocentre C are transported by a westward flowing bottom current and deposited on the elevated eastern side of a basement step.

The Amundsen Sea continental shelf is fed by two very active and fast flowing ice streams, the Pine Island and Thwaites Glacier, which account for approximately 4% of the outflow from the entire Antarctic Ice Sheet (Vaughan et al., 2001). Advances of these streams across the continental shelf during glacial maxima lead to the development of several glacial drainage troughs, of which the Pine Island Bay trough is one of the deepest (>1000 m) (Kellogg and Kellogg, 1987; Lowe and Anderson, 2002). The cross-slope profile ANT-94042 shows prograding foresets truncated by erosional unconformities (Nitsche et al., 2000), through which we infer a significant supply of glacially transported sediment to the continental slope and rise. As the Pine Island Bay trough reaches the central part of the shelf edge in front of mound Am4 (Lowe and Anderson, 2002), and mounds Am3 and 4 show highest thicknesses of glacial sediments on the along-slope profiles, we infer this area to be the main accumulation zone on

glacially transported sediments. Thicknesses of glacial sediments calculated on profile ANT-94042 are less than those on the Bellingshausen Sea continental margin, which is surprising in view of the absence of any substantial glacial drainage area or major ice streams onshore the Bellingshausen Sea. Lack of seismic data prohibits any further consideration of this question.

The reason for the relatively great thickness of 'glacial' sediments at site 323 (about 300 m), in comparison to the northernmost Petrov 98 profiles (about 200 m), may be a higher biogenic sedimentation rate. This location lies beyond the southern ACC front and thus, in a zone of higher organic production. In addition, it should be remembered that the ice rafted debris recovered near 300 m b.s.f. at site 323 can not be unequivocally related to the begin of grounding ice advances on the continental shelves.

5.6.2 Sediment accumulation rates

In order to compare the local histories of grounding ice development on the continental shelves, we approximated accumulation rates of glacially transported sediment on the continental rise. The deepest samples of sediment drilled at ODP site 1095 suggest the existence of a glacial regime since about 9.6 Ma (e.g. Barker and Camerlenghi, 2002). Drilling at site 1095 just reached the boundary between Rebesco et al.'s (1997) seismic units M3 and M4, which we adopt as the BGS horizon. Hence, we can approximate the minimum age of BGS as about 10 Ma throughout eastern and central Bellingshausen Sea where we can correlate the M3/M4 boundary. Dating of BGS as 10 Ma in the western Bellingshausen Sea and Amundsen is more speculative, as no tie to site 1095 was possible.

We calculated deposition rates of uncompacted sediments at locations in the four highest sediment thicknesses areas (Figures 5.5, 5.7 and 5.8). Of these, mound Am3 is sampled more distally, by seismic profile TH-86003, than the others. In order to calculate comparable sediment deposition rates, therefore, we chose a more proximal point sampled from our grid, halfway between the seismic profile and the shelf edge (Tab. 5).

Table 5:

Location		deposition period [m.y.]	sediment thickness [m]	sediment deposition rate [m/m.y.]
a) Drift 6	glacially transported sediments	10	1400	**140**
	pre-glacial sediments	29	1600	**55**
	total sediments	39	3000	**76**
b) Depocentre A	glacially transported sediments	10	1550	**155**
	pre-glacial sediments	37	950	**26**
	total sediments	47	2500	**53**
c) Depocentre B (eastern part)	glacially transported sediments	10	1700	**170**
	pre-glacial sediments	46	850	**18**
	total sediments	56	2550	**46**
d) mound Am3	glacially transported sediments	10	1600 *	**160 ***
	pre-glacial sediments	74	1500 *	**20 ***
	total sediments	~85	3100 *	**36 ***

*Average sediment thicknesses and sediment deposition rates calculated in the major accumulation areas. We chose locations with approximately the same distance to the shelf edge in order to enable comparisons. White triangles mark the locations on Figures 5. 5, 5.7 and 5.8. * = sampled values from the grid.*

Despite the overall increase of sediment thicknesses from east to west (Figures 5.5, 5.7 and 5.8), we observe a decrease of the total and pre-glacial sediment deposition rate. The high rate of 'pre-glacial' sedimentation off the western Antarctic Peninsula suggests a high sediment supply prior to the late Miocene. This is consistent with the interpretation of seismic unit M4 (Figure 5.2a) as an initial "drift-growth stage", with an estimated onset at 15 Ma, by Rebesco et al. (1997). Those authors mentioned that M4 may already have been deposited under glacial influence and in interaction with a bottom current prior to 9.6 Ma. As the elevated Antarctic Peninsula acts as a major barrier to tropospheric circulation, resulting in high snowfall and snow accumulation onshore (e.g. Reynolds, 1981), this region may have been more sensitive to Miocene climate changes than the adjacent regions to the west, so it is possible that ice streams developed earlier there.

In contrast to the Antarctic Peninsula, Scheuer et al. (2006) estimated a relatively low sediment deposition rate in the Bellingshausen Sea prior to 5.3 Ma (106 m/m.y. at Depocentre A) which they attributed to a wide continental shelf and low lying hinterland. Subglacial topography (Lythe et al., 2000) and bathymetry data show similar conditions apply for the Amundsen Sea, which can be invoked to explain the low deposition rate there too.

The highest deposition rate of glacially transported sediments of 170 m/m.y. in average was estimated at Depocentre B, which goes with a very high peak (deposition rate of 295 m/m.y.) in Pliocene-Pleistocene times (since 5.3 Ma) calculated by Scheuer et al.(2006). Those authors relate it to the development of very large ice drainage basins (Belgica Trough), high erosion rates on- and offshore, high ice flow velocities and the great width of the continental shelf (up

to 480 km west of Alexander Island). Deposition rates on the western Antarctic Peninsula, at Depocentre A and at mound Am3 are very similar, varying between 140 and 160 m/m.y. Even though sparse data in the Amundsen Sea make estimates of sediment thicknesses and deposition rates speculative, an estimated deposition rates of 160 m/m.y. on the upper continental rise seams reliable, with respect to the a similar width of the Amundsen Sea continental shelf to the Bellingshausen Sea and the fact that Pine Island Bay is a large glacial drainage outlet.

5.6.3 Influence of ocean bottom currents

Temperature measurements (Gordon, 1966), sea-bed photography (Hollister and Heezen, 1967), and current meter readings (Nowlin and Zenk, 1988; Camerlenghi et al. 1997) suggest a westward flowing bottom contour current follows the western margin of the Antarctic Peninsula. The influence of bottom currents on the distribution of sediments and structures of sediment deposits along the West Antarctic continental margin is well documented by several studies of contourite drifts at the Antarctic Peninsula margin (e.g. Rebesco et al., 1997) (Figure 5.2a). In addition to these, Scheuer et al. (accepted) identified a channel related sediment drift at Depocentre C in the western Bellingshausen Sea (Figure 5.2d). The development of such features seems to be related to the availability of contouritic detritus supplied from steep, unstable continental slopes with frequently-occurring turbidity currents.

The sediment accumulations on the Antarctic Peninsula margin and in the Amundsen Sea show similarities, consisting as they do of sediment mounds with steep and gentle flanks separated by erosional channels (Figures 5.2a and e). Although this may indicate a contour current influence in the Amundsen Sea, it should be remembered that the asymmetries of the contourite drifts on the Antarctic Peninsula margin are not always consistent with a westward current flow (Rebesco et al., 2002), and so the orientations of the Amundsen Sea mounds, with their steep easterly edges, can not be considered a strong indicator of the proposed current's direction. The higher elevation of the western channel levees may be related to the influence of the Coriolis force on turbidity currents.

5.6.4 Implications for geodynamics

Eagles (2006) noted that thicknesses in his grid of predicted sediment thicknesses (Figure 5.6a) were consistently greater than those in the Hayes and LaBrecque dataset, and attributed this to two causes. The first cause was underestimation of sediment thicknesses by Hayes and LaBrecque due to non-imaging of seismic basement in many of their data, which is confirmed by our new data. The second cause was long wavelength residual bathymetry anomalies formed due to crustal thickness variations and flow occurring in the mantle, known as dynamic topography. Eagles (2006) noted that dynamic uplift of 1 km would contribute to overestimates of 3.8–6.9 km in his predicted sediment thicknesses. The regional systematic overestimate of 1–3 km, shown in the comparison of Eagles' (2006) predicted sediment thicknesses with our seismic data in figure 5.6b, is thus consistent with dynamic uplift of less than 1 km. Morelli and Danesi's (2004) tomographic images provide additional evidence for dynamic topography in the Bellingshausen and Amundsen Seas, in the form of a widespread low velocity anomaly

that can be interpreted in terms of warm upwelling mantle material. Dynamic topography is also often correlated with other surface manifestations of mantle convection, notably excess volcanism, for instance around Iceland (e.g. Louden et al., 2004). Studies of volcanic rocks from Marie-Byrd Land provide ample evidence for late Cenozoic volcanic activity (e.g. Behrendt, 1999; Rocchi et al., 2002), and offshore, in the Amundsen Sea, there is evidence for excess volcanism at the Marie Byrd Seamounts, although these are assumed from seismic data and subsidence calculations on guyots to have developed prior to the younger sedimentation. Peter I Island, further east, is an active volcano that may also be attributed, along with the nearby De Gerlache seamounts, to the same cause as the regional uplift. The peak sediment thickness overestimates in Eagles' (2006) grid coincide with these centres and thus may be related to increased dynamic topography around them, or to crustal thickening associated with the volcanic activity.

5.6.5 Outlook

The modelled sediment isopach grids can be used to adjust existing paleobathymetric models for the effects of sedimentation. Such grids should be a central element of paleoceanographic models that set out to investigate the origins and effects of topographically steered currents like the ACC or AABW. To do this for the various times that might be of interest in the region will require the classification of the entire sediment package into discrete dated sediment units. As yet, the sparse data acquired in the study area did not allow the establishment of such an age model. The lack of data coming from deep penetrating ocean boreholes in the Amundsen Sea makes a dating of sediment units there especially difficult. Our classification into "pre-glacial"- and "glacially transported" sediments along seismic profiles and its northward extrapolation is the first classification of the sediments ranging across the South Pacific which can be tentatively dated by assuming that the development of grounding ice on the continental shelves started at about 10 Ma.

5.7 Summary and conclusions

A large set of seismic reflection data acquired in the Southern Pacific off West Antarctica was used to model isopach grids that provide insights into the tectonic structure and sedimentary architecture of the study area. In the future, grids like these can be used to improve existing paleobathymetric models by considering the effects of sedimentation, in order to provide more precise boundary conditions for models of palaeoceanographic development. The adoption of an age for the onset of glacial sediment supply at about 10 Ma allowed approximations of sedimentation rates on the continental rise and, thus, a comparison of local sedimentary histories.

High sedimentation rates on the western margin of the Antarctic Peninsula prior to 10 Ma points to an early glacial influence on the sediment supply to the continental rise. In contrast, pre-glacial sediment deposition rates in the Bellingshausen Sea and Amundsen Sea are about half as much as on the Antarctic Peninsula, which can be related to low relief of the sediment source area and wide continental shelves. Furthermore, this comparison may indicate that the

mid Miocene Antarctic Peninsula was more sensitive to climatic change than its neighbouring areas, resulting in the earlier development of ice streams.

The distribution of glacially transported sediments on the continental rise is in general consistent with the arrangement of recent drainage outlets on the shelf, as the thickest deposits were identified at the mouths of the Marguerite Trough (Antarctic Peninsula), Belgica Trough (Bellingshausen Sea) and Pine Island Trough (Amundsen Sea). Maximum sedimentation of glacial sediments is estimated in the western Bellingshausen Sea and central Amundsen Sea. However, differences in sediment deposition rates suggest significant local variability in the timing of glaciations and ice advances over the West Antarctic continental margin. So, we reiterate the tentative nature of our classification, which is due to sparse coverage of seismic profiles and very limited or absent drill hole information.

Acknowledgements

This study is partly funded through grant no. GO 724/3-1 of the Deutsche Forschungsgemeinschaft (DFG).

REFERENCES

Anderson, J.B., J. S. Wellner, A. L. Lowe, A. B. Mosola, and S. S. Shipp (2001), The footprint of the expanded West Antarctic Ice Sheet: ice stream history and behaviour. *GSA Today, 11*, 4-9.

Barker, P.F. (1982), The Cenozoic subduction history of the Pacific margin of the Antarctic Peninsula: ridge crest interactions, *J. Geol. Sci*., 139, 787-801.

Barker, P.F., and A. Camerlenghi (2002), Glacial history of the Antarctic Peninsula from Pacific margin sediments, in *Proc. ODP, Sci. Results 178 [online]*, edited by P. F. Barker, A. Camerlenghi, G. D. Acton, and A. T. S. Ramsay, Available from World Wide Web: <http://wwwodp.tamu.edu/publications/178_SR/synth/synth.htm>.

Bart, P. J., and J. B. Anderson (1995), Seismic record of glacial events affecting the Pazific margin of the northwestern Antarctic Peninsula, in *Geology and seismic stratigraphy of the Antarctic margin. Antarctic Research Series,* vol.68, edited by A. K. Cooper, P. F. Barker, and G. Brancolini, pp. 75-95, American Geophysical Union, Washington, DC.

Bart, P.J., and J. B. Anderson (2000), Relative temporal stability of the Antarctic ice sheets during the late Neogene based on the minimum frequency of outer shelf grounding events, *Earth Planet. Sci. Lett., 182,* 259-272.

Bart, P.J., J. B. Anderson, and F. Trincardi (2000), Seismic data from the Northern basin, Ross Sea, record extreme expansions of the East Antarctic Ice Sheet during the late Neogene, *Mar. Geol., 166,* 1-4.

Behrendt, J.C. (1999), Crustal and lithospheric structure of the West Antarctic Rift Systemfrom geophysical investigations - a review. *Global and Planetary Change, 23*, 25-44.

Brown, B. C. Gaina, R. D. Müller (2006), Circum-Antarctic palaeobathymetry: Illustrated examples from Cenozoic to recent times. *Palaeogeog., Palaeoclima.t, Palaeoecol., 231,* 158-168, *d*oi:10.1016/j.palaeo.2005.07.033

Camerlenghi, A., A. Crise, C. J. Pudsey, E. Accerboni, R. Laterza, and M. Rebesco, (1997), Ten-month observation of the bottom current regime across a sediment drift of the Pacific margin of the Antarctic Peninsula. *Antarct. Sci, 9*, 426-433.

Carlson, R. L., A. F. Gangi, and K. R. Snow (1986), Empirical reflection travel time versus depth and velocity versus depth functions for the deep sea sediment column. *J. Geophys. Res., 91*, 8249-8266.

Cooper, A. K., P. Barrett, K. Hinz, V. Traubea, G. Leitchenkov, and H. Stagg (1991), Cenozoic prograding sequences of the Antarctic continental margin: a record of glacioeustatic and tectonic events. *Mar. Geol., 102*, 175-213.

Cooper, A. K., P. F. Barker, and G. Brancolini (1995), *Geology and seismic stratigraphy of the Antarctic margin*, Antarct. Res. Ser., 68, 301 pp, CD-ROMs, AGU, Washington D. C.

Cunningham, A. P., R. D. Larter, and P. F. Barker (1994), Glacially prograded sequences on the Bellingshausen Sea continental margin near 90°W. *Terra Antarct., 1*, 267-268.

Cunningham, A. P., R. D. Larter, P. F. Barker, K. Gohl, and F.-O. Nitsche (2002), Tectonic evolution of the pacific margin of Antarctica: 2. Structure of Late Cretaceous-early Tertiary plate boundaries in the Bellingshausen Sea from seismic reflection and gravity data, *J. Geophy. Res., 107* (B12), 2346, doi: 10.1029/2002JB001897.

DeSantis, L., J. B. Anderson, G. Brancolini, and I. Zayatz (1995), Seismic record of late Oligocene through Miocene glaciation on the central and eastern continental shelf of the Ross Sea, *Antarctic Research Series, 68*, 235-260.

DeSantis, L., G. Brancolini, and F. Donda (2003), Seismo-stratigraphic analysis of the Wilkes Land continental margin (East Antarctica): influence of glacially driven processes on the Cenocoic deposition, *Deep-Sea Research II, 50*, 1563-1594.

Dingle, R.V., and M. Lavelle (1998), Antarctic peninsula cryosphere: early Oligocene (c. 30 Ma) initiation and revised glacial chronology, *J. Geol. Soc., 155* (No3), 433-437.

Dowdeswell, J.A., C. Ó Cofaigh, and C. J. Pudsey (2004), Continental slope morphology and sedimentary processes at the mouth of an Antarctic palaeo-ice stream, *Marine Geology, 204*, 203-214.

Eagles, G., K. Gohl, and R. D. Larter (2004), High resolution animated tectonic reconstruction of the South Pacific and West Antarctic margin, *Geochem., Geophys., Geosyst., 5* (No7), 1-21.

Eagles, G. (2005), Deviations from an ideal thermal subsidence surface in the southern Pacific Ocean, *Terra Antartica Reports*, special issue on Frontiers in Antarctic Earth Sciences.

Ewing, M, J. I. Ewing, R. E. Houtz, and R. Leyden (1968), Sediment distribution in the Bellingshausen Basin, in *Antarctic Oceanography, Symp., Sept. 13-16, 1966*, Santiago, Chile. Cambridge (Scott Polar Res. inst), 89-99.

Faugères, J.C., D. A. D. Stow, P. Imbert, and A. Viana (1999), Seismic features diagnostic of contourite drifts, *Marine Geology, 162*, 1–38.

Gohl, K., F. Nitsche, and H. Miller (1997), Seismic and gravity data reveal Tertiary interplate subduction in the Bellingshausen Sea, southeast Pacific, *Geology, 25*, 371-374.

Gordon, A. L. (1966), Potential temperature, oxygen and circulation of bottom water in the Southern Ocean, *Deep-Sea Research, 13*, 1125-1138.

Hampton, M. A., S. L. Eittreim, and B. M. Richmond (1987), Post-breakup sedimentation on the Wilkes Land Margin, Antarctica, in *The Antarctic continental margin, Geology and*

Geophysics of offshore Wilkes Land, edited by S. L. Eittreim, and M. A. Hampton, pp 75-89, Circum-Pacific Council for Energy and Mineral Recourses, Earth Science Series, 5A.

Hayes, D., E. and J., L. LaBrecque (1991), Sediment Isopachs: Circum-Antarctic to 30°*S*, in *Marine Geological and Geophysical Atlas of the Circum-Antarctic to 30S*, edited by D.E. Hayes, pp. 29-33, American Geophys. Union, Washington, D.C.

Hollister, C. D., and B. C. Heezen (1967), The floor of the Bellingshausen Sea, in *Deep-sea fotography, the John Hopkins studies, 3*, edited by J. B. Hersey, pp. 177-189, John Hopkins Press, Baltimore.

Hollister, C. D. and C. Craddock et al. (1976), *Initial reports of deep sea drilling project, 35*. U. S. Government Printing Office, Washington D. C., 929 pp.

Houtz, R. E., M. Ewing, D. E. Hayes, and B. Naini (1973), Sediments isopachs in the Indian and Pacific sector (105°E to 70°W), *Antarctic Map Folio Ser., Folio 17*, Plate 5, American Geophysical Society, Washington D.C.

Kellogg, T.B., and D. E. Kellogg (1987), Recent glacial history and rapid ice stream retreat in the Amundsen Sea, *J. Geoph. Res., 92* (B9), 8859-8864.

Kennett, J.P. (1977), Cenozoic evolution of Antarctic glaciation, the circum-Antarctic Ocean, and their impact on global paleoceanography. *J. Geophys. Res., 82*, 3843-3860.

Kimura, K. (1982), Geological and Geophysical Survey in the Bellingshausen Basin, off Antarctica. *Antarctic Record, 75*, 12-24.

Kuvaas, B., and Y. Kristoffersen (1991), The Crary Fan: a trough-mouth fan on the Weddell Sea continental margin, Antarctica, *Mar. Geol., 97*, 345-362.

Larter, R. D., and P. F. Barker (1991), Effects of ridge crest-trench interaction on Antarctic-Phoenix spreading Forces on a young subducting plate, *J. Geophys. Res., 96*, 19583-19608.

Larter, R. D., A. P. Cunningham (1993), The depositional pattern and distribution of glacial-interglacial sequences on the Antarctic Peninsula Pacific margin. *Mar. Geol., 109*, 203-219.

Larter, R. D., M. Rebesco, L. E.Vanneste, L. A. P. Gamboa, and P. F. Barker (1997), Cenozoic tectonic, sedimentary and glacial history of the continental shelf west of Graham Land, Antarctic Peninsula, in *Geology and Seismic Stratigraphy on the Antarctic Margin, Part 2*, American Geophysical Union, Antarctic Research Series 71, edited by A. K. Cooper and P. F. Barker, pp. 1-27, American Geophysical Union, Washington, DC.

Larter, R. D., A. P. Cunningham, P. F. Barker, K. Gohl, and F.-O. Nitsche (2002), Tectonic evolution of the pacific margin of Antarctica: 1. Late Cretaceous tectonic reconstructions, *J. Geophys. Res., 107*(B12), 2345, doi: 10.1029/2000JB000052.

Laske, G., and G. Masters (1997), A Global Digital Map of Sediment Thickness. *EOS Trans. AGU, 78 (F483)*, available from World Wide Web: <http://mahi.ucsd.edu/Gabi/sediment.html

Lazarus, D., and J.-P. Caulet (1993), Cenozoic southern ocean reconstruction from sedimentologic, radiolarian, and other microfossil data, in *The Antarctic Palaeoenvironment: A perspective on global change*, edited by L.-P. Kennet, and D. A Warnke, pp. 145-174, Am. Geophys. Union, Washington, D.C.

Louden, K. E., B. E. Tucholke, and G. N. Oakey (2004), Regional anomalies of sediment thickness, basement depth and isostatic crustal thickness in the North Atlantic Ocean, *Earth Planet. Sci. Lett., 224*, 193-211.

Lowe, A. L., and J. B. Anderson (2001), Evidence for abundant subglacial meltwater beneath the paleo-ice sheet in Pine Island Bay, Antarctica, *J. Glac., 49* (164), 125-138.

Lythe, M. B., and D. G. Vaughan, and the BEDMAP Consortium (2000), BEDMAP – Bedtopography of the Antarctic, scale 1:10,000,000. *Brit. Antarct. Surv.*, Cambridge, U.K., available from World Wide Web: http://www.antarctica.ac.uk/aedc/bedmap/database/

McCarron, J. J., and R. D. Larter (1998), Late Cretaceous to early Tertiary subduction history of the Antarctic Peninsula, *J. Geol. Soc. Lond., 155*, 255-268.

McGinnes, J. P., D. E. Hayes, and N. W. Driscoll (1997), Sedimentary processes across the continental rise of the southern Antarctic Peninsula. *Mar. Geol., 141*, 91-109.

Morelli, A., and S. Danesi (2004), Seismological imaging of the Antarctic continental lithosphere: a review. *Glob. Planet. Change, 42*, 155-165.

NGDC, National Geophysikal Data Centre, Total Sediment Thickness of the World's Oceans and Marginal Seas [online], available from World Wide Web: http://www.ngdc.noaa.gov/mgg/sedthick/sedthick.html

Nitsche, F. O., K. Gohl, K. Vanneste, and H. Miller (1997), Seismic expression of glacially deposited sequences in the Bellingshausen and Amundsen Seas, West Antarctica, in *Geology and Seismic Stratigraphy of the Antarctic Margin: 2*, Antarctic Research Series, 71, edited by P. F. Barker and A. K. Cooper, pp. 95-108, Am. Geophys. Union, Washington, DC.

Nitsche, F. O., A. P. Cunningham, R. D. Larter, and K. Gohl (2000), Geometry and development of glacial continental margin depositional systems in the Bellingshausen Sea. *Mar. Geol., 162*, 277-302.

Nowlin Jr., W. D., and W. Zenk (1988), Currents along the margin of the South Shetland Island Arc, *Deep-Sea Res., 35*, 805-833.

Ó Cofaigh, C., C. J. Pudsey, J. A. Dowdeswell, and P. Morris (2002), Evolution of subglacial bedforms along a paleo-ice stream, Antarctic Peninsula continental shelf, *Geophys. Res. Lett., 29*, (8), 1199, doi:10.1029/2001GL014488.

Ó Cofaigh, C., R. D. Larter, J. A. Dowdeswell, C-D. Hillenbrand, C. J. Pudsey, J. Evans, and P. Morris (2005), Flow of the West Antarctic Ice Sheet on the continental margin of the Bellingshausen Sea at the Last Glacial Maximum, *J. Geophys. Res., 110*, doi: 10.1029.2005JB003619.

Pudsey, C.J. and A. Camerlenghi (1998), Glacial-interglacial deposition on a sediment drift on the Pacific margin of the Antarctic Peninsula, *Ant. Sci., 10*, 286-308.

Rack, F. R. (1993), A geolocic perspective on the Miocene evolution of the Antarctic Circumpolar Current system. *Tectonophys., 222*, 397-415.

Reynolds, J., M. (1981), The distribution of mean annual temperatures in the Antarctic Peninsula, *Br. Antarct. Surv. Bull. 54*, 123-133.

Rebesco, M., R. D. Larter, A. Camerlenghi, and P. F. Barker (1996), Giant sediment drifts on the continental rise west of the Antarctic Peninsula, *Geo-Marine Lett., 16*, 65-75.

Rebesco, M., R. D. Larter, P. F. Barker, A. Camerlenghi, and L. E. Vanneste (1997), History of sedimentation on the continental rise west of the Antarctic Peninsula, in *Geology and Seismic Stratigraphy on the Antarctic Margin: 2*, Antarctic Research Series, 71, edited by A. K. Cooper, and P. F. Barker, pp. 29-49, Am. Geophys. Union, Washington, DC.

Rebesco, M., C. J. Pudsey, M. Canals, A. Camerlenghi, P. F. Barker, F. Estrada, and A. Giorgetti (2002), Case study 27: Sediment drifts and deep-sea channel systems, Antarctic Peninsula Pacific margin, mid-Miocene to present, in *Deep-Water Contourite Systems: Modern Drifts and Ancient Series, Seismic and Sedimentary Characteristics*, edited by D. A. V. Stow, C.J. Pudsey, J. Howe, J. C. Faugeres, and A. Viana, pp. 353-371, Spec. Publ. Geol. Soc. London, Memoirs 22.

Rocchi, S., P. Armienti, M. D'Orazio, S. Tonarini, J. R. Wijbrans, and G. Di Vincenzo (2002), Cenozoic magmatism in the western Ross Embayment: Role of mantle plume versus plate dynamics in the development of the West Antarctic Rift System, *Journal of Geophysical Research, 107* (B9), doi:10.1029/2001JB000515.

Rogenhagen, J., W. Jokat, K. Hinz, and Y. Kristoffersen (2005), Improved seismic stratigraphy of the Mesozoic Weddell Sea, *Mar. Geophys. Res., 25*, (No3-4). 265-282.

Rodrigues, E. A., R. E. Houtz, J. L. LaBrecque, and D. A. Drewry (1986), Total sediment thickness, south; total sediment thickness, northwest; total sediment thickness, northeast, in *South Atlantic Ocean and adjacentAntarctic continental margin, Atlas 13*, Ocean Margin Drilling Program, Regional Data Synthesis Series

SCAR Seismic Data Library, CD-ROM

Scheuer, C., K. Gohl, and G. Udintsev (accepted), Bottom-current control on sedimentation in the western Bellingshausen Sea, West Antarctica. *Geo-Marine Lett.*

Scheuer, C., Gohl, K., Larter, R. D., Rebesco, M., Udintsev, G. (2006), Variability in Cenozoic sedimentation along the continental rise of the Bellingshausen Sea, West Antarctica. *Marine Geology, 227* (3-4), 279-298.

Sijp, W., and M. H. England (2004), Effect of the Drake Passage throughflow on global climate. *J. Phys. Oceanogr., 34*, 1254-1266.

Smith, H. F. and P. Wessel (1998), New, improved version of Generic Mapping Tools released, *EOS Trans. Amer. Geophys. U., 79* (47), pp. 579.

Smith, W. H. F., and D. T. Sandwell (1997), Global seafloor topography from satellite altimetry and ship depth soundings, *Science, 277*, 1956-1961.

Stein, C., and S. Stein (1992), A model for the global variation in oceanic depth and heat flow with lithospheric age, *Nature, 359*, 123-128.

Sykes, T.J.S. (1996), A correction for sediment load upon the ocean floor: Uniform versus varying sediment density estimations-implications for isostatic correction. *Mar. Geol., 133* (1-2), 35-49.

Sykes, T. J. S., J.-Y. Royer, A. T. S. Ramsay, and R. B. Kidd (1998), Southern hemisphere palaeobathymetry, in *Geological evolution of ocean basins: results from the Ocean Drilling Program, Special Publication, 131*, edited by A. Cramp, C. J. McLeod, S. V. Lee and E. J. W. Jones, pp. 3-42, Geological Society, London, UK.

Tomlinson, J. S., C. J. Pudsey, R. A. Livermore, R. D. Larter, P. F. Barker (1992), Long-range sidescan sonar (GLORIA) survey of the Antarctic Peninsula pacific margin, in *Recent progress in Antarctic Earth Science, Terra Scientific Publishing Company, Tokyo*, edited by Y. Yoshida, K. Kaminuma, K. Shiraishi, pp. 423-429.

Tucholke, B. E., and R. E. Houtz (1976), Sedimentary framework of the Bellingshausen Basin from seismic profile data, in *Initial Reports of the Deep Sea Drilling Project, 35*, edited by C. D. Hollister, C, Craddock, et al., pp. 197-227, U.S. Government Printing Office, Washington, DC.

Vaughan, D. G., A. M. Smith, H. F. J. Corr, A. Jenkins, C. R. Bentley, M. D. Stenoien, S. S. Jacobs, T. B. Kellog, E. Rignot, and B. K. Lucchitta (2001), A review of Pine Island Glacier, West Antarctica: Hypotheses of instability vs. observations of change, in *The West Antarctic Ice Sheet: Behavior and Environment*, edited by R.B. Alley and R.A. Bindschadler, pp. 237-256, AGU Ant. Res. Series, 77.

Volpi, V., A. Camerlenghi, T. Moerz, P. Corubolo, M. Rebesco, M., and U. Tinivella (2001), 17. Data Report: Physical properties relevant to seismic stratigraphic studies, continental rise sites 1095, 1096, and 1101, ODP Leg 178, Antarctic Peninsula, in *Proceedings Volume, ODP, Sci. Results, 178*, edited by P. F. Barker, A. Camerlenghi, G. D. Acton, A. T. S. Ramsay, 1-40 [CD-Rom].

Wessel, P., and W. H. F. Smith (2004), The Generic Mapping Tool (GMT), Version 3.4.5, Technical Reference and Cookbook, SOEST/NOAA.

Yamaguchi, K., Y. Tamura, I. Mizukoshi, T. Tsuru, (1988), Preliminary report of geophysical and geological surveys in the Amundsen Sea, West Antarctica, *Proc. NIPR Symposium of Antarctic Geoscience, 2*, 55-67.

CHAPTER 6

This chapter summarises the main results and outstanding questions of the previous chapters, with respect to the aims of this thesis given in section 1.2, and briefly outlines proposed research activities in the future:

6.1 SUMMARY

The new interpretation of seismic reflection data contributed to and helped clarify the debate about late Miocene glacial dynamics on the West Antarctic continental margin in the South Pacific ocean. Analyses of profiles acquired in the Bellingshausen Sea enabled correlations between seismic units defined on the continental rise and the outer shelf, and the well-defined stratigraphy defined in ODP boreholes. An intermediate prograding sedimentary unit on the continental shelf edge indicates advances of grounding ice without significant erosion of the shelf surface, leading to deposition of glacially transported sediments on the continental slope and rise since about 9.6 Ma. Strongly eroding advances of grounded ice started at about 5.3 Ma, as shown by truncations of foresets and strong progradation. This change to strongly prograding units probably represents an important change in glacial dynamics that led to more intensively erosional ice advances. However, the dating of the first advance of grounding ice on the shelf remains questionable. A glacial advance could have removed evidence for any of the preceding advances, which makes it very difficult to set up a complete stratigraphy with the sparse data set to hand. For this reason, it has not been possible to identify evidence for single glacial-interglacial cycles in this study. The cross-slope profiles in the western Bellingshausen Sea indicate a complex history of multiple glacial advances and retreats, based on the presence of several thick prograding and aggrading sequence groups beneath the outer shelf. The dating of stratigraphic units in the westernmost Bellingshausen and Amundsen seas is more speculative as no tie to deep penetrating ocean drilling sites is possible. However, the identification in seismic data of what, for this region, are characteristically 'glacial' features such as sediment mounds or drifts on the continental rise, and frequently-occurring erosional channels caused by turbidity currents, allows a differentiation between pre-glacial and glacial sediments. Recent seismic stratigraphic models that are based on such seismic features enabled the modelling of a set of isopach grids for the Pacific sector of the Southern Ocean and, thus, a comparison of the sedimentary development in various parts of the study area. Maps of total sediment thicknesses, and the thicknesses of pre-glacial and glacially transported sediments were created.

The adoption of an age of about 10 Ma for the onset of glacial sediment supply along the South Pacific margin allowed approximations of sedimentation rates on the continental rise and, thus, a comparison of local sedimentary histories. The differences in sedimentation rates show that the glacial dynamics of the South Pacific margin vary in both time and space. The high rate of pre-10 Ma sedimentation off the western Antarctic Peninsula suggests a high sediment supply due to glacial influences prior to the late Miocene. As the elevated Antarctic Peninsula acts as a major barrier to tropospheric circulation, resulting in high snowfall and snow accumulation

onshore, this region may have been more sensitive to Miocene climate changes than the adjacent regions to the west, so it is possible that ice sheets and streams developed earlier there. In contrast, low pre-10 Ma sediment accumulation rates on the Bellingshausen and Amundsen Sea continental rise are attributed to the wide continental shelf and low lying hinterland. Consideration of the distribution of glacially transported sediments reveals another picture, as the thickest sediments were identified in front of major glacial drainage outlets. The highest deposition rate was estimated at Depocentre B, a trough mouth fan off the Belgica Trough. Average sedimentation rates of 170 m/m.y were calculated. The peak of 295 m/m.y., occurring since 5.3 Ma, indicates a trend of increasing sediment accumulation rates in Plio-Pleistocene times, related to the development of very large ice drainage basins, high erosion rates on- and offshore, and high ice flow velocities. In contrast, average deposition rates of 140 m/m.y. are calculated at drifts 6 and 7 on the western Antarctic Peninsula rise off the Marguerite Bay Trough. Drilling results from ODP Leg 178 indicate increasing deposition rates in Late Miocene times and a decrease into Pliocene times, which shows a remarkable difference in the onset time of high sediment deposition rates. This difference implies differences in the timing of the first erosional advance of grounded ice and, thus, variations of the glacial regime between the western Antarctic Peninsula and the Bellingshausen Sea continental margin. The thickest sediments, and an average sedimentation rate of 160 m/m.y. on the Amundsen Sea continental rise, were calculated for sediment mound Am3 which developed off of Pine Island Bay. As Pine Island Bay is considered to be the third largest drainage outlet of the West Antarctic Ice Sheet, the estimated high accumulation rates appear realistic. Nonetheless, such calculations in the Amundsen Sea remain speculative due to the sparse coverage of seismic profiles and very limited or absent drill hole information.

The influence of bottom currents on the distribution of sediments and structures of sediment deposits along the western Antarctic Peninsula margin has been previously documented. The channel-related sediment drift at Depocentre C can be seen as an indicator that a bottom current affected sedimentation in the western Bellingshausen Sea. The northward change in the sediment drift's structure into a classical channel-levee, whose symmetry is contrary to that of the sediment drift, is conspicuous. As well as being influenced by a topographic barrier, the submarine base of Peter I Island, the structure of Depocentre C seems to picture the course of the westward flowing bottom current. The main part of this current probably flows between the continental slope and Peter I Island, causing the development of the sediment drift, and may be diverted to the north as a contour current following the topography. The development of the wide and gently sloping depocentres A and B in the central Bellingshausen Sea, instead of channel related drifts, may be explained by a reduction in turbidity currents due to the gentle inclination of the Bellingshausen Sea continental slope. If so, the production of fine, suspended sediment on the continental rise as the source of contouritic detritus would be limited. In contrast, slope gradients on the Antarctic Peninsular are far steeper, suggesting a less stable slope and more frequently occurring turbidity currents. The sediment mounds identified in the Amundsen Sea show similarities to those developed on the Antarctic Peninsula margin, consisting of sediment mounds with asymmetrical slopes separated by erosional channels. It is not known whether a bottom current has existed in the Amundsen Sea since the onset of glacially transported sediment accumulation, but the influence of such a current on the development of these sediment mounds is possible. Speculation about this current's direction

remains difficult, as the asymmetry of the drifts on the Antarctic Peninsula margin has been shown not to be a reliable indicator of the westward-flowing current there. Furthermore, the question of whether the contour current which is assumed to be responsible for the development of the Antarctic Peninsular drifts and the southern part of Depocentre C was also active in the Amundsen Sea remains open. The correlation of basement offsets identified on one seismic profile with magnetic seafloor spreading anomalies on the continental margin of the Bellingshausen Sea allowed the definition of basement ages and identification of at least two fracture zones, named the Alexander FZ and the Peter I FZ. There identification improves previous plate kinematic models of the South Pacific. Comparison between the grid of total sediment thicknesses and Eagles´ (2006) grid of predicted sediment thicknesses, derived from a model of residual bathymetry, reveal evidence for uplift processes of the ocean floor in the Bellingshausen and Amundsen Sea, which can be interpreted in terms of warm upwelling mantle material.

6.2 OUTLOOK

Differences in sediment thicknesses and accumulation rates identified in the study area suggest significant local variability in glacial dynamics on the West Antarctic continental margin. However, the dataset in the Bellingshausen and Amundsen seas is still very limited so that the results published in this thesis have to be considered as of tentative nature. Knowledge of the behaviour of the ice sheet that developed on the continental margin remains limited, and the reason for the apparent differences in Plio-Pleistocene ice sheet dynamics and the accompanying very high sedimentation rate in the Bellingshausen Sea remains a subject of debate. Acquisition of additional cross-slope profiles at the mouths of the Belgica and Pine Island Troughs would enable correlations between continental shelf and rise deposits on the glacial outlets and, thus, the analysis of sedimentary sequences. Such correlations would improve our present interpretation of ice fluctuations, as glacial outlets probably provide the most detailed record of glacial dynamics due to the high sediment input.

The drilling of deep boreholes on the Amundsen Sea continental margin would bring geological knowledge of that region a wide step forward. Analyses of bore hole samples and correlation of the resulting stratigraphy with seismic reflectors could enable the development of an age related sedimentation model in the Amundsen Sea and, with it, a more reliable comparison with the sedimentation history of the western Antarctic Peninsula and Bellingshausen Sea.

The correlations of seismic stratigraphic pattern into the abyssal plain via additional, wide ranging seismic profiles would improve the reliability of the modelled sediment isopach grids, especially those of pre-glacial and glacially transported sediments. Digitizing and incorporation of previously acquired analogue recorded single-channel seismic profiles would also help improve and modify the isopach grids. The isopach grids can be used to adjust existing paleobathymetric models for the effects of sedimentation. Such grids should be a central element of paleoceanographic models that set out to investigate the origins and effects of topographically steered currents and water masses like the ACC or AABW. The development

of bottom currents around Antarctica, as a part of the AABW, and their effect on the sediment distribution is still little investigated, especially in the Amundsen Sea. Measurements of bottom currents via moorings of current meters on the continental rise of the Amundsen Sea would give information about modern flow velocities and directions, and help the analysis of their development in the past.

ACKNOWLEDGEMENTS

Last but not least, there are some people who I want to thank for their help and support to realize this PhD-Thesis:

I thank sincerely my doctoral advisor, Prof. Dr. Heinrich Miller, who admitted me to write this thesis at the AWI-Bremerhaven and the University of Bremen (Fachbereich 5). In addition, many thanks go to Prof. Dr. Katrin Huhn, as the second referee, for co-reviewing my work.

I kindly thank Dr. Karsten Gohl for giving me the opportunity to do this work, for his introduction into the "geophysical way of research", and for many scientific discussions between a geologist and a geophysicist. Thanks for encouraging me.

Many thanks go to Dr. Graeme Eagles. He did a lot of work correcting the English of the thesis. And even if he was not Gizmo's best friend, he did spend quite a lot of time with me discussing scientific questions, and he always amused me with his dry British humour.

I really enjoyed the collaboration with Michele Rebesco (OGS, Trieste, Italy) and Rob Larter (BAS, Cambridge, England). Working together drove me on to develop my knowledge of both sedimentary and tectonic processes on the Antarctic continental margin, and I enjoyed my stays in Trieste and Cambridge very much.

I appreciated the friendly atmosphere within the Geophysics Group at the AWI-Bremerhaven. I tasted a lot of different cakes and coffees. Special thanks go to Veit Helm for his initial introduction into the world of Landmark, Dr. Catalina Gebhardt for corrections of the manuscript, Dr. Matthias König for his help concerning AWK and GMT, and Daniela Berger for the friendly, funny, and familiar atmosphere in our office. Kind regards to Dr. Etienne Wildeboer Schut for his help to win the fight against Unix, Focus, Landmark, and other computing problems.

I kindly thank Claus-Dieter Hillenbrand and Prof. Rebecca Rendle for our collective sessions of seismic interpretation, and Sebastian, Mara and Marlen for the diverting train rides.

I am grateful to the Deutsche Forschungsgemeinschaft and the Alfred Wegener Institute for their financial support.

Finally, my deepest thanks go to my mother and Tanja. They have needed the patience of saints to support and encourage me through the last few years.

APPENDIX A

Profil	Traces	Year	Institute	Vessel	Streamer length [meter]	Airgun source [litre]
AWI-200010001	41100	2001	AWI	Polarstern	600	24
AWI-94002	8760	1994	AWI	Polarstern	2400	24
AWI-94003	5350	1994	AWI	Polarstern	2400	24
AWI-94030	9900	1994	AWI	Polarstern	600	34.4
AWI-94040	2750	1994	AWI	Polarstern	600	24
AWI-94041	11400	1994	AWI	Polarstern	600	24
AWI-94042	4900	1994	AWI	Polarstern	600	24
AWI-94043	4750	1994	AWI	Polarstern	600	24
AWI-94050	4100	1994	AWI	Polarstern	600	24
AWI-94051	535	1994	AWI	Polarstern	600	24
AWI-94052	800	1994	AWI	Polarstern	600	24
AWI-94053	500	1994	AWI	Polarstern	600	24
AWI-94054	6700	1994	AWI	Polarstern	600	24
AWI-95200	5750	1995	AWI	Polarstern	2400	24
AWI-95201	3950	1995	AWI	Polarstern	2400	24
AWI-95210	8250	1995	AWI	Polarstern	2400	24
BAS-92322	5350	1993	BAS	James Clark Ross	2400	55.9
BAS-92323	1100	1993	BAS	James Clark Ross	2400	55.9
BAS-92324	5850	1993	BAS	James Clark Ross	2400	55.9
BAS-92325	2650	1993	BAS	James Clark Ross	2400	55.9
BAS-92327	2700	1993	BAS	James Clark Ross	2400	55.9
BAS-92328	5050	1993	BAS	James Clark Ross	2400	55.9
BAS-92329	2650	1993	BAS	James Clark Ross	2400	55.9
BAS-92330	2450	1993	BAS	James Clark Ross	2400	55.9
IT-89A45	2550	1989	OGS	Explora	3000	45.6
IT-89A48	4000	1989	OGS	Explora	3000	45.6
IT-89A49	1750	1989	OGS	Explora	3000	45.6
IT-92A106	4900	1992	OGS	Explora	3000	72
IT-92A107	1100	1992	OGS	Explora	3000	72
IT-92A108	3000	1992	OGS	Explora	3000	72
IT-92A109	5300	1992	OGS	Explora	3000	72
IT-92A110	3750	1992	OGS	Explora	3000	72
IT-92A113	4600	1992	OGS	Explora	3000	72
IT-92A114	5600	1992	OGS	Explora	3000	72
IT-92A115	2700	1992	OGS	Explora	3000	72
IT-92A124	2200	1992	OGS	Explora	3000	72
IT-95130	10230	1995	OGS	Explora	3000	13.4
IT-95135	12300	1995	OGS	Explora	3000	13.4
IT-95136	8050	1995	OGS	Explora	3000	13.4
IT-95137	8425	1995	OGS	Explora	3000	13.4
IT-95138	6470	1995	OGS	Explora	3000	13.4
IT-97235	9200	1997	OGS	Explora	3000	13.4
IT-97236	6850	1997	OGS	Explora	3000	13.4
PET-98401c	3200	1998	VI / AWI	Boris Petrov	single channel	unknown
PET-98402a	750	1998	VI / AWI	Boris Petrov	single channel	unknown
PET-98403a	1350	1998	VI / AWI	Boris Petrov	single channel	unknown
PET-98404	2800	1998	VI / AWI	Boris Petrov	single channel	unknown
PET-98405	2730	1998	VI / AWI	Boris Petrov	single channel	unknown

PET-98407	1800	1998	VI / AWI	Boris Petrov	single channel	unknown
PET-98408	3150	1998	VI / AWI	Boris Petrov	single channel	unknown
PET-98409	4240	1998	VI / AWI	Boris Petrov	single channel	unknown
TH-86002	3500	1986	JNOC	Hakurei Maru	600	11.5
TH-86003	14600	1986	JNOC	Hakurei Maru	600	11.5
TH-86004	7150	1986	JNOC	Hakurei Maru	600	11.5
TH-86006	7100	1986	JNOC	Hakurei Maru	600	11.5
TH-86008	10500	1986	JNOC	Hakurei Maru	600	11.5
TH-86009	4650	1986	JNOC	Hakurei Maru	600	11.5

***Table A**: List of all seismic reflection profiles analysed in this study and their recording methods. AWI = Alfred Wegener Institute (Germany), BAS = British Antarctic Survey (UK), OGS = Istituto Nazionale di Oceanografia e di Geofisica Sperimentale (Italy), VI = Vernadsky Institute of Geochemistry and Analytical Chemistry (Russia).*